USRA

JOVE MEMORANDUM

TO: JOVE Faculty Research Associates

FROM: Maury Estes
            JOVE Program Office

DATE: May 16, 1997

SUBJECT: JOVE Annual Progress Report

Enclosed you will find an Annual Progress Report form and a copy of the JOVE Performance Expectations. The information you provide through this report is invaluable to us in providing statistics/metrics for NASA regarding the program and will be used to evaluate your performance against the JOVE Performance Expectations. A Feedback Letter regarding your performance will be sent to you in the fall.

All schools with grants which expire in May of 1997 will receive an additional form requesting information that will be necessary for grant close-out. This form should be completed only if you do not anticipate an extension of your grant or a JOVE Augmentation Grant.

This year's deadline for reports is **June 30**. Please mail 3 copies of your completed report (including attachments) to USRA/JOVE, 4950 Corporate Drive, Suite 100, Huntsville, AL 35805. **To obtain an electronic copy of the Progress Report in Microsoft Excel format contact Mona Miller via mona@space.hsv.usra.edu.**

We greatly appreciate the hard work that goes into preparing this report and look forward to learning more about your project. Please notify me or Debbie Hurst at (205) 895-0582 if you have questions.

JOVE FINAL TECHNICAL REPORT*

Note: Please print or type.

Date: 6/27/97

Dr. Benjamin K. Malphrus

Name

Morehead State University

Institution

b.malphr@morehead-st.edu

E-Mail Address

NAG8-1119

Grant Number

I. Comprehensive summary of research conducted under this NASA/JOVE grant. (Attach additional page(s) if necessary.)

See attached document.

_____

II. Please list all subject inventions/patents as a result of your Grant or provide a statement that there were none.

No patents or inventions resulted from this project.

_____

Signature

Date 6/27/97

*Complete this form only if you do not anticipate continuing your research on a No-Cost Extension or on a JOVE Augmentation Grant (JAG).

I. Comprehensive summary of research conducted under this NASA/JOVE grant.

The goal of this project has been to search for genuinely young irregular galaxies that have formed during gravitational encounters. The research has specifically involved high spatial resolution HI observations made using the VLA of NGC 5291, an interacting system consisting of a massive lenticular galaxy, companion galaxy and gaseous extensions. During the internship, data that had been collected by the mentor was calibrated, edited, reduced, and images of the HI distribution and kinematics produced. The 1995 academic year was devoted to further imaging and to the analysis of these data. Results indicated that dwarf irregular galaxies had indeed formed from material tidally removed from the interacting pair. Our observations of NGC 5291 show that some of the associations of HI and HII would be considered dwarf irregular galaxies, if they were isolated objects. Initial results were reported at the January meeting of the AAS and via a press release requested by the AAS. The 1996 academic year was devoted to further analysis of the data in an attempt to prove that the young galaxy is bound against its own internal kinetic energy and lies outside of the tidal radius of the host galaxy. An analysis method was developed that can be applied to observations of additional systems. This initial study proved the viability of the observation and analysis procedures in searching for genuinely young dwarf irregular galaxies formed in interaction fields. A scientific paper describing these observational and analysis procedures was prepared, submitted, and accepted for publication in the Astronomical Journal.

We have begun to define the role that collisions play in the building of irregular galaxies. New questions, however, are indicated by the research. What can be said about the long term stability of these potential dwarf systems? How do they evolve during the course of the interaction; do they tend to fall back into the galaxy or remain free as dwarf satellites, possibly in orbit? The next phase of the research will be devoted to developing proposals to observe other systems in attempt to prove that the phenomenon is not unique indicating that many if not *all* dwarf irregular galaxies have formed from material removed from major galaxies during mergers and gravitational encounters.

Two observing proposals were developed and submitted to the VLA. A multi-institutional research proposal involving was developed and submitted to NSF in which 21 cm observations will be combined with optical and infrared (IR) observations (provided by our collaborators at the Instituto de Astrofisica de Canarias (IAC)) and numerical simulations in a comprehensive program. This research could ultimately contribute to our understanding of galactic evolution resulting from gravitational encounters.

JOVE ANNUAL PROGRESS REPORT: ACADEMIC YEAR <u>1996-97</u>

<u>Refereed Journal Articles Published</u>: *(Include title, author(s), date of publications, volume, number, page number(s), and <u>attach a copy of the full publication</u>.)*

	Title	Benjamin K. Malphrus, Caroline E. Simpson, S. T. Gottesman, T.G. Hawarden	Date	Vol.	Number	Page #
1.	"NGC 5291: Implications for the Formation of Dwarf Galaxies"		Astronomical Journal, accepted 5/28/97			
2.	The Morehead Radio Telescope: Design and Fabrication of A Research Instrument for Undergraduate Student and Faculty Research in Radio Frequency Astrophysics"	Benjamin K. Malphrus, et. al.	Kentucky Academy of Science Bulletin,			
3.			accepted 5/15/97			

<u>Refereed Journal Articles Submitted</u>: *(Include title, authors, journal, date submitted.)*

	Title	Author(s)	Journal	Date Submitted
1.				
2.				
3.				

<u>Papers Presented</u>:   *(Include title, author(s), conference name, date, and <u>attach a copy of the abstract</u>.)*

	Title	Benjamin K. Malphrus, Caroline E. Simpson, S. T. Gottesman, T.G. Hawarden	Conference Name	Date
1.	*"The Formation of Dwarf Irregular Galaxies from Tidally Removed Debris and the Peculiar System NGC 5291"*		American Astronomical Society	1/1796
2.				
3.	*"The Discovery of Dwarf Irregular Galaxies formed from Tidally Removed Debris Surrounding the Peculiar System NGC 5291"*	Benjamin K. Malphrus, Caroline E. Simpson, S. T. Gottesman, T.G. Hawarden	NASA JOVE/NASA EPSCoR Conference	5/24/96

"The Morehead Radio Telescope-: Design and Fabrication of A Research Instrument for Undergraduate Student and Faculty Research in Radio Frequency Astrophysics"   Benjamin K. Malphrus   Kentucky Academy of Science   11/16/96

2

JOVE   ANNUAL PROGRESS REPORT: ACADEMIC YEAR <u>1996-97</u>*

Note: Please print or type.

Date: <u>6/27/97</u>

<u>Dr. Ben Malphrus</u>

Name

<u>Morehead State University</u>

Institution

E-Mail Address: <u>b.malphr@morehead-st.edu</u>

Grant Number: <u>NAG8-1119</u>

I.   RESEARCH

<u>Brief description of research results to date on your project:</u>

The goal of this project has been to search for genuinely young irregular galaxies that have formed during gravitational encounters. The research has specifically involved high spatial resolution HI observations made using the VLA of NGC 5291, an interacting system consisting of a massive lenticular galaxy, companion galaxy and gaseous extensions. During the internship, data that had been collected by the mentor was calibrated, edited, reduced, and images of the HI distribution and kinematics produced. Results indicate that a dwarf irregular galaxy had indeed formed from material tidally removed from the interacting pair. Initial results were reported at the January meeting of the AAS and via a press release requested by the AAS. The 1996 academic year was devoted to further analysis (i.e. gravitational stability) of the system. An analysis method was developed that can be applied to observations of additional systems. In addition, a scientific paper was prepared, submitted, and accepted for publication in the Astronomical Journal. The next phase of the research will be devoted to developing proposals to observe other systems in attempt to prove that the phenomenon is not unique indicating that many if not *all* dwarf irregular galaxies have formed from material removed from major galaxies during mergers and gravitational encounters. An extensive multi-wavelength, multi-instituion project has been initiatied. Two observing proposals were developed and submitted to the VLA. A multi-institutional research proposal was developed and submitted to NSF.

<u>Please identify the data sets, if any, used in your research.</u>

NASA Extragalactic Database (NED), Astrophysical Journal Abstracts, SpaceLink, SkyView, NRAO WWW pages.

<u>Communication with NASA Colleague:</u>   *(Please indicate the extent of your contact with your NASA Colleague. Is the communication producing qualitative results? Do you still consider the match to be viable?)*

Interaction with the mentor has been extensive during the 1996 academic year. I have spent a total of approximately three weeks at the mentor's institution during the academic year. In addition, we communicate regularly by electronic mail and telephone. We have collaborated on the data analysis stage closely and have co-authored a scientific paper announcing the research results that has been accepted for publication in the Astronomical Journal. We are also in the process of developing proposals for observing time on various instruments to extend the research. A multi-institutional research proposal was developed and submitted to NSF. Although it received very good reviews, the proposal was not funded. We intend to revise the proposal this summer and resubmit it in the fall. I believe that the collaboration has been extremely viable.

*This Progress Report should include information for the period 6/1/96 to 5/31/97.

III. EXTRAMURAL FUNDING

<u>**Proposals Awarded**</u>:   *(Attach the signature page, title page, and table of contents.)*

1.   **Title of Project**:   "Eastern Kentucky PRISM Regional Network."

   PI: Dr. Ben Malphrus   **Grantor**:   Kentucky Science and Technology Council and Mikrotec Internet Services, Inc.

   Agency type: ☐ **Federal** ☐ **State** ☐ **Industry** ☐ **Private** ☐ **University**

   Type of Grant: ☐ **Research** ☐ **Education** ☐ **Other** _____

   Period of Performance: _11/96-8/97_   **Total Award Amount**: $ _$137,219.00_

        First Year Funds: $ _____

        Second Year Funds: $ _____

        Third Year Funds: $ _____

2.   **Title of Proposal**:   "Partnership for Reform Initiatives in Science and Mathematics"

   PI: Dr. Ben Malphrus   **Grantor**:   Kentucky Department of Education and the Kentucky Science and Technology Council

   Agency type: ☐ **Federal** ☐ **State** ☐ **Industry** ☐ **Private** ☐ **University**

   Type of Grant: ☐ **Research** ☐ **Education** ☐ **Other** _____

   Period of Performance: _1992-1996_   **Total Award Amount**: $ _$230,000.00_

        First Year Funds: $ _$38,759.00_

        Second Year Funds: $ _$77,294.00_

        Third Year Funds: $ _$71,875.00_

        $42,072.00

   Title of Proposal: "Space Sciences Resources Travel,"

   PI: Dr. Ben Malphrus   **Agency**:   Kentucky Space Grants Consortium

   Status: _Funded_   **Pd. of Performance**: _7/01/97 - 6/30/98_   **Amount**: $ _$3,761.00_

   Title of Proposal: "Colliding Galaxies: A Search for Genuinely Young Galaxies in Interacting Systems"

   PI: Dr. Ben Malphrus   **Agency**:   NSF Extragalactic and Cosmology Division

   Status: _Not funded_   **Pd. of Performance**: _1997-1999_   **Amount**: $ _$384,846.00_

JOVE ANNUAL PROGRESS REPORT: ACADEMIC YEAR <u>1996-97</u>

III. CURRICULUM DEVELOPMENT:

<u>New Curricula</u>: *(Please list any new majors, minors, or areas of concentration, which have been implemented as a result of your institution's participation in JOVE. Indicate current student enrollments, and <u>attach a copy of the new description from your institution's course</u> catalog.)*

	Title	Department	Enrollment
New Majors			
New Minors			
New Areas of Concentration			

<u>New Courses</u>: *(List course title, department, student enrollment, <u>attach copy of course syllabus and</u> catalog description.)*

	Title	Department	Enrollment
1.			
2.			
3.			

<u>Amended Courses or Augmented Courses</u>: *(List course, title, new topics, student enrollment, and <u>attach</u> a copy of the course syllabus.)*

	Title	New Topics Description	Enrollment
1.			
2.			
3.			

III. Curriculum Development (cont'd):

<u>Reading or Independent Study Courses</u>: *(List course title, department, description, and student enrollment.)*

	Title	Department	Description	Enrollment
1.				
2.				
3.				

IV. **STUDENT INVOLVEMENT:** Indicate the impact, if any, that the JOVE Program has had on student enrollment and/or recruitment?

_____

_____

_____

<u>Student Research Assistants</u>: *(Please complete the attached form for each student listed below.)*

<u>Undergraduate Assistants</u>:   <u>Graduate Assistants</u>:

_____   _____

_____   _____

_____   _____

_____   _____

_____   _____

JOVE ANNUAL PROGRESS REPORT: ACADEMIC YEAR <u>1996-97</u>

V. OUTREACH: Please indicate your outreach efforts in each of the categories below. List the type of outreach effort (lecture, workshop, demonstration, etc.), topic, location, type of audience, and estimated number of attendees.

	Type (lecture, workshop, demo, etc.)	Topic	Location	Audience (K-12 Students, Pre-college Teachers, College Students, General Public)	# of Attendees
1.	9/26/96 "Star Party"	"Lunar Eclipse"	MSU Observatory	Public	300
2.	4/17/97 Lecture	"Comet Hale-Bop"	Montgomery Co Science Center	Students, teachers, and public	200
3.	5/19/97 2 Workshops	"Astronomy Activities for the Classroom"	Greenup Co. Elementary	Teachers	40
4.	5/20/97 Workshop	"Astronomy Activities for the Classroom"	Morgan Co. MS	Teachers	25
5.					
6.					

JOVE ANNUAL PROGRESS REPORT: ACADEMIC YEAR <u>1996-97</u>

VI. SUMMER PROGRAMS: Describe program, include location, date(s), # of attendees, length of
program, and <u>attach any relevant literature</u>.

<u>For Students:</u>

	Description	Location	Date(s)	# of Attendees	Length of Program
1.					
2.					

<u>For Teachers:</u>

	Description	Location	Date(s)	# of Attendees	Length of Program
1.					
2.					

VII. "ROADBLOCKS" TO PROGRESS/COMMENTS: Please attach additional page(s) if necessary.

_____

_____

_____

_____

_____

_____

1997 NASA/UNIVERSITY JOINT VENTURE – STUDENT INFORMATION

Name of JOVE Student Researcher: Michael Combs

Social Security Number: ▬▬▬▬▬▬

Permanent Mailing Address: PO Box 453

Dwarf, KY   41739

JOVE Faculty Advisor: Dr. Benjamin K. Malphrus

Institution Name: Morehead State University

	UNDERGRADUATE	GRADUATE
Major	Electronics	Electronics
Department	Industrial Education & Technology	Industrial Education & Technology
Class Standing	B.A. 5/97	1st year graduate
Degree Expected (e.g. BA, BS, MA, ...)		M.A.
Expected Graduation Date		5/98

JOVE Project Title: Instrumentation in Radio Astronomy

Circle **each** academic year participating as a JOVE student researcher: 93-94   94-95   (95-96)   (96-97)

Has your participation in JOVE influenced your choice of Major?   ☐ Yes   ☒ No

If so, how? _____

Has your participation in JOVE influenced your career choice?   ☒ Yes   ☐ No

If so, how?   Aerospace applications

Has your participation in JOVE influenced your plans for graduate study? ☒ Yes   ☐ No

If so, how?   NASA/JOVE provided an assistantship for my first year of graduate study

---

In order to determine the degree to which members of the diverse segments of the population are involved in this program, we request that you fill in the appropriate blocks. Completion of this section is voluntary.

☒ Male   ☐ Female   Citizenship: ___USA___

☐ American Indian or Alaskan Native   ☐ African-American/non-Hispanic

☐ Asian or Pacific Islander   ☐ Mexican-American

☒ Caucasian, non-Hispanic origin   ☐ Other Hispanic origin

1997 NASA/UNIVERSITY JOINT VENTURE -- STUDENT INFORMATION

Name of JOVE Student Researcher: Brian Matthe Lewis

Social Security Number: ▮▮▮▮▮▮▮

Permanent Mailing Address: 85 Oneida Trail

Malvern, OH 44644

JOVE Faculty Advisor: Dr. Benjamin K. Malphrus

Institution Name: Morehead State University

	UNDERGRADUATE	GRADUATE
Major	Mathematics	
Department	Mathematics	
Class Standing	Junior	
Degree Expected (e.g. BA, BS, MA, ...)	B.S.	
Expected Graduation Date	5/99	

JOVE Project Title: Surface Geometries in Radio Frequency Antennas

Circle **each** academic year participating as a JOVE student researcher: 93-94   94-95   (95-96)   (96-97)

Has your participation in JOVE influenced your choice of Major?   ☐ Yes   ☒ No

If so, how?   _____

Has your participation in JOVE influenced your career choice?   ☐ Yes   ☒ No

If so, how?   _____

Has your participation in JOVE influenced your plans for graduate study?   ☒ Yes   ☐ No

If so, how?   ___ Will definitely attend graduate school now. _____

In order to determine the degree to which members of the diverse segments of the population are involved in this program, we request that you fill in the appropriate blocks. Completion of this section is voluntary.

☒ Male   ☐ Female   Citizenship: USA _____

☐ American Indian or Alaskan Native   ☐ African-American/non-Hispanic

☐ Asian or Pacific Islander   ☐ Mexican-American

☒ Caucasian, non-Hispanic origin   ☐ Other Hispanic origin

1997 NASA/UNIVERSITY JOINT VENTURE -- STUDENT INFORMATION

Name of JOVE Student Researcher: Jennifer B. Carter

Social Security Number: ██████

Permanent Mailing Address: Route 1 Box 946

Olive Hill, KY 41164

JOVE Faculty Advisor: Dr. Benjamin K. Malphrus

Institution Name: Morehead State University

	UNDERGRADUATE	GRADUATE
Major	Physics	
Department	Physical Sciences	
Class Standing	sophmore	
Degree Expected (e.g. BA, BS, MA, ...)	B.S.	
Expected Graduation Date	5/2000	

JOVE Project Title: Interacting Galaxies

Circle **each** academic year participating as a JOVE student researcher: 93-94   94-95   95-96   (96-97)

Has your participation in JOVE influenced your choice of Major?   ☒ Yes   ☐ No

If so, how?   I have decided to major in physics and astronomy.

Has your participation in JOVE influenced your career choice?   ☒ Yes   ☐ No

If so, how?   I intend to pursue a career in astronomy.

Has your participation in JOVE influenced your plans for graduate study?   ☒ Yes   ☐ No

If so, how?   I plan to attend graduate school for astronomy.

In order to determine the degree to which members of the diverse segments of the population are involved in this program, we request that you fill in the appropriate blocks. Completion of this section is voluntary.

☐ Male   ☒ Female   Citizenship: USA

☐ American Indian or Alaskan Native   ☐ African-American/non-Hispanic

☐ Asian or Pacific Islander   ☐ Mexican-American

☒ Caucasian, non-Hispanic origin   ☐ Other Hispanic origin

1997 NASA/UNIVERSITY JOINT VENTURE -- STUDENT INFORMATION

Name of JOVE Student Researcher: Chad Jeremy Pulliam

Social Security Number:

Permanent Mailing Address: 7300 Old North Church Road

Louisville, KY 40214

JOVE Faculty Advisor: Dr. Benjamin K. Malphrus

Institution Name: Morehead State University

	UNDERGRADUATE	GRADUATE
Major	Computer Science	
Department	Mathematics	
Class Standing	Freshman	
Degree Expected (e.g. BA, BS, MA, ...)	B.S.	
Expected Graduation Date	5/2001	

JOVE Project Title: Programming Applications in Radio Frequency Astrophysics

Circle **each** academic year participating as a JOVE student researcher: 93-94   94-95   95-96   (96-97)

Has your participation in JOVE influenced your choice of Major?   ☐ Yes   ☒ No

If so, how? _____

Has your participation in JOVE influenced your career choice?   ☐ Yes   ☒ No

If so, how? _____

Has your participation in JOVE influenced your plans for graduate study? ☐ Yes   ☒ No

If so, how? _____

In order to determine the degree to which members of the diverse segments of the population are involved in this program, we request that you fill in the appropriate blocks. Completion of this section is voluntary.

☒ Male   ☐ Female   Citizenship: ___USA___

☐ American Indian or Alaskan Native   ☐ African-American/non-Hispanic

☐ Asian or Pacific Islander   ☐ Mexican-American

☒ Caucasian, non-Hispanic origin   ☐ Other Hispanic origin

1997 NASA/UNIVERSITY JOINT VENTURE -- STUDENT INFORMATION

Name of JOVE Student Researcher: Bobby Russell Ratliff

Social Security Number: ▮▮▮▮▮▮

Permanent Mailing Address: HCR 71 Box 2062

Frenchburg, KY 40322-9617

JOVE Faculty Advisor: Dr. Benjamin K. Malphrus

Institution Name: Morehead State University

	UNDERGRADUATE	GRADUATE
Major	Computer Science	
Department	Mathematics	
Class Standing	Junior	
Degree Expected (e.g. BA, BS, MA, ...)	B.S.	
Expected Graduation Date	5/99	

JOVE Project Title: Systems Administration & Data Reduction and Imaging in Radio Astronomy

Circle **each** academic year participating as a JOVE student researcher: 93-94   94-95   (95-96)   (96-97)

Has your participation in JOVE influenced your choice of Major?   ☐ Yes   ☒ No

If so, how? _____

Has your participation in JOVE influenced your career choice?   ☒ Yes   ☐ No

If so, how?   I am interested in a career in aerospace technologies.

Has your participation in JOVE influenced your plans for graduate study?   ☐ Yes   ☒ No

If so, how? _____

In order to determine the degree to which members of the diverse segments of the population are involved in this program, we request that you fill in the appropriate blocks. Completion of this section is voluntary.

☒ Male   ☐ Female   Citizenship: _____ USA _____

☐ American Indian or Alaskan Native   ☐ African-American/non-Hispanic

☐ Asian or Pacific Islander   ☐ Mexican-American

☒ Caucasian, non-Hispanic origin   ☐ Other Hispanic origin

1997 NASA/UNIVERSITY JOINT VENTURE -- STUDENT INFORMATION

Name of JOVE Student Researcher: John Farrell Pelphry

Social Security Number: ████████

Permanent Mailing Address: 245 Keeton Heights

West Liberty, KY   41472

JOVE Faculty Advisor: Dr. Benjamin K. Malphrus

Institution Name: Morehead Stae University

	UNDERGRADUATE	**GRADUATE**
Major	Electronics	
Department	Industrial Education and Technology	
Class Standing	Junior	
Degree Expected (e.g. BA, BS, MA, ...)	B.S.	
Expected Graduation Date	5/99	

JOVE Project Title: Instrumentation in Radio Astronomy

Circle **each** academic year participating as a JOVE student researcher: 93-94   94-95   95-96   96-97

Has your participation in JOVE influenced your choice of Major?   ☐ Yes   ☒ No

If so, how? _____

Has your participation in JOVE influenced your career choice?   ☐ Yes   ☒ No

If so, how? _____

Has your participation in JOVE influenced your plans for graduate study? ☐ Yes   ☒ No

If so, how? _____

In order to determine the degree to which members of the diverse segments of the population are involved in this program, we request that you fill in the appropriate blocks. Completion of this section is voluntary.

☒ Male   ☐ Female   Citizenship: USA

☐ American Indian or Alaskan Native   ☐ African-American/non-Hispanic

☐ Asian or Pacific Islander   ☐ Mexican-American

☒ Caucasian, non-Hispanic origin   ☐ Other Hispanic origin

For Release:

9:20 a.m. CST, Tuesday, Jan. 16, 1996

New Galaxies From Old?
VLA Observations Strengthen the Case

Astronomers using the Very Large Array (VLA) radio telescope have found some of the best evidence to date that small, new galaxies can form from material pulled out of older galaxies. The new observations seriously weaken models of galactic evolution that attempt to explain the various types of galaxies seen in the universe as the result of different, but independent, processes. Steve Gottesman of the University of Florida in Gainesville, Tim Hawarden of the Joint Astronomy Center in Hilo, Hawaii, Caroline Simpson of Florida International University in Miami and Benjamin Malphrus of Morehead State University in Morehead, Kentucky, presented the results today to the American Astronomical Society meeting in San Antonio, TX.

The astronomers used the VLA, a facility of the National Science Foundation, to study a galaxy system some 180 million light-years distant in the constellation Centaurus called NGC 5291. NGC 5291 is a peculiar spiral galaxy that appears to be interacting with a nearby object called the Seashell. The VLA observations show a large, elongated cloud of neutral hydrogen gas surrounding NGC 5291 and the Seashell.

Within that gas cloud there are several concentrations. These mostly coincide with faint "knots" which were first seen on optical photographs taken twenty years ago with the UK Schmidt Telescope in Australia for the ESO/SRC Southern Sky Survey. In a detailed study at that time, using the 4-meter Anglo-Australian Telescope (AAT) and the 65-meter Parkes radio telescope, the knots were shown to be giant star-forming regions and the system was found to contain an extremely large cloud of gas. Though details were lacking then, astronomers suggested that the larger knots would turn out to be galaxies either in

- more -

the process of formation or recently formed from the material of the parent system.

Subsequently, similar suggestions were made about concentrations of material in the "tidal tails" ejected by galactic collisions elsewhere in the sky, but it was not possible to put the suggestions on a firm footing. This latest research, however, shows conclusively that one of the knots in the NGC 5291 system is indeed a dwarf irregular galaxy similar to the Magellanic Clouds, companion galaxies to our own Milky Way. The knot of gas, in which stars are being formed, has about 5 billion times the mass of the Sun.

"In order for it to be considered an independent galaxy, it must meet two conditions -- its mass must remain gravitationally bound against its own kinetic energy and it must remain bound against the gravitational effect of the primary galaxy. This knot in the NGC 5291 system has the stable properties, the required mass, and sufficient distance from the remnant galaxies that, were it an isolated system, it would be classified as an actively star-forming dwarf irregular galaxy," said Gottesman.

In addition, the researchers' analysis of the VLA observations indicates that several other knots seen in the region probably are protogalaxies or young dwarf irregular galaxies in various stages of development.

"It was a great thrill to see the VLA images confirm in detail the association between the neutral hydrogen concentrations and the star-forming knots which we predicted 17 years ago, and especially rewarding to see our suspicion that some knots would turn out to be young galaxies so nicely verified," said Hawarden, who was part of the earlier research team.

The new observations, combined with earlier evidence from interacting systems such as Arp 105 and NGC 7252, strengthen the idea that galaxy collisions must be considered an important agent of galactic evolution. "This is strong evidence that galaxies, especially in clusters where they can interact with each other and with any hot medium present in the cluster, can and do evolve in dramatic ways, including being able to form genuinely young systems," Simpson said.

Malphrus added, "An important implication of this research is that genuinely young galaxies may evolve from the debris formed of material tidally removed by galactic interactions. We look forward to verification of this by the discovery of additional examples of genuinely young irregular galaxies in interacting systems."

The astronomers used the VLA, a 27-antenna radio telescope west of Socorro, NM,

at times when its antennas were spaced in two different configurations in order to gain both high resolving power and high sensitivity for the images. Observations of the radio spectral line of neutral hydrogen allowed the astronomers to use the Doppler shift in frequency of the received radio emissions to derive information about the velocity of the gas in different parts of the cloud.

Reduction and analysis of the data were made possible by a grant received from the National Aeronautics and Space Administration Joint Ventures in Research (NASA-JOVE) Project. Initial observations were made with the Very Large Array, an instrument of the National Radio Astronomy Observatory, a facility of the National Science Foundation operated under cooperative agreement by Associated Universities Incorporated. Digitized image and object positions were obtained using the Guide Star Astrometric Support Program developed at the Space Telescope Science Institute (STScI), which is operated by the Association of Universities for Research in Astronomy, Inc., for NASA. This research has made use of the NASA/IPAC Extragalactic Database (NED) which is operated by the Jet Propulsion Laboratory, California Institute of Technology, under contract with the National Aeronautics and Space Administration.

For More Information Contact:

Dr. Benjamin K. Malphrus	(606) 783 2212	b.malphr@msuacad.morehead-st.edu
Dr. Caroline Simpson	(305) 348 1565	simpsonc@galaxy.fiu.edu
Dr. Tim Hawarden	(808) 935 0407	hawarden@jach.hawaii.edu
Dr. Steve Gottesman		sgottes@ll.iac.es

Radio and Optical Images of the NGC 5291 Region
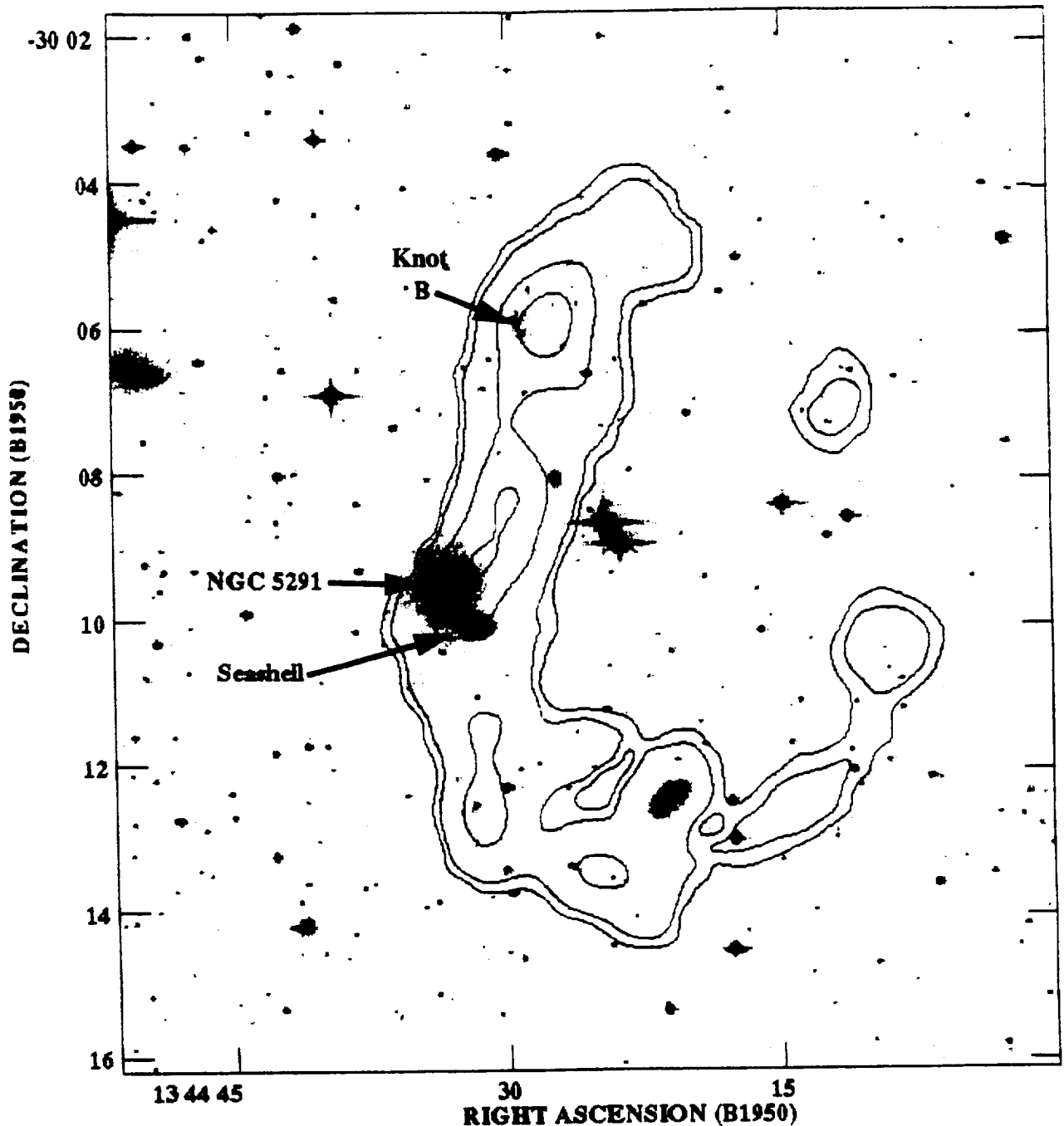
A Young Galaxy Emerges From the Debris of a Galactic Collision

In this image, contours (lines) representing the strength of radio emission from neutral atomic hydrogen are superimposed on an optical image (greyscale). "Knot B" is the optical object that coincides with a large concentration of hydrogen gas, and has been shown by detailed analysis to be an independent, star-forming galaxy. The gas from which it formed is believed to have been ejected by the interaction of the older galaxies, NGC 5291 and the Seashell.

Photo Credit: Steve Gottesman, Tim Hawarden, Caroline Simpson, Benjamin Malphrus; ESO/SRC Sky Survey and Space Telescope Science Institute; and NRAO/AUI.

NGC 5291: Implications for the Formation of Dwarf Galaxies

Benjamin K. Malphrus

Department of Physical Sciences, Morehead State University, Morehead, KY 40351

b.malphr@morehead-st.edu

Caroline E. Simpson

Department of Physics, Florida International University, Miami, Florida 33199

simpsonc@fiu.edu

S. T. Gottesman

Department of Astronomy, University of Florida, Gainesville, Florida 32611

gott@astro.ufl.edu

Timothy G. Hawarden[1]

Joint Astronomy Centre, 660 North A'ohoku Place, Hilo, Hawaii 96270

hawarden@jach.hawaii.edu

---

[1]Royal Observatory, Blackford Hill, Edinburgh EH9 3HJ, United Kingdom

ABSTRACT

The possible formation and evolution of dwarf irregular galaxies from material derived from perturbed evolved galaxies is addressed via an H I study of a likely example, the peculiar system NGC 5291. This system, located in the western outskirts of the cluster Abell 3574, contains the lenticular galaxy NGC 5291 which is in close proximity to a disturbed companion and is flanked by an extensive complex of numerous knots extending roughly 4' north and 4' south of the galaxy. In an initial optical and radio study, Longmore *et al.* (1979) showed that these knots have the spectra of vigorous star-forming regions, and suggested that some may in fact be young dwarf irregular galaxies.

High resolution 21-cm line observations taken with the VLA are presented here and reveal that the H I distribution associated with this system encompasses not only the entire N-S complex of optical knots, but also forms an incomplete ring or tail that extends approximately 3' to the west. The H I associated with NGC 5291 itself shows a high velocity range; the Seashell is not detected. The formation mechanism for this unusual system is unclear and two models – a large, low-luminosity ram-swept disk, and a ram-swept interaction – are discussed.

The H I in the system contains numerous concentrations, mostly along the N-S arc of the star-forming complexes, which generally coincide with one or more optical knots; the larger H I features contain several $\times$ 10^9 $M_\odot$ of gas. Each of the knots is compared to a set of criteria designed to determine if these objects are bound against their own internal kinetic energy and are tidally stable relative to the host galaxy.

An analysis of the properties of the H I concentrations surrounding the optical star-forming complexes indicates that at least the largest of these is

a bound system; it also possesses a stellar component. It is suggested that this object is a genuinely young dwarf irregular galaxy that has evolved from the material associated with the system and that this entire complex contains several proto- or young dwarf irregular galaxies in various stages of development. We are therefore witnessing the early evolution of a number of genuinely young galaxies. Given the evident importance of the NGC 5291 system as a "nursery" for young galaxies, careful modeling is required if we are to understand this remarkable galaxy.

Subject headings:

1. Introduction

NGC 5291 lies at $\alpha = 13^h 47^m 24\overset{s}{.}3$, $\delta = -30° 24' 26''$ (J2000), in the western parts of the cluster Abell 3574[2] (Abell 1958) of which it is probably a member. We adopt a value for H_0 of 75 km s^{-1} Mpc^{-1}; the cluster recession velocity of 4350 km s^{-1} (e.g. Richter 1984) then implies a distance of 58 Mpc. Pedersen *et al.* (1978) presented and briefly discussed deep images of the system taken with the ESO 3.6m telescope, drawing attention to the immense complexes of optical knots which extend several galactic diameters to the north and south and hypothesizing that these are H II regions (or at least, sites of recent star formation) from their blue colors. In the Second Reference Catalog of Bright Galaxies (de Vaucouleurs *et al.* 1976) NGC 5291 is classified as a peculiar elliptical (Ep?) with a nearby companion. Longmore *et al.* (1979, hereafter L79), using deep IIIaJ plates from the UK Schmidt Telescope for the Southern Sky Survey, reclassified NGC 5291 as SA.0+.

Table 1 summarizes the properties of the NGC 5291 system, while Figure 1 shows a *B*-band image of NGC 5291 taken by Pedersen *et al.* (1978) with the ESO 3.6m telescope. The main bodies of the galaxies NGC 5291 and its companion (dubbed "the Seashell" by L79 because of its appearance) are themselves relatively unremarkable. The overall lenticular morphology of the former is evident in the bulge-disc structure, and its late lenticular sub-type in the weak, smooth, possibly spiral, structure and dust lane evident to the NE. The Seashell is basically smooth in texture, and therefore probably also lenticular in underlying type; perhaps slightly earlier than NGC 5291, since no dust structure is visible. It displays dramatic evidence of its tidal distortion, in its contorted disk morphology and sharply defined edge. Nevertheless, the most unusual feature of this double system is not so much the morphology of the main bodies of the galaxies but the clearly-associated

---

[2]a.k.a. Shapley 1346-30 (Shapley 1936), IC 4329 (de Vaucouleurs & de Vaucouleurs 1964), and Klemola 29 (Klemola 1969).

swarms of knotty condensations, ranging in size down to the resolution limit of the image, and extending $\sim 4'$ both north and south of the pair.

EDITOR: PLACE FIGURE 1 HERE.

EDITOR: PLACE TABLE 1 HERE.

Longmore *et al.* (L79) obtained optical spectra of NGC 5291, the Seashell and of a number of the outlying knots, confirming that these last are indeed the locations of vigorous star formation as suggested by Pedersen *et al.* (1978), and have the spectra of H II regions. Longmore *et al.* also made 21-cm observations of the system, using the 64m Parkes (HPBW $= 15'$) and 100m Effelsberg (HPBW $= 9'$) telescopes, which revealed that $\sim 5 \times 10^{10} M_\odot$ ($H_0 = 75$ km s^{-1} Mpc^{-1}) of H I gas was present in the complex. The velocity ranges both of the optical features and of the H I are > 650 km s^{-1} and are centered on that of NGC 5291, with which they are clearly associated. This H I distribution was not resolved, however, although the H I centroid could be seen to be offset $\sim 1\overset{'}{.}5$ to the west of the optical system (primarily, it is now apparent from our new data, as a consequence of the source geometry).

In their paper, L79 drew attention to the luminosities and sizes of the brighter H II objects in the complex and particularly pointed out that they appeared to have all the properties of dwarf irregular galaxies, and that, if these are bound entities, they are eventually likely to be lost from the parent galaxy and will assume an independent existence as young dwarf systems. Two models describing the formation of these objects were then postulated, namely, ram-sweeping and local compression of a pre-existing, very extended H I disk and consequent collapse of the denser concentrations into star-forming cloud complexes, or the formation of these complexes from clumps of material tidally removed from the main bodies of the galaxies by the effects of the interaction.

Longmore *et al.* discussed the overall properties of the system and noted the very evident interaction between NGC 5291 and the Seashell. However they pointed out that the high relative velocity of the two galaxies ($\sim$ 600 km s^{-1}, in an apparently retrograde sense) which they measured made the creation of such massive and extensive tidal features seem unlikely. The asymmetric, curved optical structure and the geometrical offset of the H I centroid, together with the system's location in the northwest edge of a cluster then led them to suspect the presence of ram-sweeping. They speculated that NGC 5291 initially possessed a very extended, tenuous disk of H I, and suggested that this disk is now being compressed from the east as the galaxy falls into the Abell 3574 cluster and encounters an intracluster medium. Instabilities triggered by this ram-sweeping process would then, they suggest, have given rise to the observed star-forming complexes, while the sweeping-up and compression of the H I would give rise to the asymmetric distribution they observed.

To investigate further these scenarios, and the intriguing possibility that the star-forming objects in the extended complex are, indeed, dwarf galaxies in the process of formation, high resolution H I observations were taken using the Very Large Array (VLA) Radio Telescope[3] and are presented here. The observations described in this paper of the system, the debris field, and its contents show that it is even more complex and unusual than previously suspected.

In section 2 of this paper, we present the observational procedures and data reduction; section 3 contains a description of the H I distribution and kinematics, and section 4 discusses the analysis and interpretation of the results, including discussions of both the primordial disk and interaction hypotheses. Conclusions and a summary are presented in

---

[3]The VLA is operated by The National Radio Astronomy Observatory; the National Radio Astronomy Observatory is a facility of the National Science Foundation operated under cooperative agreement by Associated Universities, Inc.

section 5.

2. Observations and Data Reduction

High spatial resolution spectral line observations of the 21-cm emission from the region of NGC 5291 were made in 1989 by STG and R. Byrne with the Very Large Array radio telescope (VLA) in its CnB and DnC hybrid configurations, using a 64 channel spectrometer with a total bandwidth of 6.25 MHz. The resulting channel separation of 97 KHz provides velocity resolution of 25.6 km s^{-1}: the observations were made at a central velocity of 4386 km s^{-1}. Data were collected for two polarizations, right and left circular, which were then averaged together to enhance the signal-to-noise ratio in the final images.

The hybrid configurations have a long north arm to maintain resolution at extreme southern declinations where projection effects for the beam are large. At the declination of NGC 5291 the more extended CnB array provides spatial resolution of 14″ × 13″ while the compact DnC array, with lower spatial resolution (50″ × 39″) is more sensitive to weak extended emission. A third set of data was produced by combining that from both arrays – this takes advantage both of the higher resolution of the CnB array data and of the higher sensitivity of the DnC array observations. The spatial resolution of the combined data set (hereafter referred to as the combined array data, or the C+D array data) is 26″ × 15″. The observational parameters for all three sets of data are shown in Table 2.

EDITOR: PLACE TABLE 2 HERE.

Calibration and editing of the data were performed using the AIPS data reduction package available from NRAO. The phase and amplitude response of the receiving system were calibrated using the continuum sources 1354-152 and 1313-333 for the CnB array

observations, and 1313-333 for the DnC array observations. The calibrators were observed every thirty minutes for the duration of the observations. These calibration sources and the instrumental bandpass were in turn calibrated for radio frequency flux using the primary standard 3C 286.

The data from each configuration was edited and calibrated independently and converted to separate high resolution and high-sensitivity image cubes; the two data sets were also combined in the uv-plane to produce the C+D combined array dataset.

The data reduction was complicated by the presence of an internal interference spike at 1400 MHz, uncomfortably close to the observed frequency (1400.8 MHz) of the H I hyperfine transition at the systemic velocity of NGC 5291. Calibration involves the use of a continuum data set which is normally created by averaging together the central two-thirds of the channels in the bandpass. The continuum data set created during our observations was therefore affected by the interference spike, which was present in a few of the central channels. Rather than attempting to identify and remove the contaminated data piecemeal, a new interference-free continuum data set was created by identifying 21 interference-free channels (those well away from the problematic frequency) in the line dataset and averaging them in the uv-plane.

After calibration, the line data were examined and edited. The channels affected by the interference spike were easily identified and the affected data were removed by "clipping" data points above a specified value determined from an examination of the unaffected channels. This process minimized the removal of uncontaminated data points and hence resulted in the removal of very few data points ($\sim 2\%$ of the total) in unaffected channels. The contaminated channels, however, suffered the loss of approximately half of the data, thus degrading their signal-to-noise. Fortunately, not more than three channels were severely affected, due to the narrow frequency range of the interference spike. The

poorer quality of the data from the heavily clipped channels resulted in some loss of signal during the blanking and integrating processes (described below), and slightly reduced the column densities and H I masses calculated from the integrated dataset.

The uv data set was Fourier transformed to produce images of the intensity distribution of the source for each channel. The data cube of channel maps resulting from this process includes not only the 21-cm line emission from the observed source, but also the continuum emission from other sources. Continuum estimation was performed by combining channels which were free of line emission from both ends of the data cube, thirteen from the low frequency end and eleven from the high frequency end. This averaged continuum map was then subtracted from each channel of the cube.

Since the images are produced using a fast Fourier transform, any unsampled points in the uv-plane are automatically set to zero. In addition, the finite nature of the uv data set produces a truncation effect, so that the fast Fourier transform process results in a synthesized beam with extensive sidelobes: the "dirty beam." The continuum-subtracted data cube, consisting only of 21-cm line emission from the source, is actually a representation of the source brightness distribution convolved with the dirty beam. Confusion caused by the dirty beam was corrected by using the AIPS CLEAN routine (Högbom 1974, Clark 1980). The resulting point-source model was then convolved with the "clean beam," a 2-D Gaussian with the same full-width half-maximum (FWHM) as the dirty beam, to remove grating responses and sidelobes.

The data cubes were CLEANed down to 2 × the average r.m.s. noise (σ) as determined by a statistical analysis of the signal-free channel maps. Synthesized beamsizes representing the effective spatial resolution of the Gaussian CLEAN beams were calculated for all three data sets; these values are provided in Table 2. The average r.m.s. noise after CLEANing was determined to be 0.60 mJy per beam solid angle for the CnB array data, 0.71 mJy per

beam solid angle for the DnC array data, and 0.56 for the combined array data (Table 2).

After the data cubes were CLEANed, final imaging was performed by the integration of signal from ~ 40 contributing channels. This was done using the AIPS routine MOMNT, which conditionally blanks the data cube using a mask created by smoothing the data in both velocity and space (α, δ) and then integrates the blanked dataset. Blanking is performed in an attempt to isolate the signal from the noise by suppressing the noise. The data for NGC 5291 were blanked and integrated using a mask created by Hanning smoothing in velocity, and convolving in right ascension and declination with a Gaussian corresponding to twice the FWHM of the clean beam. The blanking and integrating levels were set to approximately 1.5 times the r.m.s. noise level on the unsmoothed data. Moment maps representing the H I column density (integrated flux) distribution (0th moment), velocity field (1st moment), and velocity dispersion (2nd moment) were created by this process.

3. Results

3.1. H I Spatial Distribution

Moment maps from the high sensitivity DnC array data, the high resolution CnB array data, and the combined C+D data were produced using the method described above. Figure 2 shows a grayscale image of the integrated H I flux distribution from the CnB array data overlaid with the 2σ contour level of the H I distribution from the DnC array data. We have indicated the positions of the original optical knots identified by L79 (A–H), as well as the discrete H I features (I–M) detected in the VLA observations that also appear to be associated with optical knots identified from either the optical image in Figure 1 or

the Digitized Sky Survey image[4]. Also identified are the locations of NGC 5291 and of the Seashell. *The H I forms what appears to be an incomplete ring structure extending about 9.'9 north-south (163 kpc) and 5.'6 east-west (93 kpc).*

EDITOR: PLACE FIGURE 2 HERE.

The single-dish observations by L79 found the centroid of the H I to be offset $\sim$ 1.'5 to the west of the optical objects. This appears to be an effect of the presence of the westward arc, which was unresolved by the 9′ and 15′ beams of the Effelsberg and Parkes telescopes. To test this, we smoothed the integrated intensity image from the present DnC array observations with a 9′ Gaussian to replicate the resolution of the Effelsberg observations. This indeed produced a smooth distribution with the peak intensity located $\sim$ 1.'5 to the west of NGC 5291.

A grayscale image of the H I integrated flux from the combined C+D array data is shown in Figure 3. The optical image from the Digitized Sky Survey (derived from a UK Schmidt IIIaJ plate) overlaid with these H I contours is shown in Figure 4. The H I is highly structured on scales at least down to the CnB beam size and many of the concentrations are clearly associated with optical knots.

EDITOR: PLACE FIGURE 3 HERE.

EDITOR: PLACE FIGURE 4 HERE.

The spatial association of the H I concentrations with the larger optical knots is very striking. Figure 3 shows that the H I distribution in the complex is generally clumpy; the

---

[4]Obtained using Skyview; see acknowlegements
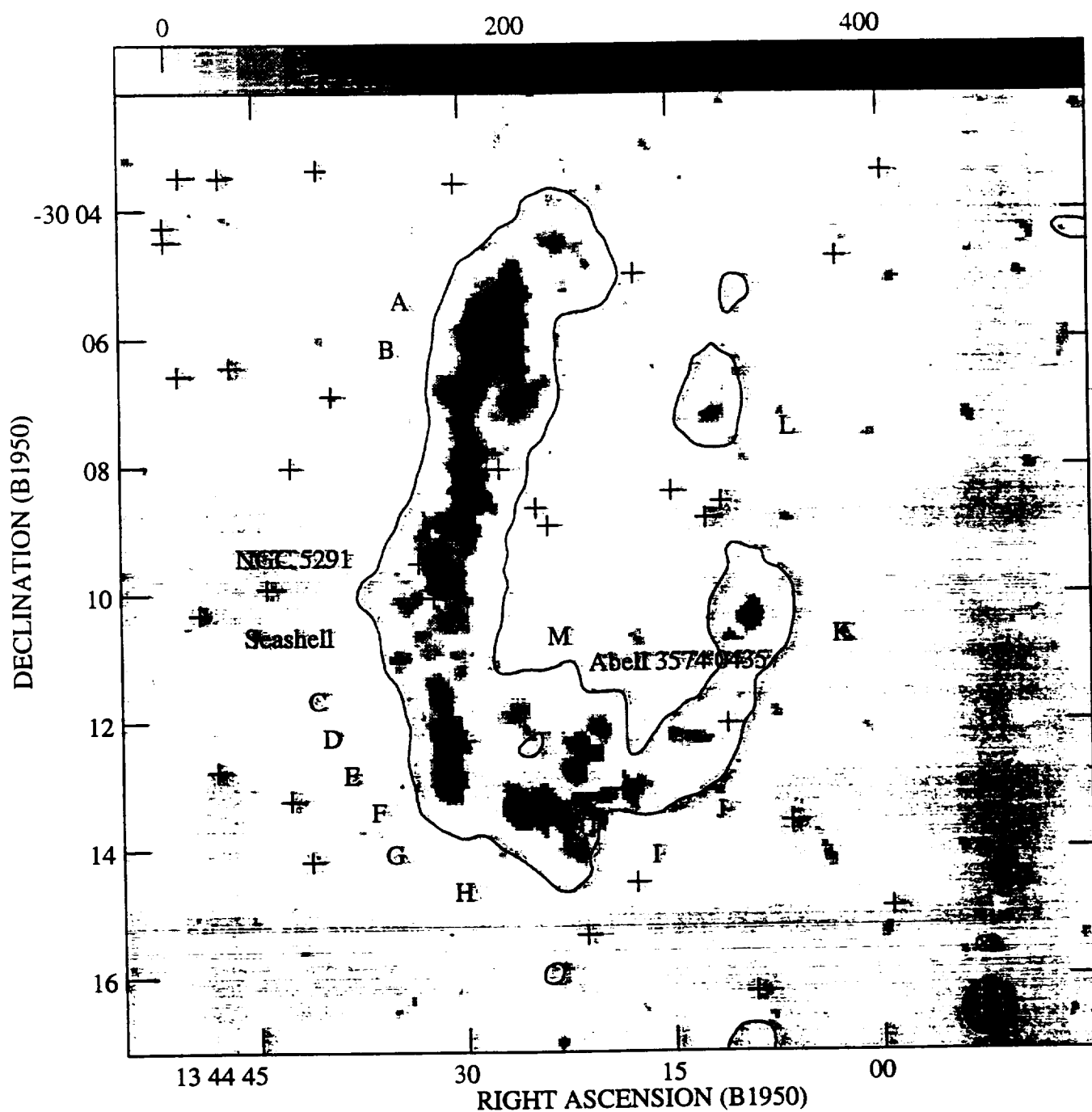
Fig. 2. Grayscale image of HI integrated intensity from BnC array data, with 2σ contour from CnD array data overlaid. BnC array beamsize (14″ × 13″) indicated by upper ellipse in lower right corner; CnD array beamsize (50″ × 39″) indicated by lower ellipse. Crosses indicate objects listed in the HST Guide Star Catalog. Optical knots indicated by letters.
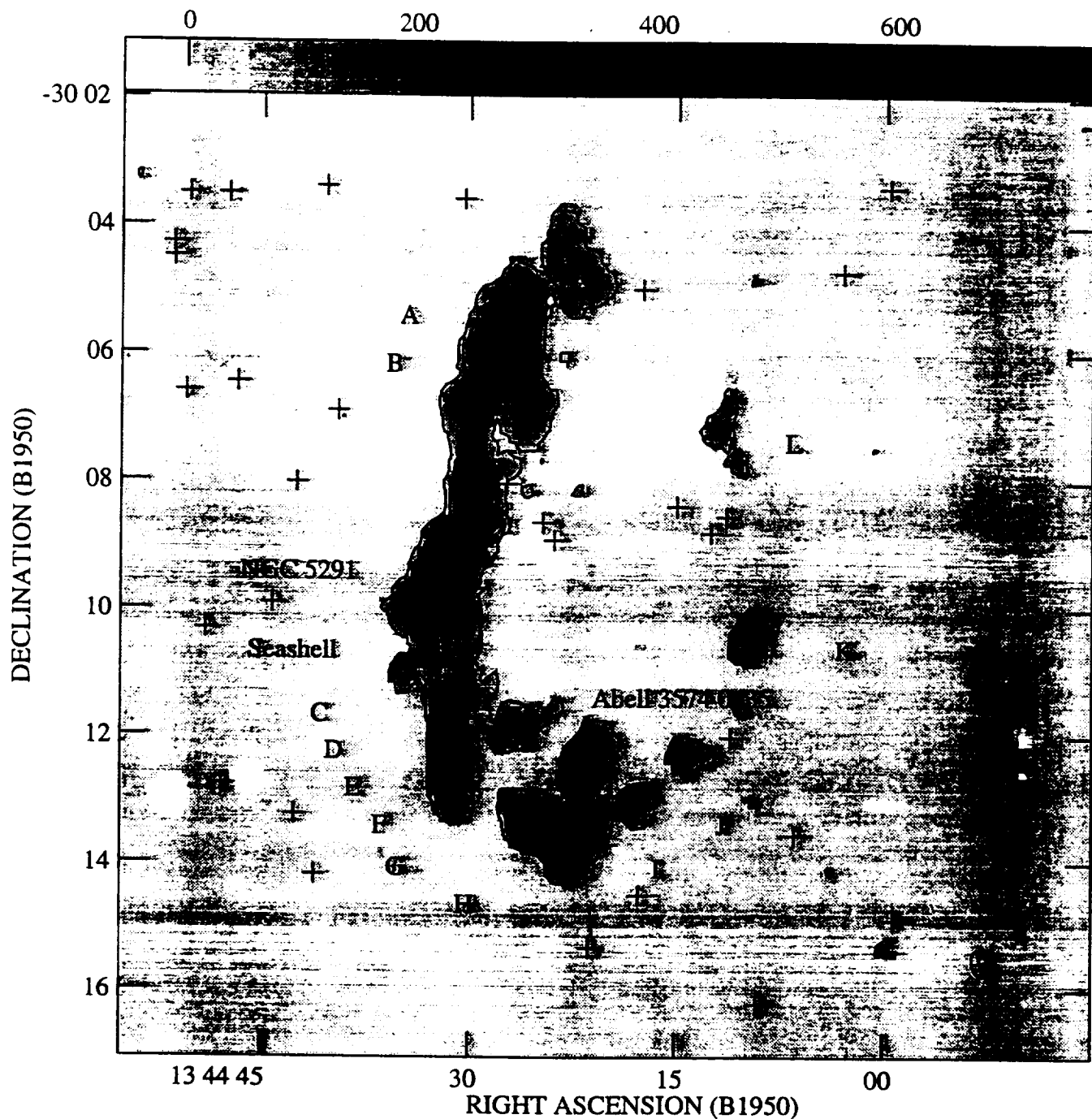
Fig. 3. Grayscale image of the HI integrated intensity from BnC+CnD combined array data. Contour levels are 1.1 (2σ), 5, 10, 15, and 20 $\times$ 10^{20} atom cm^{-2}. The beamsize $(26'' \times 15'')$ is indicated by the ellipse in the lower right corner. Crosses indicate objects listed in the HST Guide Star Catalog. Optical knots indicated by letters.
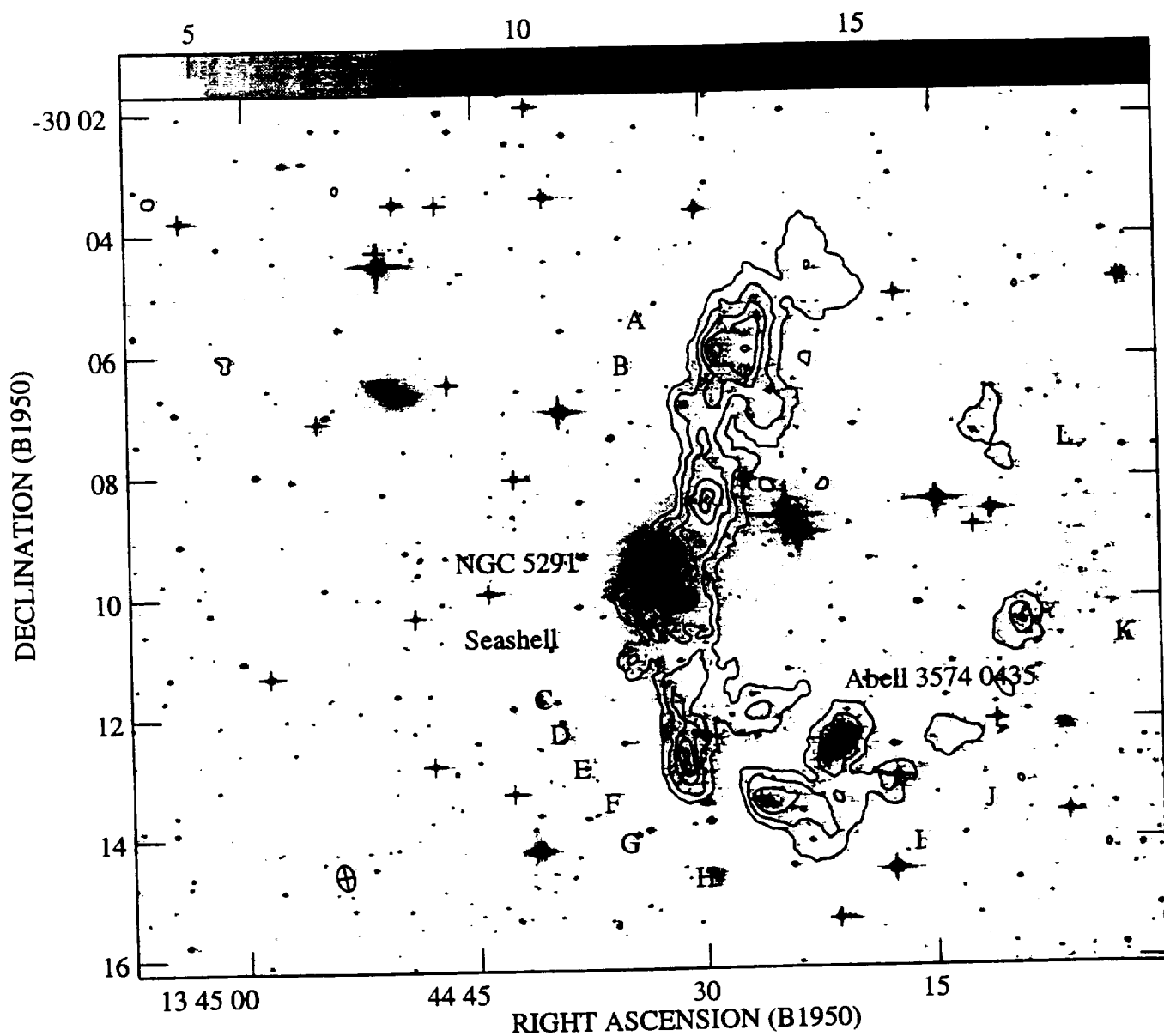
Fig. 4. HI integrated intensity from the BnC+CnD combined array data superimposed over the digitized optical image taken from the UK Schmidt IIIaJ Sky Survey plate. Contour levels are 1.1 (2σ), 5, 10, 15, and 20 $\times$ 10^{20} atom cm^{-2}. The beamsize (26$''$ $\times$ 15$''$) is indicated by the ellipse in the lower left corner. Crosses indicate objects listed in the HST Guide Star Catalog. Optical knots indicated by letters.

amount and location of H I associated with the optical knots observed by L79 are clearly visible in Figure 4. The greatest concentration of H I is associated *not* with NGC 5291 itself, but with optical Knot B. More detailed inter-comparison of the optical and H I images shows that many of the H I features and clumps have underlying optical knots. Several of these – those associated with the H I lying north of Knot A and also to the southwest of Knot B, and possibly with Knot M as well – have been observed spectroscopically[5] and confirmed to be emission line regions (H II complexes) like Knots A to H. The observed H II regions have optical velocities in good agreement with those of the associated H I features (Hawarden *et al.* 1997), while the rest are very similar in appearance in Figure 1 to the confirmed H II complexes.

The existence of the westernmost H I emission, including the concentrations labeled as knots K and L, was not previously suspected; examination of the optical image (Figure 1) reveals faint optical knots coinciding with the H I features I–M as well. Knots I, J, and M appear to be associated with several faint optical features rather than one large one as for the other knots. However, we note that these objects could be chance superpositions of faint background galaxies; spectroscopy is needed to verify these associations.

A strong, highly resolved H I feature (clearly visible in Figure 3) lies ~ 0.5 west of a point about a third of the way from the nucleus of NGC 5291 to the brightest northern knot, B. There is no single bright optical feature underlying this H I concentration, but it does appear to be associated with a swarm of faint optical knots on Figure 1, which also have the appearance of H II complexes.

Some H I, $\sim 20\%$ of the total amount in the system, is evidently associated with the main body of NGC 5291, most of it lying slightly to the west and north of the center of

---

[5]by the late Dr. David Allen at the AAT

the galaxy (Figure 3). The association of this material with the galaxy is confirmed by the correspondence of its flux-weighted systemic velocity, 4370 km s^{-1} (see section 3.3, with that of the galaxy as determined from optical observations (4335 km s^{-1}, L79; 4330 km s^{-1}, Hawarden et al. 1997).

While some H I also lies in a similar projected position relative to the Seashell, this material has a velocity $\sim$ 4380 km s^{-1}, several hundred km s^{-1} too high to be associated with that galaxy (which has $cz = 3950$ km s^{-1}: Duc 1995 or 3730 km s^{-1}: L79; see below). The velocity range covered in the VLA observations is $\sim$ 3590 to 4870 km s^{-1} and includes both these values; however no H I was detected near these velocities. Evidently the Seashell contains little or no H I at present: we derive (see below) an upper limit to its H I mass (single-channel 5σ detection) of 5.7×10^7 $M_\odot$.

Perhaps the Seashell was an H I-poor lenticular, a classification which is consistent with its relatively smooth (if distorted) structure (even on the UV image of L79) and also its moderately red colors (Daly et al. 1987). If any H I it may initially have possessed was located in the outskirts of the system it would probably have been lost in the encounter with NGC 5291, but the apparent absence, anywhere in this system, of detectable H I at the velocity of the Seashell strongly suggests that this was not the case. Using the cooled grating spectrometer CGS4 on the 3.8m UK Infrared Telescope (UKIRT), we have secured a K-band spectrum covering the first overtone ($\lambda = 2.3\mu$m) bandhead of CO in stellar atmospheres. This spectral feature is unusually weak in the Seashell, which implies that it cannot recently have housed a nuclear starburst since strong nuclear CO absorption in the atmospheres of red supergiants is to be expected in the aftermath of such an event. Together with its weak optical emission lines, this further argues against there having been a significant amount of H I in the central parts of the Seashell.

The galaxy located in the southwest part of the overall H I complex is number 435 in Richter's (1984) list of galaxies in the cluster and surrounding area. He classifies it Sc; from Figure 1 we refine this to SA(s)c. Richter gives a heliocentric velocity of 4088 km s^{-1}, strongly suggesting that it is a member of the cluster. While its H I component is well detected on our images among the gas associated with the southern end of the NGC 5291 complex, its velocity is quite different, so that no confusion arises. Evidently Richter 435 has no connection with the NGC 5291 complex.

Five arc-minutes to the northeast a second prominent galaxy is also included in the VLA primary beam but is not detected in H I. This is a barred spiral listed as number 446 by Richter, who gives a radial velocity of 4409 km s^{-1}, in excellent agreement with the L79 velocity of 4420 km s^{-1} and a more recent AAT velocity of 4414 km s^{-1}; its velocity is clearly close to that of NGC 5291. Richter classifies this system Sd, which suggests that it should be H I-rich and should have been detected in our images. However, scrutiny of Figure 1 shows a generally smooth structure, except for some curious lateral spurs attached to the bar, suggesting that R446 is actually a lenticular or very early spiral: we propose a classification R'SB(s)0/a. Such a system would be quite likely to contain little H I.

Figure 5 shows the radio continuum emission as determined from those channels free of line emission. There is continuum emission associated with the optical body of NGC 5291 as well as that of Knot B which is presumably due to ionization from O and B stars. The low level (3σ) of the detected emission precludes quantitative analysis.

EDITOR: PLACE FIGURE 5 HERE.
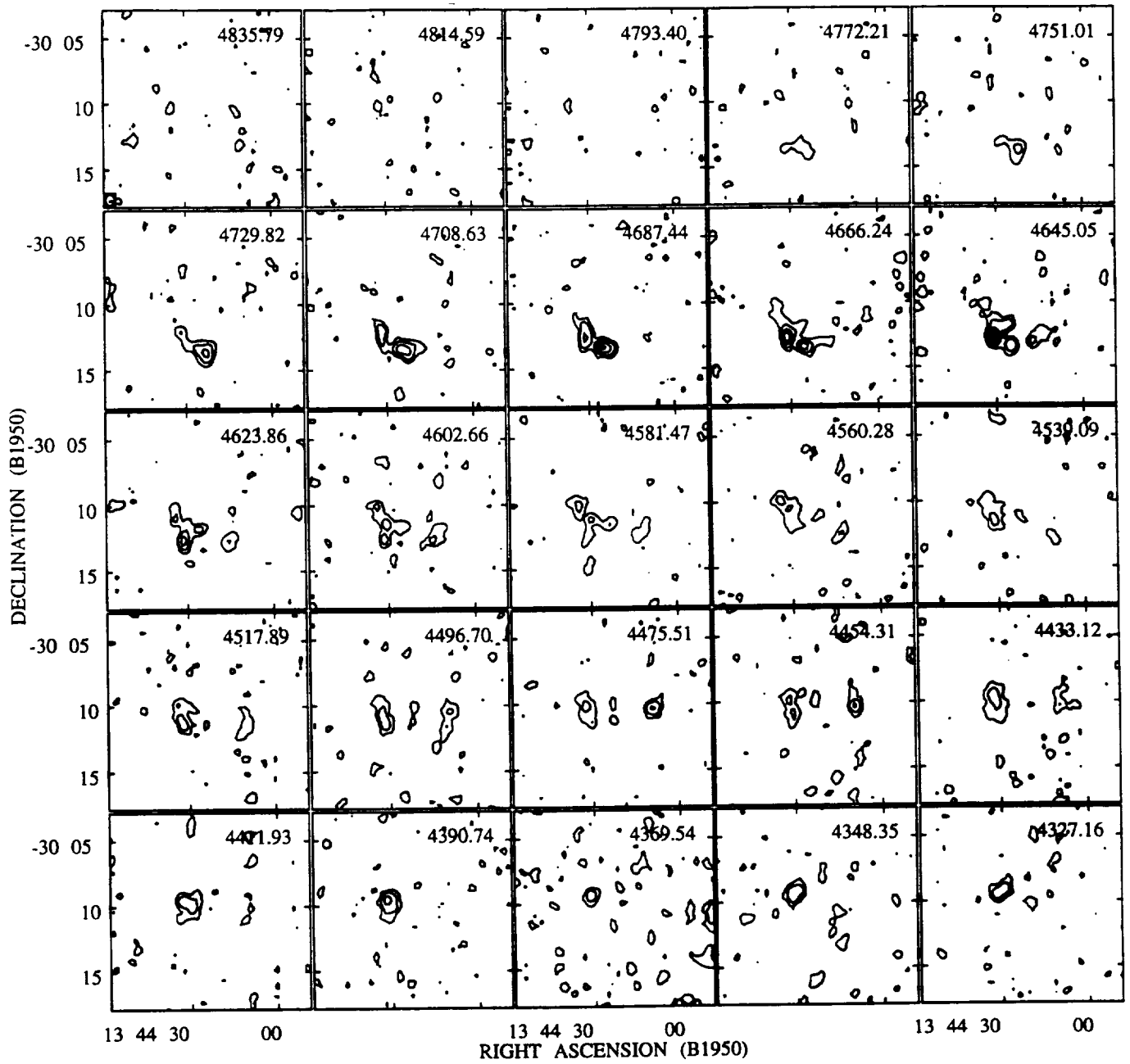
Fig. 5a. Individual channel maps produced from the CnD array observations. Contour levels are at 2, 5, 10, 15, and 20σ. Heliocentric velocities are listed in the upper right of each image.
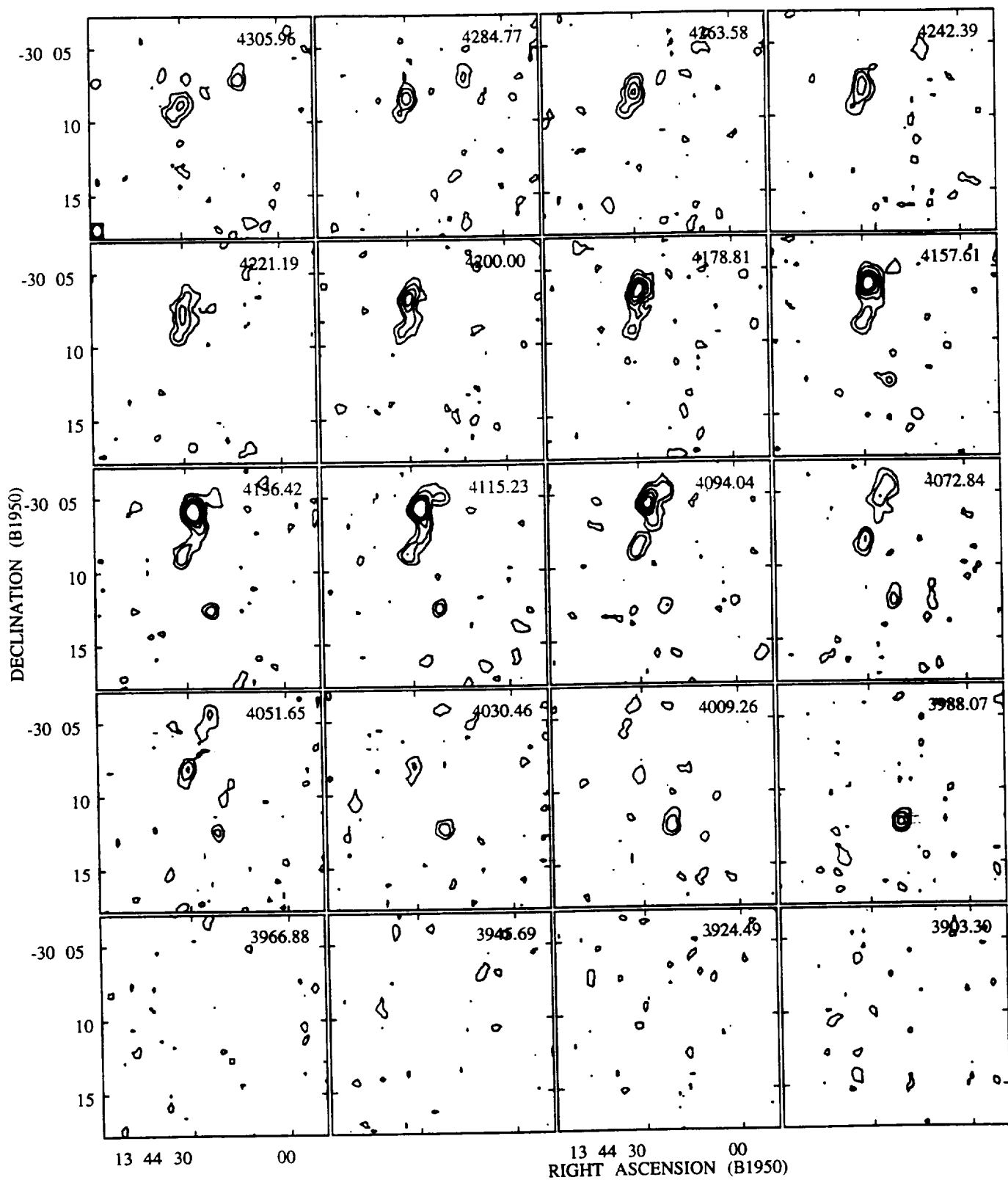
Fig. 5b. Individual channel maps produced from the CnD array observations. Contour levels are at 2, 5, 10, 15, and 20σ. Heliocentric velocities are listed in the upper right of each image.

3.2. H I Column Densities and Masses

Figures 2 and 3 represent the integrated intensity (column density) of the H I flux from the system. The column density of the H I along the line of sight for a given position (α, δ) may be determined for a source by integrating the brightness over all velocities using the following expression (Mihalas & Binney 1981):

$$N_{\text{HI}}(\alpha, \delta) = 1.82 \times 10^{18} \int_{-\infty}^{\infty} T_{\text{B}}(\alpha, \delta) \, dv, \tag{1}$$

where T_{B} is the brightness temperature in Kelvin and v is the velocity in km s^{-1}. The peak column densities found for the identified features (the galaxies and knots) on the moment maps are listed in Table 3. These values were determined using the DnC array data, which is most sensitive to extended emission. The highest column density in the entire complex, 12.6×10^{20} atoms cm^{-2}, is associated with Knot B. The peak column densities for NGC 5291 and the H I Concentration are 10.7×10^{20} and 10.6×10^{20} atoms cm^{-2}, respectively. Peak column densities for the rest of the labelled knots range from 1.4×10^{20} to 7.4×10^{20} atoms cm^{-2}. The detection threshold (2σ level) is 1×10^{20} atoms cm^{-2}.

The integrated flux from the H I gas may be found by integrating equation (1) over the solid angle subtended by the feature, and expressing the brightness temperature in terms of the observed flux $S(\nu)$. The H I mass may then be calculated as follows (Mihalas & Binney 1981):

$$M_{\text{HI}} = 2.36 \times 10^{5} \, D^2 \int_{-\infty}^{\infty} S(v) \, dv, \tag{2}$$

where M_{HI} is expressed in solar masses, D is the distance in Mpc, $S(v)$ is the flux in Janskys summed over the area of the feature, and v is velocity. The areas used to determine the masses for each knot are indicated in Figure 6, and the corresponding calculated H I masses are listed in Table 3.

EDITOR: PLACE TABLE 3 HERE.

EDITOR: PLACE FIGURE 6 HERE.

The H I masses associated with Knot B and the H I Concentration are roughly comparable: 2.48×10^9 $M_\odot$ and 2.03×10^9 $M_\odot$ respectively. The H I mass associated with NGC 5291 is 1.60×10^9 $M_\odot$. This value represents only 21% of the total H I mass of the complex (see below); *over three-quarters of the total H I mass is located in the extensions.* The H I masses of the other knots range from 7×10^7 $M_\odot$ to 9×10^8 $M_\odot$ (Table 3).

The total H I mass detected with the VLA for the entire complex is 1.80×10^{10} $M_\odot$. This is approximately 36% of that detected in the single-dish observations by L79 (Table 1). Our estimate does not include the H I mass of Abell 3574 0435 (9.92×10^8 $M_\odot$) which must have been included in the large beams of the telescopes at Parkes (15′ FWHM) and Effelsberg (9′) used by L79. This would only add 5% to the total H I mass, however, and so cannot account for the discrepancy.

It is well known that single-dish spectra are prone to substantial instrumental effects that make them unreliable for weak extended emission-line spectra. The Effelsberg data may be an overestimate of the H I present. Employing a very wide bandwidth, L79 were observing for broad and weak spectral features, which is notoriously difficult with an autocorrelation receiver. Indeed the data taken by the Parkes radio telescope were not used for this reason. Baseline curvatures can add to or subtract from apparent line strengths, especially on very broad lines such as that from the NGC 5291 complex. It is therefore possible that the discrepancy between the masses determined from the VLA and single-dish observations is somewhat less than reported. It is questionable, however, whether the entire difference between the VLA and single-dish fluxes could be attributable to baseline errors. Examination of the H I spectra in L79 suggests that an overestimate of around 40% is the most that could reasonably be attributed to an unrecognized baseline rise around the systemic velocity of 4400 km s^{-1}. New, high-sensitivity single-dish observations, secured

with a system having stable baselines and a beam at least as large as that set by the VLA minimum spacing, would clearly be most valuable to resolve this problem.

There are four possibilities for accounting for the "missing H I", more than one of which could be simultaneously true. The single dish measure could indeed be a 30% to 40% overestimate, as discussed above. It is also possible that some of the H I could be so extended in velocity and/or space as to fall below the surface density detection threshold of the observations. We note, however, that if the "missing mass" were to fill in the ring, then the H I surface density would be approximately 2.0×10^{21} cm^{-2}, which is well above the detection threshold of the DnC array.

3.3. Kinematics

Individual velocity channel maps of the D array data in a $15' \times 15'$ area are presented in Figure 7. It is clear that H I in the NGC 5291 complex has an overall ordered velocity structure, with velocities varying (for the most part) in a regular manner from low values in the north to high in the south.

EDITOR: PLACE FIGURE 7 HERE.

The cumulative velocity field of the gas can be determined by calculating the intensity-weighted mean velocity of the gas at each position (α, δ). This is accomplished by taking the first moment of the column density relationship (equation 1) with respect to velocity as follows:

$$\langle v(\alpha, \delta) \rangle = \frac{\int_{-\infty}^{\infty} T_{\mathrm{B}}(\alpha, \delta)\, v(\alpha, \delta)\, dv}{\int_{-\infty}^{\infty} T_{\mathrm{B}}(\alpha, \delta)\, dv}. \tag{3}$$

Figure 8 shows the first moment map of the complex. The isovelocity contours are separated by 25 km s^{-1}. The wide N – S velocity range is evident. The maximum velocity,

in the south of the complex, is 4750 km s^{-1}; the minimum, in the north. is 4040 km s^{-1}, giving a (large) total velocity range of 710 km s^{-1}. The flux-weighted heliocentric velocity of the gas associated with NGC 5291 itself is 4370 km s^{-1}, whereas that for the entire complex is 4406 km s^{-1}. The difference in the flux-weighted velocities show that the gas density is not symmetrically distributed in velocity space with respect to the galaxy.

The velocity structure, though necessarily simplified in this figure by averaging, nevertheless shows considerable complexity just north and south of the main body of NGC 5291: here the isovelocity contours are much closer-spaced than in the outlying regions, and considerable E–W velocity shear across, e.g. the H I Concentration of Figure 2 is also apparent. The overall behavior is not very dissimilar to that which would be expected from a galaxy seen edge-on, but with additional complexities.

The general velocity trend apparent in the main, eastern arc of H I is also visible in the western arc as well, but here the gradient appears roughly linear overall. The velocity of the (northern) knot L in the western arc is $\sim$ 145 km s^{-1} higher than the H I in the eastern arc at the same N-S position. In the southern part of the western arc, an opposite trend is (barely) apparent: knots J and K have (average) velocities $\sim$ 60 and 50 km s^{-1} lower than the H I in the corresponding parts of the eastern arc.

EDITOR: PLACE FIGURE 8 HERE.

The spatial distribution of the velocity dispersion of the H I is shown in Figure 9. The velocity dispersions are calculated for each position by taking the second moment of equation 1 with respect to velocity:

$$\sqrt{\langle v^2(\alpha, \delta) \rangle} = \sqrt{\frac{\int_{-\infty}^{\infty} T_{\rm B}(\alpha, \delta)\ (v(\alpha, \delta) - \langle v \rangle)^2\ dv}{\int_{-\infty}^{\infty} T_{\rm B}(\alpha, \delta)\ dv}}. \tag{4}$$
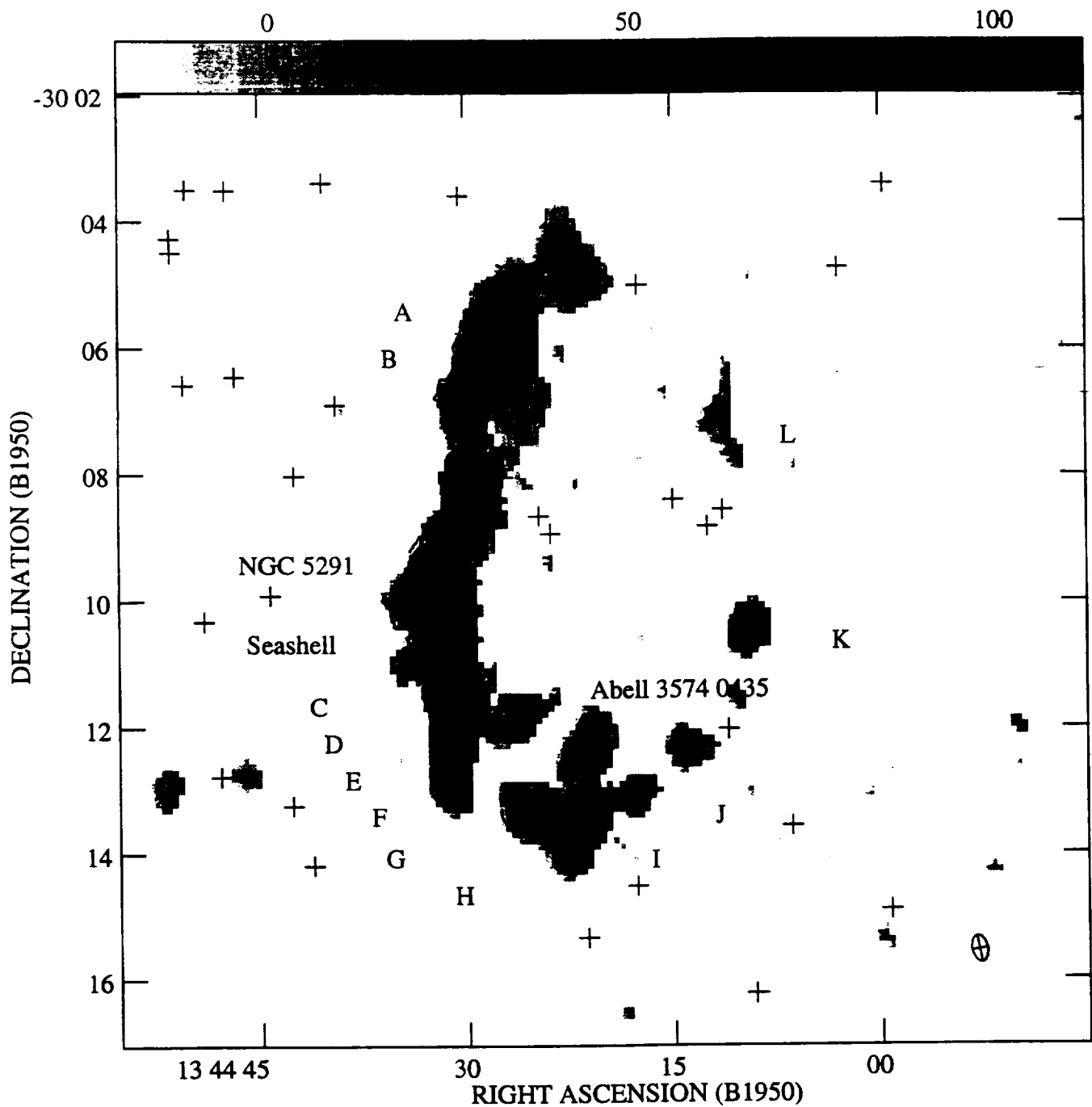
Fig. 7. Isovelocity contours superimposed on the velocity dispersion image (second moment map) produced from the BnC+CnD combined array observations. The contours are 10, 25, 30, 50, 75, 100 km s^{-1}; the velocity resolution is 21 km s^{-1}.
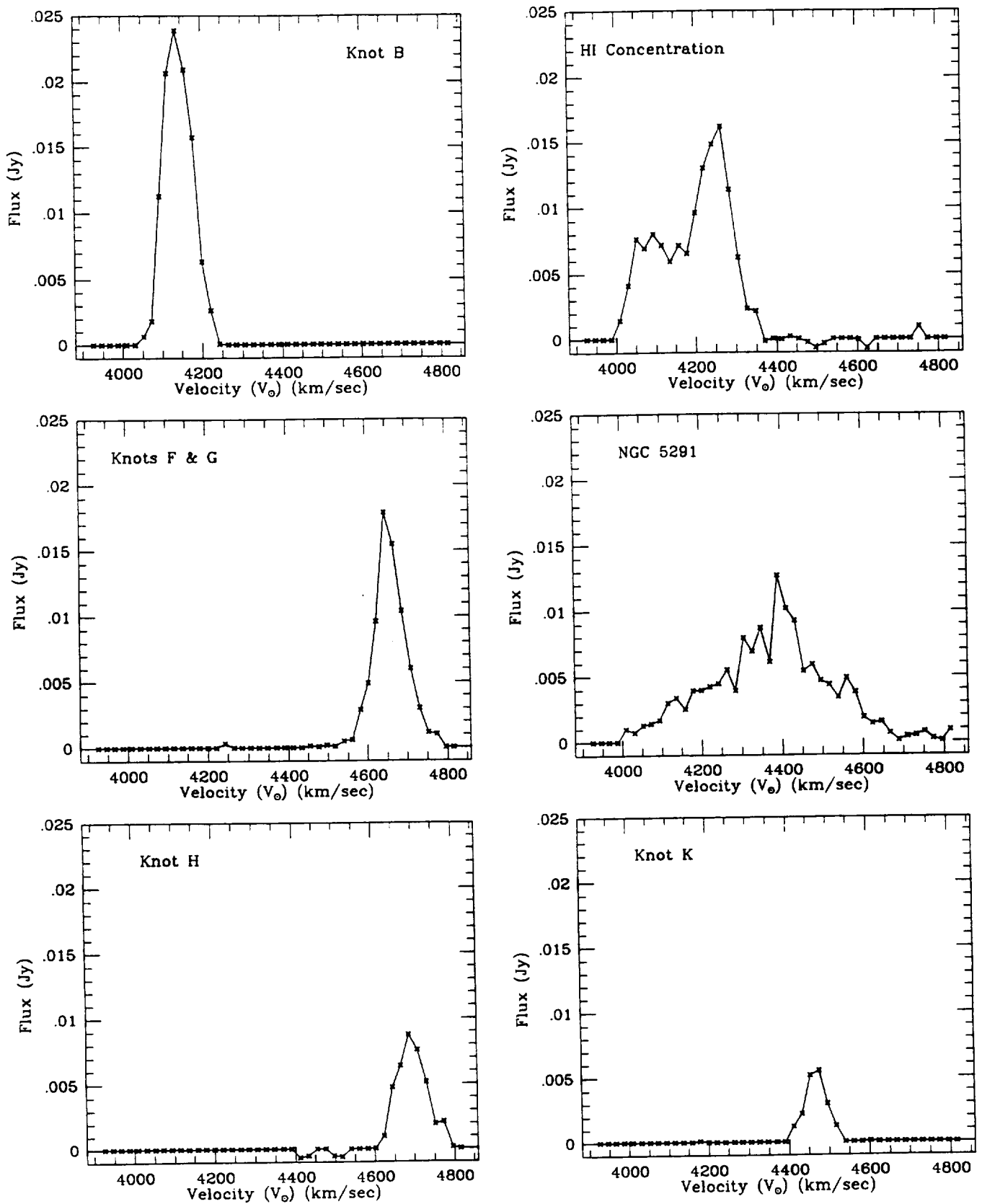
Fig. 8a. Velocity profiles for components of NGC 5291 complex. Vertical axis (flux in Janskys) drawn to same scale for all six objects, with a peak flux of 0.025 Jy.
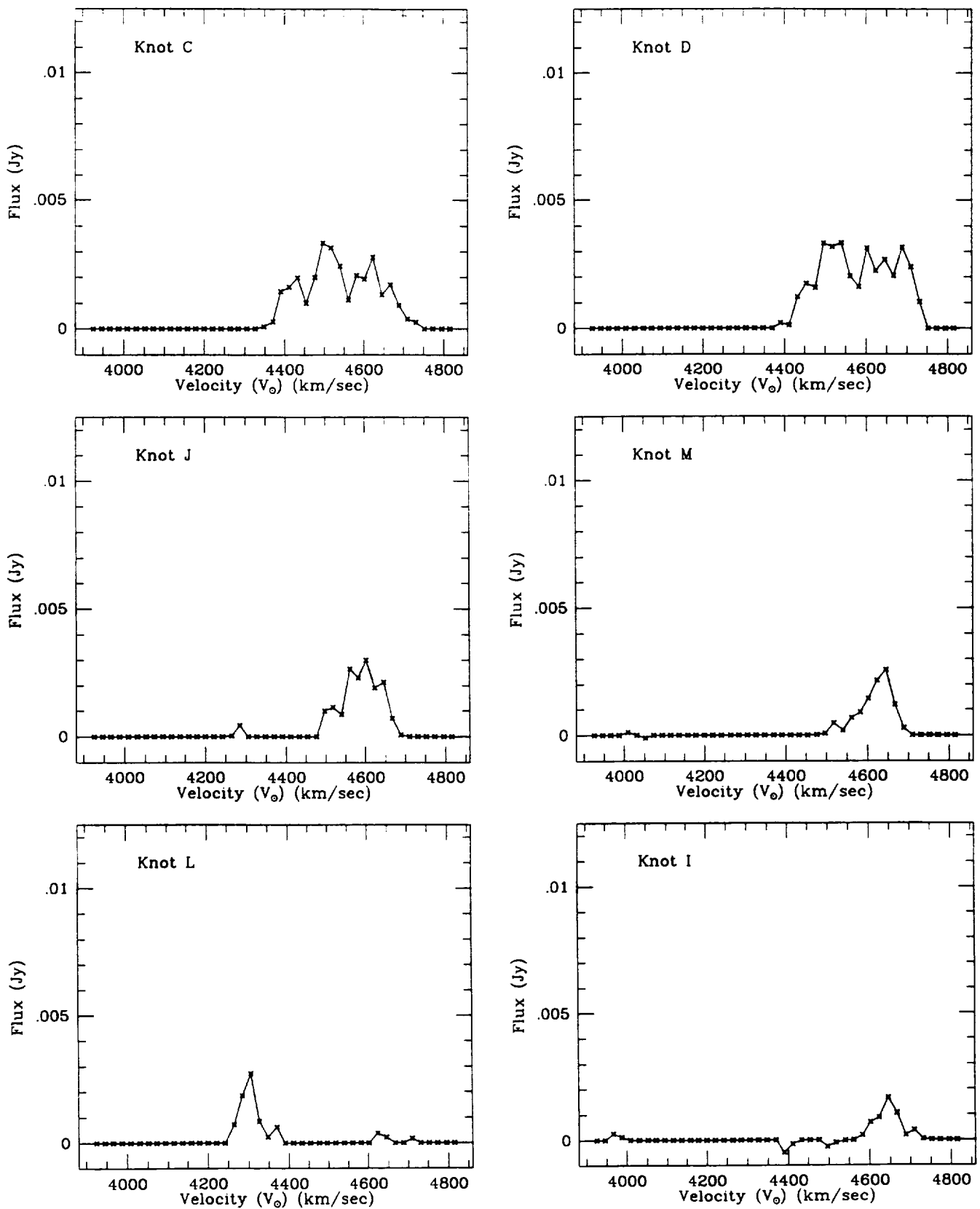
Fig. 8b. Velocity profiles for components of NGC 5291 complex. Vertical axis (flux in Janskys) drawn to same scale for all six objects, with a peak flux of 0.0125 Jy. Note that the vertical scale is therefore half of that used for Fig. 8a.

EDITOR: PLACE FIGURE 9 HERE.

It can be seen in Figure 9 that there are two regions of very high dispersion, on the order of 100 km s^{-1}. These regions, one encompassing both NGC 5291 and the H I Concentration, and one associated with Knot D, imply the presence in the line of sight of bodies of gas with widely ranging velocities (see Figure 11). These are further discussed below.

4.   Discussion

4.1.   Physical Nature of the System

The obvious, strong, distortion of the Seashell, presumably by interaction with NGC 5291, immediately suggests that the far-flung outlying structures in the system were caused by tidal effects from this interaction. However the large velocity difference between the two galaxies measured by L79 (640 km s^{-1}), and its apparently retrograde sense, made the great amplitude of the resulting disruption difficult to understand in terms of tidal effects. This led them to seek alternative hypotheses for the origin of the outlying features.

Since the major problem with the tidal disruption scenario was the difficulty of moving so large a mass of material to such large radii they hypothesized, instead, a pre-existing, very extensive, and presumably primordial H I disk. This was a logical extrapolation of the properties of several other H I-rich early-type systems listed by L79, and analogous to the then-undiscovered Malin 1 (Bothun *et al.* 1987; see also Sprayberry *et al.* 1995 for more details of the properties of this class of galaxies).

Longmore *at al.* then proposed two trigger mechanisms for the intense but localized star formation activity seen in the outlying complexes. The first suggestion was that NGC

5291 has suffered an almost orthogonal, off-center, penetration by a companion galaxy (though probably not the Seashell) which has caused an eccentric kinematic density wave to propagate through the disk, producing a ring galaxy with offset nucleus (see, e.g., Lynds & Toomre 1976; Theys & Spiegel 1976). They tentatively identified Richter 446 (to the northeast) as a potential culprit, but did not pursue the hypothesis because the ring was incomplete.

The second trigger mechanism was suggested to L79 by the location of NGC 5291 in the outskirts of a galaxy cluster, the concentration of the H II complexes in an arc convex toward the cluster and centered on the galaxy and by the westward offset of the centroid of the H I emission. These led L79 to speculate that the postulated H I disk is being ram-swept, more or less from one edge, as the galaxy moves mostly eastwards through an intracluster medium, and that it is this process which has triggered star formation, by compression of the previously too-tenuous H I disk.

We have noted that the H I offset, at least, now appears to reflect the detailed distribution of the gas as seen at low resolution. The kinematics, but especially the morphology of the H I in this system as revealed by the higher resolution VLA data presented here, encourage us to reinstate as a possible scenario the original interpretation of the outlying features as the products of tidal disruption consequent on an encounter, most likely with the Seashell. The ring-arc seen in the H I may represent tidally removed debris along the path of motion of the component galaxies of the system, similar to the Magellanic stream. Alternatively, the arms, counter-arms and bridges of an interaction, first discussed by Toomre & Toomre 1972 are seen at very large projection.

We also note that the western H I arc repairs the "incomplete ring" noted by L79 as evidence against a possible orthogonal penetration by some galaxy other than the Seashell. As they suggested, Richter 446 is the most probable candidate as it does appear poor in gas

and possibly disturbed, as might befit a system which has passed though, and been swept clean by, a giant neighbor.

In the rest of this section we discuss the case for ram-sweeping, and revisit the "primordial disk" and "tidal disruption" scenarios for the creation of the outlying complexes in the NGC 5291 system, and thus of the candidate "young galaxies" lying within them. There is supporting evidence for both creation models, as well as for ram-sweeping. Each of the two formation scenarios, however, has limitations based on analysis of the existing optical, radio, and x-ray data.

4.1.1. Ram Sweeping

As NGC 5291 is located in the northwest part of the Abell 3574 cluster, ram-sweeping would be expected to produce compression along the leading (east) edge, assuming that the system is moving toward the center of the cluster, located to the southeast. On all hypotheses one would expect to find that the star formation regions (SFRs) are associated with H I concentrations. If ram-sweeping is occurring, one further expects that since the SFRs are presumably of higher density than the less concentrated H I the latter will tend to be displaced in tail-like structures trailing "downwind" from the SFRs. Furthermore one expects the density gradient of the H I to be steeper on the side towards the compressing wind than on the opposite side.

The gradient in the H I distribution is indeed higher on the eastward edge of the *east* side of the ring-arc (Figure 4), which provides some evidence that compression of the eastward edge of the H I is occurring, at least on the east side of the complex. The distribution of the H I around the H II complexes (SFRs) B and H, in particular, exactly fulfills the predictions of this scenario for ram-sweeping by a flow from the east: the densest

H I lies on or slightly west of the optical features, the H I density gradient is steeper to the east and shallow, and the H I much more extended, to the west. These effects are also present in the complex south of knot B: to the east a "prow" of H I wraps steep density gradients close around a knotty optical feature but tapers more gradually to the west. However, we note that this sweeping to the west does *not* appear to be true for the knots in the western arc (particularly K and L), which show a slightly higher density gradient on their *western* edges.

Further evidence that ram-sweeping is operating may be indicated by the slightly asymmetric distribution of the atomic hydrogen in the vicinity of the optical body of the galaxy. As seen in Figure 4, the gas appears to extend farther to the west of the optical emission than to the east, which is expected if the H I is being swept to the west.

To examine further the validity of ram-sweeping, Hawarden *et al.* 1997 have obtained x-ray images of NGC 5291, first with the Einstein Observatory's Imaging Proportional Counter (IPC) in 1980 and then with the ROSAT High Resolution Imager (HRI) in 1996. An archival observation of the super-Seyfert galaxy IC 4329A with the ROSAT Position-Sensitive Proportional Counter (PSPC) (now defunct) is also available. It was expected that if ram-sweeping was indeed occurring to a significant extent, density enhancement (and possibly, if the galaxy is moving supersonically, heating) of the ICM "upstream" of the H I should result in enhanced x-ray emission from just ahead of the H I being swept. Possible ablation effects were also anticipated.

In fact NGC 5291 is a quite prominent extended x-ray source. Although the resolution (2.'6) is not sufficient to examine the distribution of the x-ray emission in detail, the Einstein image (Figure 10) shows a source coincident with the galaxy and possibly extended N-S along the H II complexes and an apparent "tail" to the west, as might be associated with ablation by a westward flow. The north-south extent of the x-ray emission is approximately

7′, somewhat smaller than the 10′ extent of the H I gas. Compression of the x-ray emission along the eastern edge is also evident.

EDITOR: PLACE FIGURE 10 HERE.

The ROSAT images (Hawarden & Chaytor 1997, Hawarden *et al.* 1997) have confirmed some, but not all, of this impression. While there certainly exists extended emission which may be spatially associated with the H II complexes to the north of NGC 5291, several (variable) sources underly the "tail" seen in the Einstein image; when these are removed the tail is reduced. The ROSAT images lie to the *west* of the H I and H II complexes to the south of the galaxy.

4.1.2. Large H I Disk Model

Longmore *et al.* concluded from both the optical and H I velocity field that the complex of knots and the H I itself were entirely associated with NGC 5291. As noted above, their interpretation therefore was that of a low luminosity S0 galaxy surrounded by a large (160 kpc) primordial H I disk, similar to the then-unknown Malin 1. Their estimate of the total mass in the NGC 5291 system, assuming it was a disk in keplerian rotation, was $\gtrsim 9 \times 10^{11}$ $M_\odot$, making it one of the most massive systems then known.

As set out above, this scenario supposes that the outlying star-forming regions in NGC 5291 have been produced by local compression of the H I disk by the ram-sweeping process, giving rise to instabilities and collapse of large bodies of gas to form the H II complexes now observed in the optical.

The overall kinematics of the gas in the system, as seen in Figure 8, could be consistent with a heavily disturbed massive rotating disk centered upon NGC 5291. The eastern

gradients seen in both the H I and x-ray data, as well as the x-ray "tail" to the west are also consistent with a ram-swept disk system.

The previously unsuspected ring-arc morphology of the H I complex may argue against the existence of a large disk however. As discussed in section 3.2, above, no atomic hydrogen was found "filling in" the ring-arc. The association of the westernmost knots (I-L) is also difficult to understand if the NGC 5291 complex is to be interpreted as a large disk. Compression and subsequent knot formation along the *trailing* edge are then difficult to explain, although it is *possible* that the western arc traces out a (large!) spiral feature.

There is also evidence that the gas associated with the NGC 5291 system is not primordial. Metallicity measurements of the gas in the knots, approximately one-third solar (Duc 1995, Hawarden *et al.* 1997), is higher than expected for primordial material, and indicates enrichment from prior star formation. Either the knots formed from pre-enriched material such as found in the outer parts of actively star-forming spiral galaxies, or there has been self-enrichment occurring in the vigorously star-forming optical knots. This last would increase the metallicity of the gas to an extent dependent upon the amount of mixing in the object (i.e. from stellar winds, etc).

4.1.3. Interaction Model

Although in many ways the NGC 5291 complex does not closely resemble a "classical" interacting system, many properties of the extensions could be consistent with the scenario attributing their properties to a tidal origin. The most striking evidence is the optical morphology of the system. As stated above, the Seashell, with its strongly distorted disk and sharply-defined, curved southwestern edge is evidence that an interaction could be of importance, since one is certainly affecting (or has recently affected) this galaxy. Its

projected position close to NGC 5291 makes the latter the logical candidate to have caused the disruption, and thereby to have been disrupted in its turn to produce the outlying features (though we cannot use these to support the identity of NGC 5291 as the disrupter without prejudging the issue of their origin).

NGC 5291 itself *may* show the beginnings of a faint optical "tail" and dust lane extending to the north and slightly west, opposite to the position of the Seashell, although it is just as likely that these features may instead be part of a spiral arm. If they are tidal in origin however (i.e. it is a "tail" and not an "arm"), this type of morphology, delineated by tidal arms opposite a companion, with long patchy tails and scattered clumpy debris resembling dwarf galaxies, could be consist with a high velocity grazing interaction (Elmegreen *et al.* 1993).

Most of the features of the H I distribution detailed in these observations could probably be explained in terms of an interaction. Over three-quarters of the total H I mass is found in the extensions. The Seashell either is a gas free system or has been stripped of its atomic hydrogen, and there is more gas associated with the H I Concentration and with Knot B than with NGC 5291 itself. These characteristics are similar to those seen in NGC 7252 (Atoms-for-Peace) and NGC 3921, as reported by Hibbard & van Gorkom 1996. They examined a sequence of interacting/merging galaxies, and found that the more evolved the interaction, the lower the percentage of H I associated with the bodies of the parent galaxies. They also reported substantial offsets between the H I and the optical structures of their systems, and found that in the latest stage, essentially all the atomic gas was located in the tidal extensions.

In addition to the optical and H I morphologies, the one-third solar metallicity of the gas in the knots is consistent with that expected in material stripped from the outer disk of a gas-rich system with an active star-forming history (although note the caveat about

self-enrichment mentioned above). The H II regions in the tails of the Antennae (NGC 4038/39) also have metallicities about one-third solar (Mirabel *et al.* 1994).

The kinematics of the gas (Figures 7 and 8) may also consistent with an interaction-dominated system. Interactions commonly produce plumes with monotonic slowly-increasing velocities away from the main bodies, especially if the the material in the plumes is escaping, so that the outermost features are not returning to the systemic velocity as occurs in "bound" plumes like those in NGC 7252 (Figure 4 of Hibbard *et al.* 1994). In an interaction, orbital decay occurs as energy is transferred from the galaxies to their particles. The particles receive energy and angular momentum from the relative motion of the passage, which produces the tail-like structures and orbital decay. The tails produced by these encounters move radially away and fan outwards from the parent systems and the velocity increases along the tail. At the base, the tail particles are more tightly bound, turn quickly in their orbits and fall back towards the remnants. The more distant matter is less tightly bound and falls back more slowly, if at all. This monotonic increase in velocity along the tail is a prominent feature of the H I structure in the NGC 5291 system. The relative velocity reaches a maximum, and then as the feature arcs to the NW and SW, the line-of-sight velocity component decreases as the tangential motions become more important. The velocity map (Figure 8), for example, quite closely resembles that of the merger NGC 4676 in Figure 13 of Hibbard & van Gorkom 1996. In NGC 5291 the reducing velocity differences of the material in the western arc could also perhaps be ascribed to the slowing of bound material as in NGC 7252, although it is also consistent with the velocity contours which might be expected if the western arc were an H I feature delineating the edge of a distorted disk.

We can draw some additional conclusions about the issues to be considered if the interaction scenario is to be verified. As noted, from the optical image the most obvious

candidate for the partner in this destructive minuet, owing to its contorted shape, is the Seashell. However, as first noted by L79, it is difficult to support this model if the passage is retrograde. The construction of tidal tails is most pronounced if the victims rotate in the same direction as the passage, and is further enhanced if the latter is roughly coplanar with the disk of the victim (i.e. the closer the alignment of the same-sign angular momentum vectors of the participants, the greater their disruption of one another). Such a prograde (but not necessarily coplanar) passage is needed to produce the morphology we observe in the NGC 5291 system. However, the Seashell appears to be approaching the observer in the region for which the H I in the system is receding. Therefore, a prograde orbit requires a special orientation for the NGC 5291-Seashell interaction, and one with a high velocity passage. It is clear that careful modelling (along the lines of that discussed by Barnes 1994 and Hibbard & Mihos, 1995 will be required to clarify the possibility of constructing a successful scenario.

Alternatively, the Seashell may not be the culprit here. In addition to the orthogonal interaction/ring-galaxy hypothesis put forth by L79, M. Balcells (1996, personal communication) has suggested that Knot B is an irregular that has entered the system at almost the escape velocity and is now spiraling into the center of NGC 5291; perhaps it was a satellite to the Seashell. Such a model has many resemblances to the relation between M31, the Milky Way, and the LMC (Lynden-Bell 1994). The dense H I distribution shown in Figure 3 looks very much like a trail of debris torn from a system dominated by the Knot B complex. Much of the ring-arc might denote the orbit of the passage, although the amount of H I involved is considerable, possibly one-half the total mass. The projected difference in velocity between Knot B and NGC 5291 is 185 km s^{-1} and the projected separation is 61 kpc. This would be a bound system if the mass of NGC 5291 were several times its calculated (minimum) value (section 4.2). However, even one deeply plunging passage could be extremely damaging if not totally destructive to the "magellanic" system.

If, however, this system has been produced by an interaction between NGC 5291 and the Seashell, some of the specifics can be inferred from the velocity field. The relative velocity between NGC 5291 and the Seashell is either approximately 450 km s^{-1}(Duc 1995) or 630 km s^{-1}(L79), and the projected separation is 10.7 kpc (L79). Using the lower value, the mass necessary to gravitationally bind the Seashell and NGC 5291 is then 5×10^{11} $M_\odot$. The indicative (keplerian) mass for NGC 5291 is 1.5×10^{11} $M_\odot$ (see section 3.2, below), which is a factor of 3 less than this binding mass. However, there are the usual uncertainties associated with the unknown orbital phase terms and inclinations to the line of sight which easily bracket this figure. Furthermore, Barnes (1994) shows that the overall dynamics of encounters are largely controlled by the extended dark halos of the systems. As part of the interaction, dark halos transfer angular momentum and energy, imparting spin and raising broad tidal features. It is this halo interaction that brings about the merger and extracts luminous tails from galactic disks. In the models considered by Barnes, the ratio of halo to disk masses is 5:1, which is within the range of corrections to visible masses found by van Moorsel (1987) in a study of binary galaxies. Given all the uncertainties, we believe that it is entirely possible that the Seashell and NGC 5291 are bound and merging.

While somewhat suggestive of the debris fields produced in some galaxy encounters, the optical image (Figure 1) alerts us to the unusual nature of this system. Although appearance is dependent on both geometry and viewing angle, the complex shoals of objects (known to be H II regions) to the north and south of the main body in Figure 1 do not *closely* resemble the tails and countertails seen in canonical interacting or merging galaxies such as the "Antennae" NGC 4038/9 and the "Atoms for Peace" galaxy NGC 7252 (e.g. Hibbard & van Gorkom 1996). Nor, indeed, does this system closely resemble any of the systems in the atlases of Arp 1966 or Arp & Madore 1987.

The classical interactors produce tails and countertails which are relatively narrow

and quite smooth, sometimes studded along their lengths "string-of-pearls" fashion with a number of condensations, often H II regions, which generally number a dozen or less and are quite inconspicuous compared to the continuous structure. In the NGC 5291 complex, in contrast, there is little continuous structure discernable beyond the visible galaxy. There are perhaps two faint features extending $\sim 1\rlap{.}'5$ to the SSE and, reinforced by an inner dust lane to resemble a weak spiral arm, slightly west of north (Figure 1), but these do not underlie the main swarms of H II knots. It may also be noted that the H II knots in NGC 5291 are mostly not arranged in a line (except, perhaps, to the south between D and G), but appear to be spread out laterally (i.e. knots H through M: the western arc) much more than is usual in the long filamentary arms and tails in the classical interactors. A final discrepancy is evident in the unusually large *number* of the H II knots.

The energetics of the gas in the NGC 5291 system imply that a significant fraction of the gas is unbound (at 20 kpc ($72''$)) unless the galaxy contains a massive halo. The escape velocity is about 255 km s^{-1}, well below the maximum velocities observed). However, large velocities and energetics are apparently not rare in the early phases of galaxy mergers. Similar situations exist for NGC 4676 and especially for Arp 295 (Hibbard & van Gorkom 1996). For these three systems (NGC 5291, NGC 4676, and Arp 295) a mass of order 10^{12} $M_\odot$ is required to bind the H I. Thus, either substantial amounts of gas escape from the systems or they possess dark matter. We presume both to be true. Certainly Hibbard & van Gorkom (1996) note the role of escaping gas in the scenario they describe for galaxy mergers. The existence of large kinetic energies in NGC 5291 is thus neither unusual nor unexpected, if in fact it is in the early stages of a galaxy merger. Mirabel and colleagues (Mirabel *et al.* 1991, Mirabel *et al.* 1992), find similar situations for the Superantennae (with a tail 260 kpc in length) and Arp 105; at the tip of a tidal tail, star formation is occurring. These are objects with masses in excess of the LMC, and which Mirabel and his associates believe were detached from the progenitor galaxies $\sim 10^8$ years ago. Star

formation is now occurring well after ejection of the tidal debris. Knot B represents an analogous situation; we will argue that Knot B is a stable entity (section 3.2).

The formation and evolution of dwarf irregular galaxies from tidally removed material in interacting systems has been postulated by Zwicky (1956) and Schweizer (1978). Much attention has recently been devoted to clumps in tidal tails, as prominent Hα, H I and stellar enhancements have been shown to exist in these regions (e.g. Mirabel *et al.* 1991, Mirabel *et al.* 1992, Hibbard *et al.* 1994, Hibbard & van Gorkom 1996). This discovery of regions of star formation associated with the tidal tails of interacting galaxies is evidence that gravitational condensation is possible in tidally removed material. Previous high spatial resolution observations of the H I in tidal tails have shown that the distribution of gas in these regions is often clumped into organized regions of high density with masses on the order of 10^9 $M_\odot$ (Hibbard *et al.* 1994). These concentrations are very similar to dwarf irregular galaxies in terms of their sizes, masses, colors, and stellar and gas distributions. The observed star formation rates are also very similar to those found in actively star-forming dwarf irregular galaxies.

Numerical modeling simulations have also been performed to test the possibility that material ejected during a tidal encounter will remain bound, or develop into sub-units on the scale of dwarf- and even full-sized irregular galaxies (e.g. Barnes & Hernquist 1992, Elmegreen *et al.* 1993). The models by Barnes & Hernquist (1992) produced strings of bound subsystems along the unbound tidal tails of two model spirals, passing each other in a prograde, direct, initially parabolic encounter prior to merging. They find in their simulations that distinct clumps form in tidal tails, and that these objects are gravitationally bound and stable against tidal stripping. These clumps form from the stellar component; the most massive of these clumps are able to capture significant amounts of gas.

Rather similar results were obtained by Elmegreen *et al.* (1993). They claim that the interaction will increase the energy of the interstellar medium (ISM) and thereby raise the Jeans mass. This process erases fluctuations smaller than 10^8 $M_\odot$. They show that the formation of these objects at the ends of tidal tails is a natural consequence of the model, and that they will continue to exist as distinct objects long after the tails have faded.

Hibbard *et al.* (1994), amongst others, suggest that the giant H II regions seen near the ends of the tidal tails in NGC 7252 are examples of such objects; other candidates are discussed by Mirabel and collaborators (Mirabel *et al.* 1991, Mirabel *et al.* 1992, Mirabel *et al.* 1994). Indeed, Hibbard & Mihos (1995), in their model of NGC 7252, find that at least one of these stable clumps will ultimately orbit the remnant as a satellite, with peri/apocentric distances of 14 and 120 kpc and an orbital period of about 4 Gyr.

It seems clear that interactive processes can and do produce bound systems resembling dwarf irregulars in this way. Unfortunately, objects like Knot B, or the features in the Superantennae and Arp 105 discussed by Mirabel *et al.* (1991, 1992), have gas masses that are an order of magnitude greater than the total masses of the clumps that appear in models. It is not clear that current models can account for such *large* associations forming in tidal tails. However, they may adequately explain the smaller knots and nebulosities observed.

Since ram-sweeping is the most obvious explanation for the asymmetry of the atomic gas and the large x-ray halo and tail, it is possible that we are seeing an interacting system that is subsequently being ram-swept as it passes through an intracluster medium. However, neither the ram-swept large disk nor the ram-swept interaction hypothesis alone can easily explain all of the observed characteristics of this unusual system. Detailed dynamical modelling is essential if more certain diagnoses are to be obtained.

4.2. Analysis of Dwarf Galaxy Candidates in the NGC 5291 System

Regardless of the formation mechanism, it is clear that there are large star-forming regions associated with the NGC 5291 system. As pointed out by L79, the optical knots in the NGC 5291 complex resemble dwarf galaxies in size and content. Two conditions must be met for a concentration of material to remain bound in the outer regions of such a complex field. These conditions require that the object (1) remains bound against its own internal kinetic energy (is self-gravitating), and (2) remains bound against the tidal force of the parent galaxy. We here examine whether the knots observed in the NGC 5291 complex can remain bound against these two disruptive influences, as then the likelihood of their eventual detachment from NGC 5291, to become independent systems, is quite high (see L79). We note that the following arguments are independent of the process which has given rise to the overall structure of the complex. (Ram-sweeping in fact causes compression, providing extra containment and facilitating the production of a bound subsystem; if this is the initiating process our estimates, below, will be even more conservative.)

To begin to understand the NGC 5291 system it is necessary to develop an estimate of the total mass present. This may be done in a number of ways, making different assumptions and therefore arriving at substantially different results. The simplest of these is to assume, with L79, that the system is a bound rotating disk extending out to the outermost H I and H II features, and that their velocities are projected orbital velocities. This results in mass estimates similar to those of L79 (who made this assumption), scaled for our larger assumed Hubble constant: $M_{tot} \sim 10^{12}$ $M_\odot$, where we have implicitly assumed that the galaxy is not far from edgeways-on. This value is large, but not without precedent in early-type spirals: for example, NGC 5084 (Gottesman & Hawarden 1986) has a mass $\sim$ 1.5×10^{12} $M_\odot$, though much less of this is H I than appears to be the case in NGC 5291.

A second approach is to ignore the H I and H II features in the outskirts of the complex,

as under the interaction hypothesis of their origin, they may well not be bound to NGC 5291 at all. A *lower* limit to the mass of NGC 5291 may be determined using a different Keplerian approximation:

$$M_K = \frac{rv^2}{G}.$$ (5)

and estimating the orbital velocity as the full width at 20% peak intensity of the H I velocity profile of the H I in the central optical image, corrected for inclination:

$$v = \frac{\frac{1}{2}\Delta v_{20}}{\sin i}.$$ (6)

From Table 3 we have $\Delta v_{20} = 464$ km s^{-1}. For the extent of the gas we adopt the optical major axis extent, 1.'1 (NED)[6] and a distance of 58 Mpc, resulting in a linear diameter of 18.2 kpc. For an inclination of 60° (L79) the total mass becomes 1.5×10^{11} $M_\odot$. Allowing for a dark halo, we increase this value by a factor of 5, as in the models by Barnes (1994).

4.2.1. Binding Mass

For an object to maintain gravitational stability, its gravitational potential energy must equal or exceed its internal kinetic energy. To estimate the binding mass, M_b, necessary for an object to meet condition (1), we start with the well-known energy equation for two gravitating point masses:

$$v^2 = G(M + m)\left[\frac{2}{r} - \frac{1}{a}\right],$$ (7)

where a is the semi-major axis of the orbit, and m is the mass of a "test particle" at a distance r. Setting a equal to infinity for a parabolic orbit and assuming $M \gg m$, we end

---

[6]The NASA/IPAC Extragalactic Database

up with the classic escape velocity equation. Rearranging, we find an expression for the minimum mass required to bind the system:

$$M_b = \frac{rv^2}{2G}.$$ (8)

We approximate the internal kinetic energy by means of the half-width of the H I velocity profile at the 20 level ($\frac{1}{2} \Delta v_{20}$). Assuming an isotropic velocity dispersion:

$$v = \sqrt{3} \left(\frac{1}{2} \Delta v_{20} \right).$$ (9)

The velocity profiles for NGC 5291 and the individual knots are shown in Figure 11. Alternatively, if the H I is in an inclined plane, the $\sqrt{3}$ correction is equivalent to an inclination of 35 deg. Our final expression for the binding mass now becomes

$$M_b = \frac{r \left[\sqrt{3} \left(\frac{1}{2} \Delta v_{20} \right) \right]^2}{2G}.$$ (10)

As long as the knots are essentially spherical, and we are only considering the dense H I cores, this is not likely to be much in error.

EDITOR: PLACE FIGURE 11 HERE.

We have evaluated the binding masses for the major knots in the NGC 5291 complex. To do this, we have estimated the radius of each object from the cores of the H I associated with each knot as delineated by the high resolution CnB array data. Knots D, J, and L have cores which are unresolved by the CnB array beam, while F – G is nearly so. We have therefore used the beamwidth as an upper limit to their diameters. The velocity widths and H I masses have been determined from the spectra in Figure 11. These spectra were calculated by summing the flux in each channel of the more sensitive (but lower resolution) DnC array data cube, within the high density regions ("cores") as delineated by the high resolution CnB array data; the method makes the exact shapes of the spectra somewhat

uncertain. The velocity widths were measured at 20% of the peak value to eliminate some of the uncertainty due to these fluctuations. Table 3 lists the velocity widths, radii, resultant binding masses, and H I masses for each object.

To determine whether the knots were self-gravitating, we have compared the measured H I mass for each knot (Table 3) to the binding mass. Values range from 0.82 for Knot B to 0.02 for Knot C. However this is a conservative test, which assumes that there is no other contributor to the mass than the observed H I. In the case of knots B and F–G there are clearly two other components: the stars and the ionized component in the optically-visible SFR associated with the H I feature, and observed in the radio continuum. Allowing for these masses, Knot B is self-gravitating, as is region F–G. Knots H, K and the H I Concentration may be marginally bound as well. The case for the stability of Knot B against its internal energy is clearly a very strong one. We would have to be underestimating the mass by more than a factor of 4 before the properties of Knot B are peculiar compared to a typical irregular galaxy.

4.2.2. Tidal Condition

To evaluate the second condition, we calculated the tidal limit for each dwarf candidate. The tidal radius is the radius within which material in a knot must lie to remain bound against the tidal force between the object and the parent galaxy. An object whose actual radius is smaller than its tidal radius will be stable against tidal disruption.

The tidally limited radius, r_T, can be expressed by (von Hoerner 1957):

$$r_T = R_G \left[\frac{m}{3M} \right]^{\frac{1}{3}}, \tag{11}$$

where r_T is the tidal limit of a test particle orbit in the satellite galaxy, M is the mass of the parent galaxy, m is the mass of the satellite galaxy (both assumed to be point sources),

and R_G is the projected separation between the two galaxies.

Determining the tidal limit requires that the total mass of NGC 5291, the candidate's separation from it, and the radius of each object be known. The effective tidal radius (r_T) has been calculated for each knot using its measured separation distance from NGC 5291 (listed in Table 3) and the knot's H I mass. The total mass estimate used for NGC 5291 is $7 \times 10^{11} M_\odot$, which includes the factor of five to allow for a dark halo.

This calculation provides a conservative tidal limit which is correct in detail for a point source potential, and quite reasonable for this system. We have increased the minimum mass by a factor of five to allow for the halo mass. Furthermore, the mass of an isothermal, spherical halo increases directly as R_G. Thus r_T is proportional to $(R_G)^{2/3}$. As our value for M cannot be reduced and R_G is underestimated owing to projection effects, our assumed values for R_G and M should lead to a realistic lower limit to the tidal radius r_T. We assume that the knots, as they are small, are essentially spherically symmetric and any model dependence on M propagates slowly at the one-third power. Therefore, we believe that the tidal radius can only be larger than indicated by equation 11.

This tidal limit is compared to each object's radius as measured from the H I data to determine its tidal stability. As seen in Table 3, most of the high-density cores of the objects meet this criterion. Knots C, M, and the H I Concentration do not, although for the H I Concentration, the H I radius (1.9 kpc) just barely exceeds the tidal limit (1.8 kpc).

Candidate components that meet both the binding and tidal criteria are very possibly irregular galaxies in various stages of evolution. It may be argued that a subset of these objects become independent irregulars. An understanding of the likelihood of this process of galaxy formation will allow us to estimate its contribution to the overall dwarf population, especially in clusters where interactions and ram-stripping are more likely to occur.

5. Conclusions and Summary

The high-resolution H I observations presented and discussed above shed considerable light on the nature of the NGC 5291 system, but do not finally resolve the causes of its peculiarities. Nevertheless we now have a much clearer picture of the basic parameters.

NGC 5291 is being significantly perturbed by interaction, either with another galaxy, or with the intracluster medium of Abell 3574, or both. What remains unclear is the relative weight of these processes in arriving at the present condition of the system. However we are at least in the position of being able to describe that condition in some detail. NGC 5291 is attended by veritable shoals of star-forming H II complexes, the brighter specimens of which are associated with concentrations of H I on our VLA images.

The H I observations establish clearly that a major speculation of L79 was in several elements correct: at least one (Knot B) and possibly several (H, K, and the H I Concentration) of the H I/H II features are bound against their own internal energies and stable against tidal disruption by the nearby galaxy. These objects are therefore prime candidates for young irregular galaxies produced from stripped galactic material. An argument particularly may be made for Knot B, which possesses a large young stellar component (Duc 1995) in addition to its H I mass and performance on the stability criteria. Knot B appears in every way to resemble an LMC-sized (or larger) "dwarf" irregular galaxy and would certainly be categorized as such were it to be detached from its parent galaxy, as appears likely in the next gigayear or so: it is a true, young, galaxy.

We suggest that the other knots may be dwarf irregular galaxies in formative stages of evolution; Knot B representing the largest and perhaps most highly evolved of these candidates. An important implication of this work is the verification that genuinely young galaxies may evolve from components of the debris fields of destructive interactions between parent systems and both their companions (via tidal effects) and their environments (via

ram-sweeping).

Understanding of the processes involved in this formation, and hence, for example, the age of the new entity, requires solving the puzzle of the dominant process in the NGC 5291 system. We have attempted to set out the obvious evidence for the ram-sweeping of a large disk or of a tidally disrupted system, without selecting either. This is because we consider it essential that careful modeling of the system and its processes on both these scenarios be undertaken, if a correct understanding is to be obtained. Such an understanding is in turn essential if the lessons to be learned from the availability of a young dwarf irregular galaxy are properly to be absorbed.

It has been suggested that half or more of the dwarf irregular galaxies in compact clusters have formed from gravitational encounters of the more massive galaxies in the cluster (Hunsberger *et al.* 1996). The observations presented herein, along with a growing body of evidence presented by many other researchers, seriously weaken models of galactic evolution that attempt to explain the various types of galaxies seen in the universe as the result of different, independent processes. To date however, too few systems have been observed to determine if a new class of genuinely young galaxies is truly indicated, or if instead this formation process is rare in the universe. Further investigations are needed to establish the extent to which gravitational encounters are involved in the building of dwarf irregular galaxies.

REFERENCES

Abell, G.O. 1958, ApJS, 3, 211

Arp, H.C. 1966, "Atlas of Peculiar Galaxies" (Calif. Inst. of Tech., Pasadena)

Arp, H.C. & Madore, B.F. 1987. "A Catalogue of Southern Peculiar Galaxies and Associations" (Cambridge Univ. Press, Cambridge)

Balcells, M. 1996, private communication

Barnes, J.E. 1994, in The Formation and Evolution of Galaxies, edited by C. Muñoz-Tuñon and F. Sanchez (Cambridge University Press, Cambridge), p. 399

Barnes, J.E., & Hernquist, L. 1992, Nature, 360, 715

Bothun, G.D., Impey, C.D., Malin, D.F. & Mould, J.R. 1987, AJ, 94, 23

Clark, B.G. 1980, ApJ, 89, 377

Daly, P.N., Phillipps, S., Disney, M.J., 1987, A&AS, 68, 33

Duc, P.-A. 1995, Ph.D. Dissertation, University of Paris

Elmegreen, B., Kaufmann, M., & Thomasson, M. 1993, ApJ, 412, 90

Gottesman, S.T. & Hawarden, T.G. 1986, MNRAS, 219, 759

Hawarden, T.G. & Chaytor, D.H. 1997, BAAS, (in press)

Hawarden, T.G., Longmore, A.J., Allen, D.A., Gottesman, S.T., & Miller, L. 1997, in preparation

Hibbard, J. E., & Mihos, J. C. 1995, AJ, 100, 140

Hibbard, J. E., & van Gorkom, J. H. 1996, AJ, 111, 655

Hibbard, J. E., Guhathakurta, P., van Gorkom, J. H., & Schweizer, F. 1994, AJ, 107, 67

Hunsberger, S.D., Charlton, J.C., & Zaritsky, D. 1996, ApJ, (in press)

Hogbom, J.A. 1974, ApJS, 15, 417

Klemola, A.R. 1969, AJ, 74, 804

Longmore, A.J., Hawarden, T.G., Cannon, R.D., Allen, D.A., Mebold, U., Goss, W.M., & Reif, K. 1979, MNRAS, 188, 285 (L79)

Lyden-Bell, D. 1994, in The Formation and Evolution of Galaxies. edited by C. Muñoz-Tuñon and F. Sanchez (Cambridge University Press, Cambridge), p. 85

Lynds, R., & Toomre, A. 1976, ApJ, 209, 382

Mihalas, D., & Binney, J. 1981, in Galactic Astronomy (W.H. Freeman and Company, New York), p. 489

Mirabel, I.F., Dottori, H., & Lutz, D. 1992, A&A, 256, L19

Mirabel, I.F., Duc, P.-A., & Dottori, H. 1994, in Dwarf Galaxies, ESO Conference No. 49, edited by G. Meylan and P. Prugniel (European Southern Observatory, Munich), p. 371

Mirabel, I.F., Lutz, D., & Maza, J. 1991, A&A, 243, 367

Pedersen, H., Gammelgaard, P. & Laustsen, S. 1978, The Messenger, 13, 11

Richter, O.-G. 1984, A&AS, 58, 131

Schweizer, F. 1978, in The Structure and Properties of Nearby Galaxies, IAU Symposium No. 77, edited by E. M. Berkhuijsen and R. Wielebinski (Reidel, Dordrecht), p. 279

Shapley, H. 1936, Harvard Bull., 903, 17

Sprayberry, D., Impey, C.D., Bothun, G.D. & Irwin, M.J. 1995, AJ, 109, 558

Theys, J.C., & Spiegel, E.A. 1976. ApJ, 308, 650

Toomre, A., & Toomre, J. 1972, ApJ, 178, 623

de Vaucouleurs, G. & de Vaucouleurs, A. 1964, Reference Catalog of Bright Galaxies (University of Texas Press)

de Vaucouleurs, G., de Vaucouleurs, A., & Corwin, H.G. 1976, Second Reference Catalog of Bright Galaxies (University of Texas Press)

van Moorsel, G.A. 1987, A&A, 176, 13

von Hoerner, S. 1957, ApJ, 128, 45

Zwicky, F. 1956, Ergebnisse der Exakten Naturwissenschaften, 29, 344

Fig. 1.— B-band Image of the NGC 5291 complex taken with the ESO 3.6m telescope (Pedersen *et al.*, 1978: reproduced by permission).

Fig. 2.— Grayscale image of H I integrated intensity from the CnB array data, with 2σ $(0.36 \times 10^{20}$ atom $cm^{-2})$ contour from DnC array data. CnB and DnC array beamsizes indicated by lower $(14'' \times 13'')$ and upper $(50'' \times 39'')$ ellipses in lower left corner. Crosses indicate the optical knots identified by L79 (A - H) and the H I features discovered with the VLA (I - M).

Fig. 3.— Grayscale image of the H I integrated intensity from the C+D combined array data. Contour levels are 1.1 (2σ), 5 10, 15, and 20×10^{20} atom cm^{-2}. The beamsize $(26'' \times 15'')$ is indicated by the ellipse in the lower right corner. Optical and H I knots are indicated with labeled crosses.

Fig. 4.— Contours of the H I integrated intensity from the C+D combined array data superimposed over the digitized optical image from the UK Schmidt IIIaJ Sky Survey plate. Contour levels are 1.1(2σ), 5, 10, 15, and 20×10^{20} atom cm^{-2}. The beamsize $(26'' \times 15'')$ is indicated by the ellipse in the lower right corner. Optical and H I knots are indicated with labeled crosses.

Fig. 5.— Radio continuum contours over optical image. Contour levels correspond to 3, 5, and 10σ $(1\sigma = 2.7 \times 10^{-4}$ Jy/beam). The beamsize $(26'' \times 15'')$ is indicated by the ellipse in the lower right corner. Optical and H I knots are indicated with labeled crosses.

Fig. 6.— Grayscale image of H I integrated intensity from the C+D combined array data. Outer contour indicates 2σ level from DnC array data. Inner contours indicate boundaries used for determining H I masses of knots.

Fig. 7.— (a) Individual channel maps from the DnC array data. Contour levels are 2, 5, 10,

15, and 20σ. The heliocentric velocity for each channel is listed in upper right corner.

Fig. 8.— Velocity (first moment) map from the C+D combined array data. Isovelocity contours are 25 km s^{-1} apart and run from 4000 km s^{-1} to 4725 km s^{-1}.

Fig. 9.— Velocity dispersion (second moment) map from the C+D combined array data. Contours are 10, 25, 30, 50, 75, and 100 km s^{-1}.

Fig. 10.— Einstein X-ray image courtesy T. Hawarden. The very strong source in the northeast (upper left) of the image is the Seyfert galaxy IC 4329A; the NGC 5291 complex is the extended source in the center of the frame. North is up; east is left. The grid lines are 2 minutes by 20$'$.

Fig. 11.— (a) Velocity profiles for components of NGC 5291 complex. Vertical axis (flux in Janskys) is drawn to same scale for all six objects. The peak intensity is 0.025 Jy. (b) Velocity profiles for components of NGC 5291 complex. Vertical axis (flux in Janskys) is drawn to same scale for all six objects. The peak intensity is 0.0125 Jy; note that the vertical scale is one-half of that used for (a).

VLA OBSERVING APPLICATION

A

rcvd:

(1) Date Prepared: May 31, 1997

(2) Title of Proposal: **The Evolution of Tidal Debris in Interacting Galaxies**

(3) AUTHORS	INSTITUTION	Who Will Come To The VLA?	For Grad Students Only Observations For Ph.D. Thesis?	Anticipated Ph.D. Year
B. K. Malphrus	Morehead State University, KY	x		
S. T. Gottesman	University of Florida	?		
C. E. Simpson	Florida International University, FL	x		
G. Tenorio-Tagle	Institute of Astronomy, Cambridge University, UK	?		
C. Munoz-Tunon	Instituto de Astrofisica de Canarias, Spain	?		
H.-J. Deeg	Instituto de Astrofisica de Canarias, Spain	?		

(4) Related VLA previous proposal number(s):

(5) Contact author
for scheduling: Caroline E. Simpson
address: Dept. of Physics
Florida International University
Miami, FL 33199

(6) Telephone: (305) 348-1565
Telex:
Internet: simpsonc@fiu.edu
Other E Mail:
Telefax: (305) 348-3053

(7) Scientific Category: ○ astrometry,geodesy & techniques, ○ solar, ○ propagation, ○ planetary, ○ stellar, ○ pulsar, ○ ISM, ○ galactic center, ○ galactic structure & dynamics (HI), ⊗ normal galaxies, ○ active galaxies, ○ cosmology

(8) Configurations (one per column) (A, B, C, D, BnA, CnB, DnC, Any)	D					
(9) Wavelength(s) (400, 90, 20, 18, 6, 3.5, 2, 1.3, 0.7 cm)	20 cm					
(10) Time requested (hours)	18.5					

(11) Type of observation: ⊗ mapping, ○ point source, ○ monitor, ○ continuum, ○ lin poln, ○ circ poln, ○ solar, ○ VLBI,
(check all that apply) ⊗ spectroscopy, ○ multichannel continuum, ○ phased array, ○ pulsar, ○ high-time resolution
○ other_____

(12) ABSTRACT (Do not write outside this space. Please type.)

D configuration 21 cm observations of a sample of interacting galaxies are requested as part of a multi-wavelength project to investigate the role of gravitational encounters in the formation of dwarf galaxies. We intend to identify dwarf galaxy candidates in interacting systems, observe the systems at optical, infrared, and 21 cm wavelengths to study both their stellar and HI distributions and kinematics, analyze these data to determine whether the candidates are dwarf galaxies in formation, and perform numerical modeling of these objects. High sensitivity (D configuration) observations are required to map the extended diffuse HI often found in the outer regions of these interacting systems. These data will be used to identify candidate tidal dwarfs and analyze their gravitational and tidal stability; and will provide needed parameters for numerical simulations, including an investigation into the statistical production of tidal dwarfs. This work could lead to revisions of current models of galaxy evolution, which has important implications for cosmological models.

NRAO use only

(13) Observer present for observations? ⊗ Yes ○ No   Data reduction at? ○ Home ⊗ AOC or CV (2 weeks notice

(14) Help required: ○ None ○ Consultation ⊗ Friend (extensive help)

(15) Spectroscopy Only:

	line 1	line 2	line 3	line 4
Transition (HI, OH, etc.)	HI			
Rest Frequency (MHz)	1420			
Velocity (km/s)	637–5061			
Observing frequency (MHz)	1417–1396			
Correlator mode	1A			
IF bandwidth(s) (MHz)	6.25			
Hanning smoothing (y/n)	N			
Number of channels per IF	128			
Frequency Resolution (kHz/channel)	48.828			
Rms noise (mJy/bm, nat. weight., 1 hr)	1.55			
Rms noise (K, nat. weight., 1 hr)	0.47			

(16) Number of sources __6__ (If more than 10 please attach list. If more than 30 give only selection criteria and LST range(s).)

(17) NAME	Epoch: 1950 ⊗ 2000 ○ RA hh mm	Dec ± xx.x°	Config.	Band (cm)	Band-width (MHz)	Total Flux line (Jy)*	cont. (Jy)	Largest angular size	Required rms (mJy/bm)	Time requested (hours)
Arp 158	01 22	+33.77	D	21	6.25	0.028		2.5'	1.1	2.5
Arp 31	01 48	+21.67	D	21	6.25	0.139		2.9'	4.8	0.5
Arp 78	01 56	+18.76	D	21	6.25	0.192		7.2'	2.7	0.5
Arp 135	02 37	+38.85	D	21	6.25	0.084		8.7'	1.0	3.5
Arp 213	04 03	+69.68	D	21	6.25	0.207		5.2'	4.0	0.5
Arp 298	23 00	+08.60	D	21	6.25	0.008		1.5'	0.5	11.0

*this should be the total flux at the peak of the line

Notes to the table (if any):

(18) Restrictions to elevation (other than hardware limits) or HA range (give reason):

(19) Preferred range of dates for scheduling (give reason):

(20) Dates which are not acceptable:

(21) Special hardware, software, or operating requirements:

(22) Please attach a self-contained <u>Scientific Justification</u> not in excess of 1000 words. (Preprints or reprints will be IGNORED!) Please include the full addresses (postal and e-mail) for first-time users or for those that have moved (if not contact author). When your proposal is scheduled, the contents of the cover sheets become public information (Any supporting pages are for refereeing only).

v3.0 6/94

Scientific Justification

D array observations of a set of interacting galaxies are requested as part of a multiwavelength project to investigate the role of gravitational encounters in the building of dwarf irregular galaxies. We propose to study the nature of the interaction and to search for genuinely young dwarf galaxies that may have formed from breakaway debris. 21 cm observations will be combined with optical and infrared (IR) observations (provided by the collaboration with the Instituto de Astrofisica de Canarias (IAC)) and numerical simulations in a comprehensive program.

A new model of the evolution of galaxies is emerging based on HST and other observations and numerical simulations. Interactions are being shown to play a major role in the evolution of galaxies. Consequences of these encounters may account for a significant fraction of the dwarf galaxies observed today (Hunsberger et al. 1996). Numerical modeling has shown that dwarf galaxies are unlikely to form in clusters as density fluctuations in proto-cluster clouds (Burkert & Silk 1997); some other mechanism may be at work in the building of these galaxies.

Numerical simulations show that material ejected during a tidal encounter can develop into stable sub-units on the scale of dwarf irregular and even full-sized irregular galaxies (e.g. Barnes & Hernquist 1992, Elmegreen et al. 1993). Observations of regions of star formation (e.g. Mirabel et al. 1991, Mirabel et al. 1992) and high density HI condensations (Hibbard et al. 1994) associated with the tidal tails of interacting galaxies show that gravitational condensation is possible in tidally removed material. Using a gravitational and tidal stability analysis, Malphrus et al. 1997 show that a large star-forming region ("Knot B") in NGC 5291's tidal complex is self-gravitating and strongly resembles a star-forming dwarf galaxy.

Objects like Knot B have gas masses that are uncomfortably large for many models. What kind of satellite systems are generated by an interaction? Are tidally stable clumps produced and is it likely that they will become genuine satellites? What percentage of the existing dwarf galaxies today have resulted from gravitational encounters?

Proposed Observations

To address these questions, the collaboration is undertaking a multi-wavelength observational program to be augmented by numerical simulations. We propose to search for small ejecta around a sample of galaxies which exhibit evidence of gravitational interaction. 21 cm observations will be used to investigate the HI distribution, dynamics, and kinematics of these systems and their interaction fields. Wide and narrow-band optical images will be used to identify dwarf galaxy-like companions (Deeg et al. 1997), while imaging in the near-IR as well as multifiber spectroscopy will be done to measure velocities and determine the physical nature, level of excitation, and metallicity of dwarf candidates, and to estimate star formation rates and ages. Numerical modeling will be done in conjunction with colleagues at the University of Florida and with Dr. Marc Balcells of the IAC.

D array observations of a subset of the interacting systems being studied by the IAC group are requested (see figures). These objects represent a variety of Arp types and a range of merging interactions. For example, Arp 78 and Arp 298 may be representative of early phases of interactions and possile mergers. The components are well separated showing tidal arms and plumes, faint nebular companions and strong absorption lanes. In contrast Arp 158 appears to represent a very advanced stage of a merger as the main body is complex with several centers of emission and a faint tail with knots. The other systems probably lie between these extremes.

We argue that these six systems represent close passages witnessed at different stages in the merging process. For Arp 78, Arp 158 and Arp 298, small nebular knots are clearly visible on the Arp and DSS images. The IAC group (see Deeg et al. 1997) has identified 21 non-stellar objects (NSOs) in the Arp 135 (NGC 1023) field, while more than 100 are seen in the Arp 78 (NGC 772) field. If these interacting systems form a temporal sequence, the distribution of ejected matter will vary as a function of the evolutionary stage of the

1

interaction. As the interaction ages, much of the material drawn out in the early phases will fall back into the principle galaxy(ies). This may explain the difference between the Arp 135 and Arp 78 fields. We need to assess the energetics and stability of dwarf candidates, and we will apply the methods developed in our study of the NGC 5291 system (Malphrus *et al.* 1997).

We will see a correlation between the broad distribution of HI and the non-stellar objects. Indeed, STG (working with data supplied by the IAC collaborators and by John Hibbard) found such a correlation between HI and the NSOs for NGC 520. Clearly, observations of the atomic hydrogen emission from these systems is crucial to our understanding of the evolution and energetics of these sytems; these data will constrain the dynamics and geometry of models.

Observational Parameters

To investigate the possible formation of genuinely young galaxies from tidal debris, we require broad angular sensitivity to diffuse HI that may be tidally expelled into space by the interaction. Therefore, the CS array is not of prime interest here as we require sensitivity and *not* coverage of the UV plane. Based on the results from the D array data, we will apply for C array time in the future to get improved resolution.

A bandwidth of 6.25 MHz is required to accommodate the large velocity widths (200–500 km/s) of these systems and to examine the nearby velocity field for candidate tidal dwarfs. To achieve a velocity resolution of 10 km/s, we require a 128 channel spectrometer with a frequency resolution of 48.8 kHz (1 IF, without on-line Hanning smoothing). We have requested enough time to achieve a signal-to-noise of 10:1. The total time requested includes calibration and move time.

Conclusion

We hope to begin to define the role that collisions play in the building of irregular galaxies. What can be said about the long term stability of these potential dwarf systems? How do they evolve during the course of the interaction? The combination of optical and radio observations discussed are designed to answer such questions. This research will contribute to our understanding of galactic evolution resulting from gravitational encounters.

Barnes, J.E., & Hernquist, L. 1992, Nature, 360,715

Burkert, A., Silk 1997 UC Berkeley Preprint

Deeg,H.J., Munoz-Tunon, C., Tenorio-Tagle, G., Telles, E., Vilchez, J.M., Rodriguez-Espinosa, J.M., Duc, P.A., Mirabel, I.F. 1997, "A Catalog of Dwarf Galaxy Candidates Around Interacting Galaxies", A&A, submitted

Elmegreen, B., Kaufmann, M., & Thomasson, M. 1993, ApJ, 412, 90

Hibbard, J. E., Guhathakurta, P., van Gorkom, J. H., & Schweizer, F. 1994, AJ, 107, 67

Hunsberger, S.D., Charlton, J.C., Zaritsky, D. 1996, ApJ462,50

Malphrus, B.K., Simpson, C.E., Gottesman, S.T., & Hawarden, T.H. 1997, AJ, submitted

Mirabel, I.F.,Dottori, H.,& Lutz, D. 1992, A&A, 256, L19

Mirabel, I. F., Lutz, D., & Maza, J. 1991, A&A, 243, 367
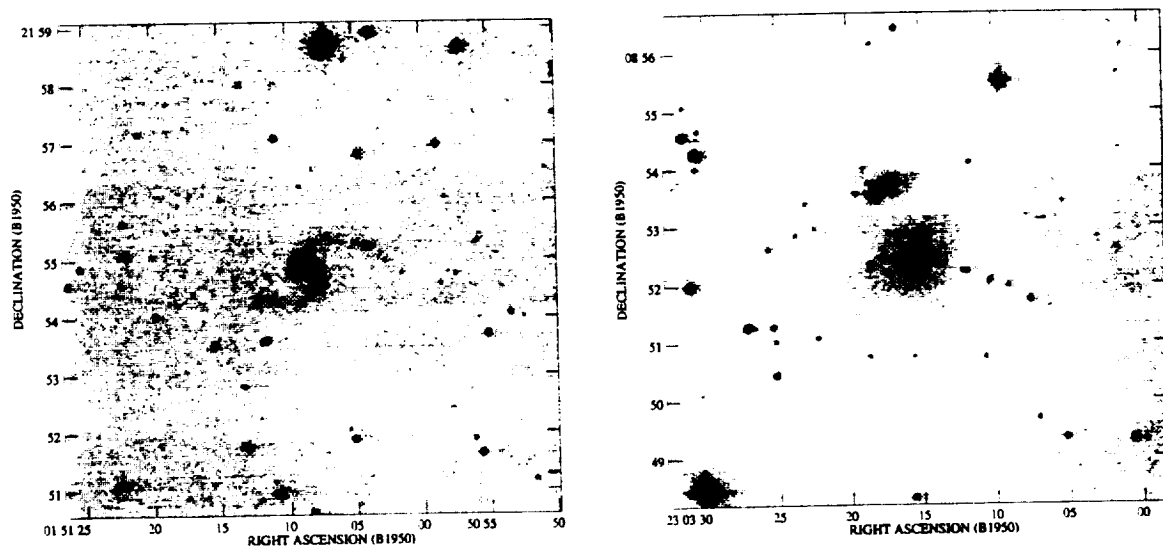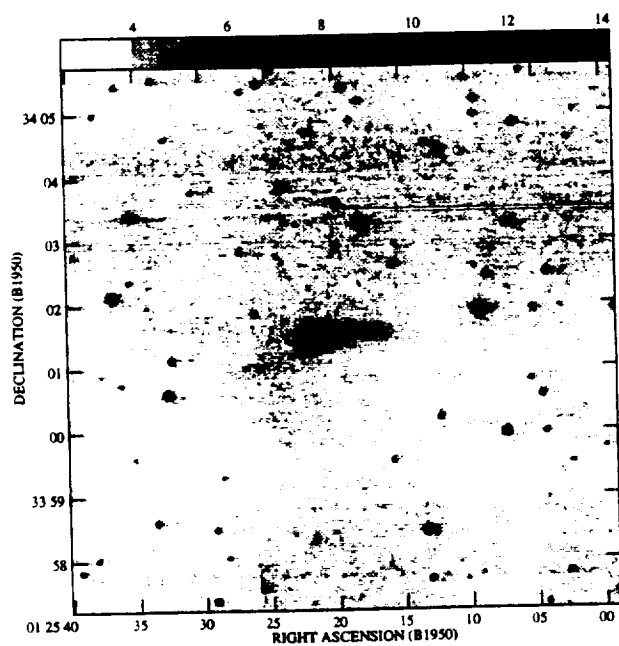
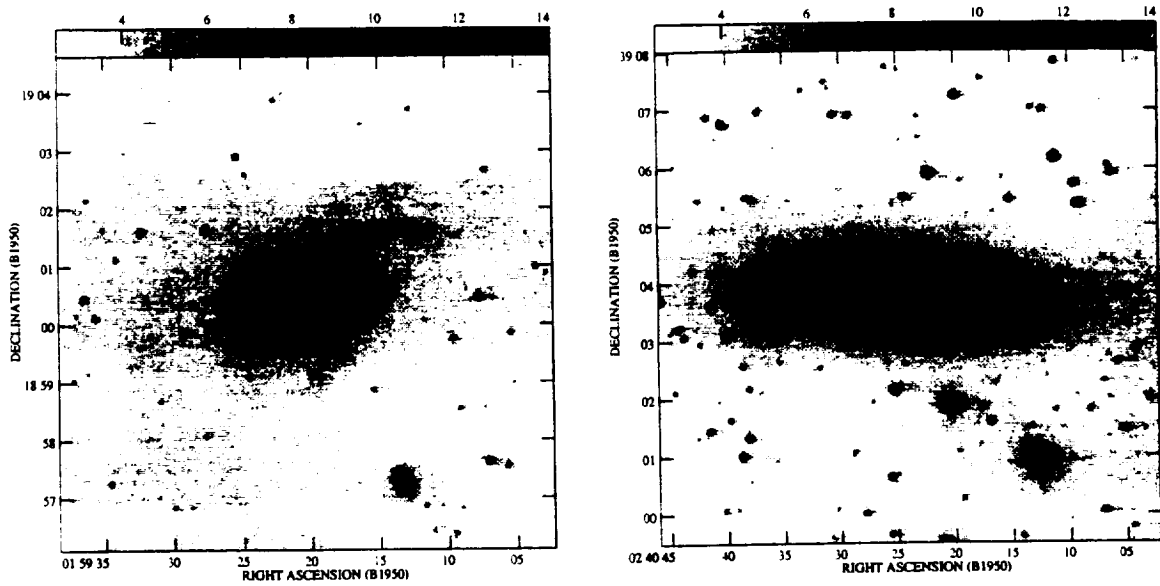Fig. 1.— Arp 31 (left); NGC 7469 = Arp 298 (right)

Fig. 2.— NGC 523 = Arp 158

3

Fig. 3.— NGC 772 = Arp 78 (left); NGC 1023 = Arp 135 (right)
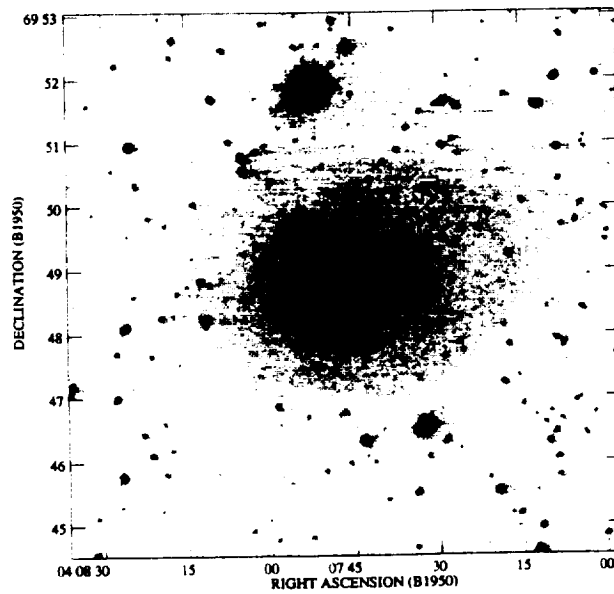

Fig. 4.— Arp 213

4

The Morehead Radio Telescope: Design and Fabrication of a Research Instrument for Undergraduate Faculty and Student Research in Radio Frequency Astrophysics

Benjamin K. Malphrus, Eric Thomas, Michael Combs. Brian Roberts, Bob Ratliff, Brian Roberts. Chad Pulliam. Jennifer Carter, John Pelfry, Dara Preece, and Viju Hullur
Morehead Astrophysical Observatory, Morehead State University, Morehead, KY 40351

Russell Brengelman, David Cutts, Charles Whidden,
Department of Physical Sciences, Morehead State University, Morehead, KY 40351

Rodney Stanley and William Grizes
Department of Industrial Education and Technology, Morehead State University, Morehead, KY 40351

Drew Henderson
Information Technology, Morehead State University, Morehead, KY 40351

Daniel Puckett
ACE Engineering, Morehead, KY 40351

AND

Jeff Kruth
Kruth- Microwave Electronics, Hanover, Maryland

ABSTRACT

Faculty and students of the Departments of Physical Sciences and Industrial Education and Technology at Morehead State University have designed and assembled the Morehead Radio Telescope (MRT) to provide a research instrument for undergraduate astronomy and physics students and an active laboratory for physics, engineering, and computer science undergraduates and faculty. The instrument functions as a research and educational instrument for undergraduate students, faculty, and science teachers throughout Kentucky. The goals of the MRT program are to enhance the curricula in physics, physical science, electronics, and science education programs by serving to provide: 1.) a research instrument for investigations in astronomy and astrophysics; 2.) an active laboratory in astronomy, physics, electrical engineering, and computer science; and 3.) a research instrument and laboratory for science teacher education and inservice programs. The telescope incorporates a modular design in which components may be easily removed for use in laboratory investigations and for student research and design projects. The performance characteristics of the telescope allow a varied and in-depth scientific program. The sensitivity and versatility of the telescope design facilitate the investigation of a wide variety of astrophysically interesting phenomena. The MRT provides hands-on experience in research and instrumentation technology in a cutting-edge science- one that is in the midst of scientific revolution.

INTRODUCTION

Observational astrophysics is literally in the midst of scientific revolution in that new instrumentation, namely space platforms and telescopes operating at previously invisible frequencies (i.e. Gamma ray, X-ray, ultraviolet, infrared, and radio) have been utilized in the discoveries that have required new paradigms to explain the fundamental structure and function of cosmic phenomena and of the universe itself. The MRT design provides an instrument capable of supporting scientific research in observational astrophysics at radio frequencies. The design and fabrication of the basic MRT systems is complete- first light was achieved on October, 12, 1996. An overview of the MRT Instrumentation, detailed description of major subsystems (antenna, alt-azimuth drive and control systems, opto-isolator circuitry, receiver systems, and controlling computer and interface), theoretical performance characteristics, intended scientific programs, and project significance, is provided herein.

MRT Instrumentation

The basic design of the MRT includes a wire-mesh parabolic reflecting antenna, alt-azimuth tracking positioner control and drive systems, receiver and signal processing system, a controlling computer with an interface device, and supporting electronics and hardware (Figure 1.0). The system is designed around a total power receiver which converts radiation from space concentrated by the antenna system to an electrical signal which is amplified, modified and interpreted. The MRT system is controlled by a Macintosh IIsi controlling computer and utilizes a National Instruments Lab NB Interface board, optical isolation system, and robotic drive and control systems developed by MSU faculty and students. The controlling computer positions the telescope, instructs it in robotic tracking of cosmic sources, and controls data collection and storage. The data from a particular experiment is then transferred via ftp to a Sun Sparcstation for imaging and analysis (Malphrus 1992).

Antenna :

The MRT employs a high gain forty-foot high antenna designed for L-Band operation. A surplused Army NIKE-Hercules ANS-17 Radar antenna was obtained and modified for radio astronomy applications. The antenna was selected because of its extremely large aperture, excellent aperture efficiency (afforded by its innovative offset feed design), and low cost . It includes L-Band, horn-fed, parabolic reflector and azimuth positioning system. The unmodified positioning system provided azimuth coverage of 360 degrees at a continuos antenna rotation speed of approximately six revolutions per minute.

The main purpose of the antenna is to trace the objects in space and collect and concentrate radio signals from space. These radio signals are then focused by the reflector to a single focal point on the antenna horn where a waveguide system transmits the wave to a terminus where the front-end receiver is located. A probe inserted into the waveguide to coax transitions converts the electric field of the radio wave to an electrical signal via electromagnetic induction. The electrical signal is then amplified and conditioned by the receiver front-end which then sends the data to the back-end receiver and controlling computer to be analyzed.

**Figure 1.0 Morehead Radio Telescope:
Systems and Subassemblies**

Reflecting Surface

Precision Clinomete

Superstructur

Feed Horn

Waveguide System

Focal Feed Support

Waveguide to Coax Transition

Front-End Receiver

Elevation Axis
and Bearings

Elevation Stop B

Counterweights

Elevation Control B

Elevation Positioning
System

Astronomer
(to scale)

Azimuth Indicator

East End Access Panel

Limit Switches

Pedistal:
   Azimuth Drive System
   Translators
   Power Supplies
   Optical Encoders
   Opto-isolator Circuitry
   Supporting Electronics

Dimensions and Motion	
Reflecting Surface:	44 ft x 11 ft (13.42 m x 3.35 m)
Total Surface Area:	484 ft^2 (50m^2)
Focal Distance:	3.50 m
Moving Weight:	1,155 kg
Total Weight:	4,527 kg
Positioner:	Automated Az.-alt. system
Elevation Range:	0° to 90°
Azimuth Range:	0° to 360°
Slew Rates:	20 min/360° Az. 10 min/90° el.
Data Collection:	Automated tracking and transit modes

Azimuth and Elevation Drive and Control Systems

Positioning the telescope is accomplished by azimuth and elevation drive and control systems designed and built by MSU faculty and students and ACE Engineering. The systems utilize a common controlling computer and interface board and independent electro-mechanical drive-train and positioning control systems. A block diagram of the azimuth drive and control systems is provided in Figure 2.0. The azimuth drive system incorporates a traditional translator, stepper motor, and gearing system that drives a 6-foot diameter bull gear inside a rotating turret to which the telescope superstructure, antenna, and feed support system (the moving components of the telescope) are attached. The elevation drive system incorporates a more radical rod and reel type design. A fixed axle is positioned at the center of gravity of the moving component of the telescope. The fixed axle is affixed to rotating couplers located on top of a supporting elevation positioning assembly. Motion in elevation is accomplished by controlling the motion about this axle with a rod and reel assembly positioned at the base. Cables attached to pick points on the focal feed support structure are reeled in out around a rod driven by the elevation control assembly. The elevation control assembly consists of a translator, stepper motor, gearing and coupling system that controls the rotation of the rod, motion of the cables, and ultimately motion of the telescope about the elevation axis (Figure 3.0) (Malphrus 1996).

Multiple Use Systems

Macintosh IIsi Controlling Computer:

The Macintosh Controlling Computer has 16 MB of RAM and 1 GB of hard disk memory with a mathematics co-processor. The Lab-NB which is a low-cost multifunction analog, digital, and timing I/O (Input/Output) board is installed in the computer. It contains a 12-bit successive approximation A/D converter with eight analog inputs, two 12-bit D/A converter with voltage outputs, 24 lines of transistor-transistor logic compatible I/O, and three counter/timer channels for timing I/O. Lab-NB is used with Lab VIEW, a software system that features interactive graphics, a state-of-the-art user interface, and a powerful graphical programming language. This software is used to send the input pulses to both the azimuth and elevation translators to move the telescope and analyze the data collected from the optical encoder and clinometer and is also used to collect the data from receiver system. The signal path from the controlling computer to the drive and positioning systems is outlined in Figure 4.0.

Interface Board:

A National Instruments LAB-NB Interface Board is used to interface computer with the electromechanical hardware. It is a 50 pin board with analog input channels, bi-directional data lines for ports A; B; & C, control signals, counter inputs; outputs; and gates. It is primarily used to interface the computer's I/O board with the hard wiring of the telescope's drive, control, and receiver systems.

Opto-Isolators :

The Opto-Isolators are electronic circuits designed and built by MSU students and faculty and ACE Engineering. The purpose of the opto-isolators is to isolate high voltage components of the system from low voltage components of the system. There are two types of opto-isolators - transmitters which transmit the signals from low voltage circuits and receivers which receive the signals from high voltage circuits. A system of opto-isolators is incorporated into the drive and control circuitry for total optical isolation. A schematic diagram of the MRT system as-wired is given in Figure 5.0.
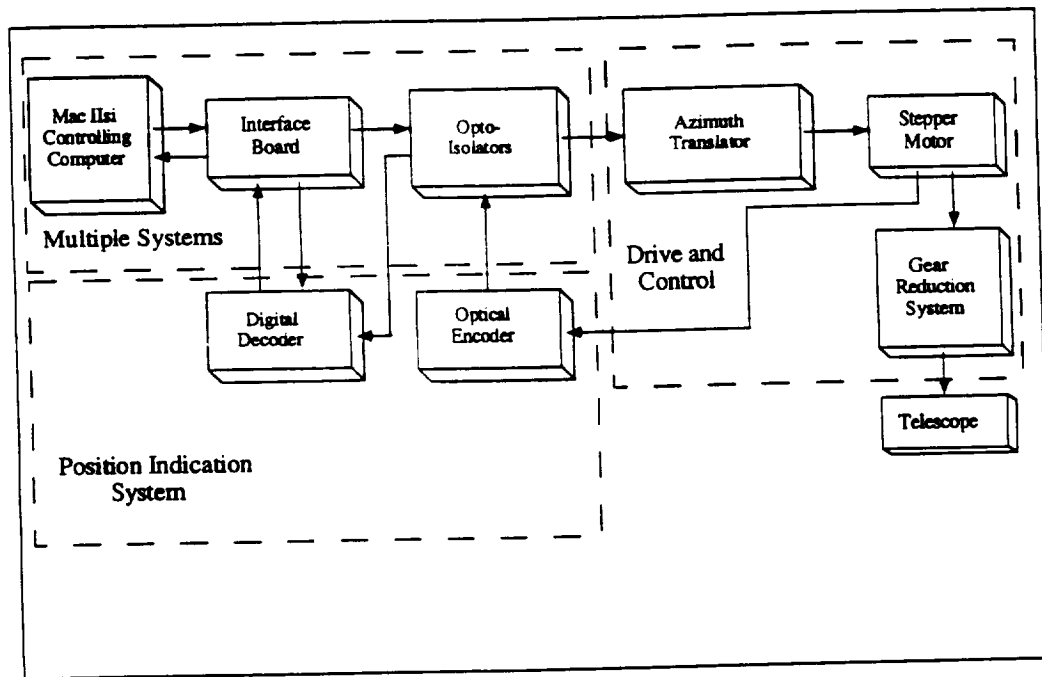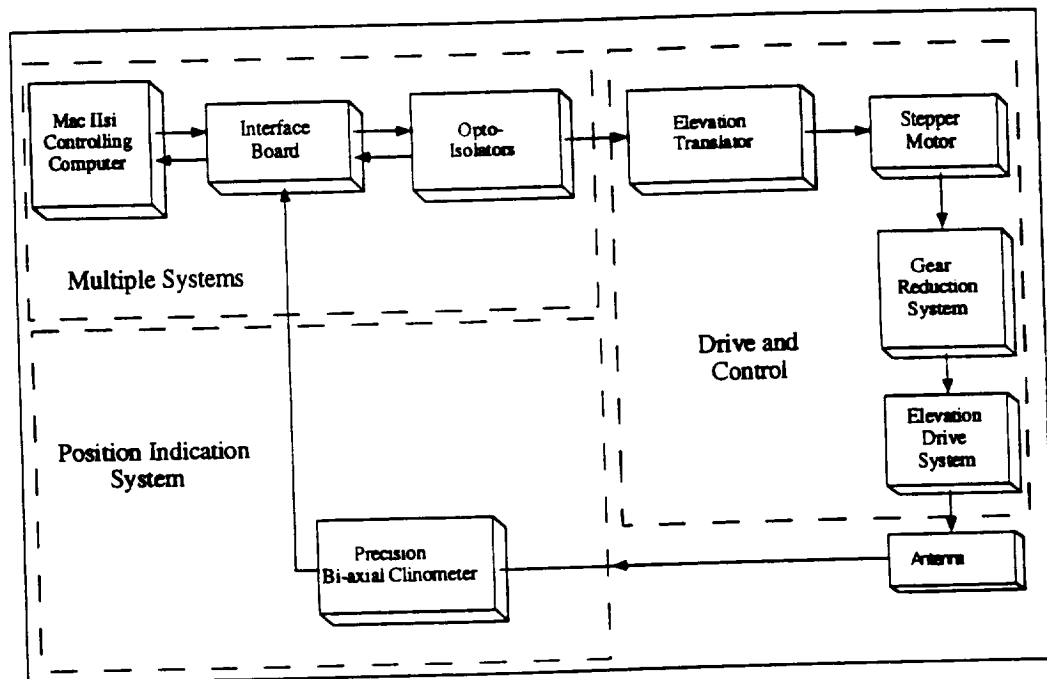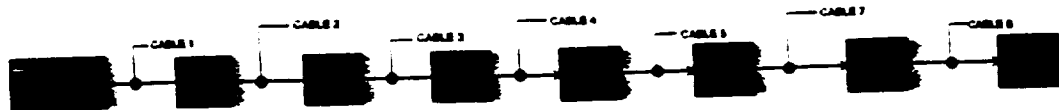
Figure 2.0   MRT Azimuth Control and Drive System

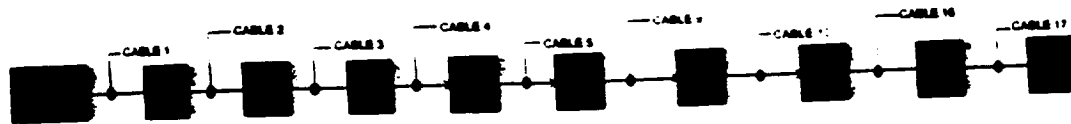Figure 3.0   MRT Elevation Control and Drive System

Figure 4.0

AZMITH SIGNAL DRIVE

FLOW1.WPS
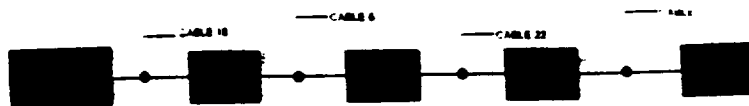11/21/95
Path=C:\MSWORKS\MRT_DWG\T-STRIPS
page 1 of 4

ELEVATION SIGNAL DRIVE

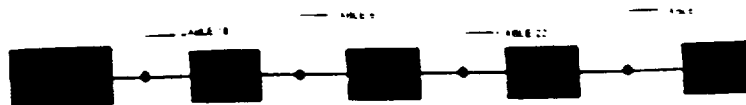FLOW1.WPS
11/21/95
Path=C:\MSWORKS\MRT_DWG\T-STRIPS
page 2 of 4

RETURN SIGNAL FROM CLINOMETER

FLOW1.WPS
11/21/95
Path=C:\MSWORKS\MRT_DWG\T-STRIPS
page 4 of 4

RETURN SIGNAL FROM ENCODER

FLOW1.WPS
11/95
Path=C:\MSWORKS\MRT_DWG\T-STRIPS

R1,R2,R3,R4 = 2.2K ohm

R5,R6,R7,R8 = 220 ohm

R9,R10,R11,R12 = 220 ohm

Figure 5.0 Optoisolator circut

Drive and Control Systems:

Azimuth Translator :

The Translator is a self-contained unit incorporating the power circuits and logic elements needed for bi-directional control of a stepping motor. The azimuth translator was designed and built by MSU students in cooperation with ACE Engineering. It can be triggered by pulses from an internal oscillator or from an external pulse source and will drive the motor at rates of 1000 steps per second. The unit can be operated in ambient temperatures from 0° Celsius to +40° Celsius. The Azimuth translator is used to control the azimuth stepper motor and an Elevation translator is used to control the elevation stepper motor.

Stepper Motors :

The SLO-SYN stepping motors operate on phase-switched DC motor. The motor shaft advances 200 steps per revolution (1.8° per step) when a four-step input sequence (full-step mode) is used and 400 steps per revolution (0.9° per step) when an eight-step input sequence is used. Logic devices are normally used for switching the speeds. Counter clockwise rotation is obtained by reversing the order of the switching steps of the clockwise rotation.

Gear Reduction System :

Precision-built parallel shaft speed reducers are specifically designed to provide long, trouble-free service on heavy duty low speed, high torque applications. They are directly coupled to the stepper motors in the drive trains of both axes. For the Azimuth system, three speed reducers with ratios 12.5:1, 30:1, 10:1 are coupled back to back to provide a gear reduction of 3750:1. This elaborate gear reduction system allows the drive train to move the azimuth axis of the telescope at the rate of one revolution per 23 hours 56 minutes (sidereal day) in the tracking mode and at the rate of one revolution in 45 minutes in the slew mode. For the Elevation System, one speed reducer with ratio of 15:1 is incorporated and sufficient to drive the telescope at an appropriate tracking rate and a slew rate of 10° per minute.

Position Indication Systems:

Azimuth Indication System :

The Azimuth indication system is based on measuring the rotation of an axle in the drive system with an optical incremental shaft encoder. The Optical incremental shaft encoder is a noncontacting rotary to digital position feedback device mount on the azimuth drive shaft at the stepper motor assembly . The internal monolithic electronic module converts the real-time shaft angle, speed and direction into TTL-compatible outputs. The encoder is used to count the rotations of the stepper motor shaft. This is basically used as a feedback data to trouble shoot if the count is not equal to the number of the pulses sent to the stepper motor.

Elevation Indication System :

The Elevation indication system is based on precisely measuring the tilt of the antenna focal plane with a high-precision biaxial clinometer. The Model 9000 Precision Biaxial Clinometer developed

by Applied Geomechanics is a low-cost biaxial clinometer for a wide variety of industrial and scientific applications (Figure 6.0). A precision electrolytic transducer comprises the sensing element. It has two orthogonal tilt angles (X and Y tilt) and one temperature channel as it's output channels. The unit can be operated from -10 degrees to 50 degrees Celsius. The clinometer is mounted on the parabolic reflector of the MRT and one of the orthogonal tilt angle (Y tilt) is used for our purpose. As the antenna is moved from the local horizon to the zenith, the electrolytic transducer's voltage is changes accordingly and this value is collected by the computer and the software converts this value to the degrees to know the exact inclination of the antenna.

MRT Receiver System

I. INTRODUCTION

The MRT receiver system design and fabrication program was a joint effort between MSU faculty and Kruth-Microwave Electronics Company. The program to design, fabricate and test a complete radio astronomy receiver system for the reception of signals in the 1420 MHz region was undertaken in 1993 and completed in 1995. A modular, flexible approach was chosen to permit simple up-grades as evolving experimentation needs require. Standard microwave/RF components were used where possible to reduce development time and to increase reliability. Custom low noise amplifiers were built to mate with existing antenna feed assemblies. Initial design work was performed by Malphrus and Cutts at Morehead State University; all additional work was performed at the Maryland facilities of K-MEC. The system design is comprised of single receiver with integral low noise amplifier that directly mated to the existing waveguide flange of the MRT antenna.

II. SYSTEM DESIGN

The overall receiver system design utilizes a low noise, sensitive, stable receiver to convert the 1420 MHz Hydrogen line frequency to a frequency region suitable for processing by standard laboratory equipment. A DC voltage derived from an envelope detector is incorporated in the final stage. In this context, low noise means less than 100 degrees Kelvin, with a goal of 35 degrees or less. Traditionally, this would have required cryogenic cooling of the first stage semiconductor amplifier. However, advances in GaAs FET technology allowed the fabrication of amplifiers with 35 degree noise temperatures with the device junctions at room temperature (Kruth 1994).

The MRT receiver system incorporates an FET LNA design. The system is comprised of two major subsystems- the front and back-end receiver systems. The front-end receiver is mounted at the waveguide terminus mounted on the focal feed support of the MRT superstructure. A back-end IF processor consisting on one channel of 160-21.4 MHz, and one channel of 21.4-2 MHz conversion is utilized for back-end processing with associated power supplies, monitor circuitry, and controlling computer. A block diagram of the overall system design is provided in Figure 7.0.

Major Receiver components include:

LNA assembly, assembled w/ Front-end Receiver
Receiver Down converter, 1420 MHz to 160 MHz
WJ IFC-162 160 MHz to 21.4 MHz IF Converter
21.4 MHz to Baseband IF Processor
Fluke 6160 Synthesizer for Microwave Oscillator Control
5 MHz Frequency Standard
Power Supply/ Housing for IF Processor
Misc. RF circuitry, cabling, filters, attenuators, etc.

TOP VIEW

0.125 (3,2) 4PLCS

1.76
(44,7)

1.76 (44,7)

2.00 (50,8)

2.00 in
(50,8)
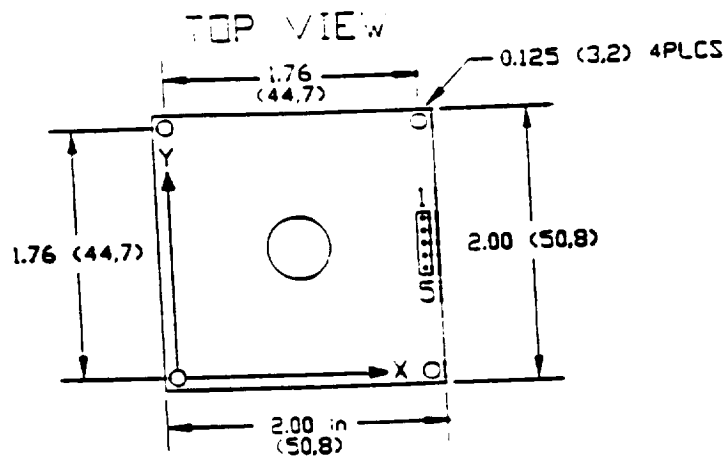
Pin #	Signal	Color
1	POWER	RED
2	GROUND	BLACK
3	X-OUTPUT	GREEN
4	Y-OUTPUT	BLUE
5	TEMPERATURE	YELLOW

0.64 (16.3)

TRANSDUCER

IC'S

5-PIN HEADER
SIGNAL AND POWER
CONNECTION

PCB
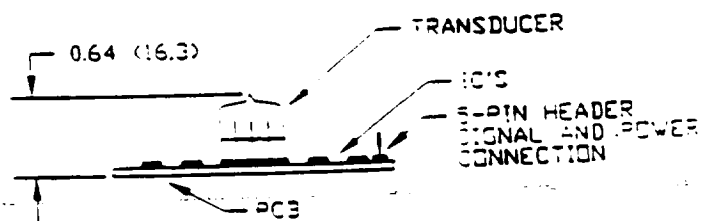
Figure 6.0 Biaxial Precision Clinometer Basic Diagram

RCVR
DWN-CNV

PWR/CNT/MNTR
I.F.
REFERENCE

Cable Bundle

SYSTEM BLOCK DIAGRAM

1
2
Power Supply
+ Control

1
2
IF PROCESSOR

1
FLUKE
6160
2

5MHZ
REFERENCE
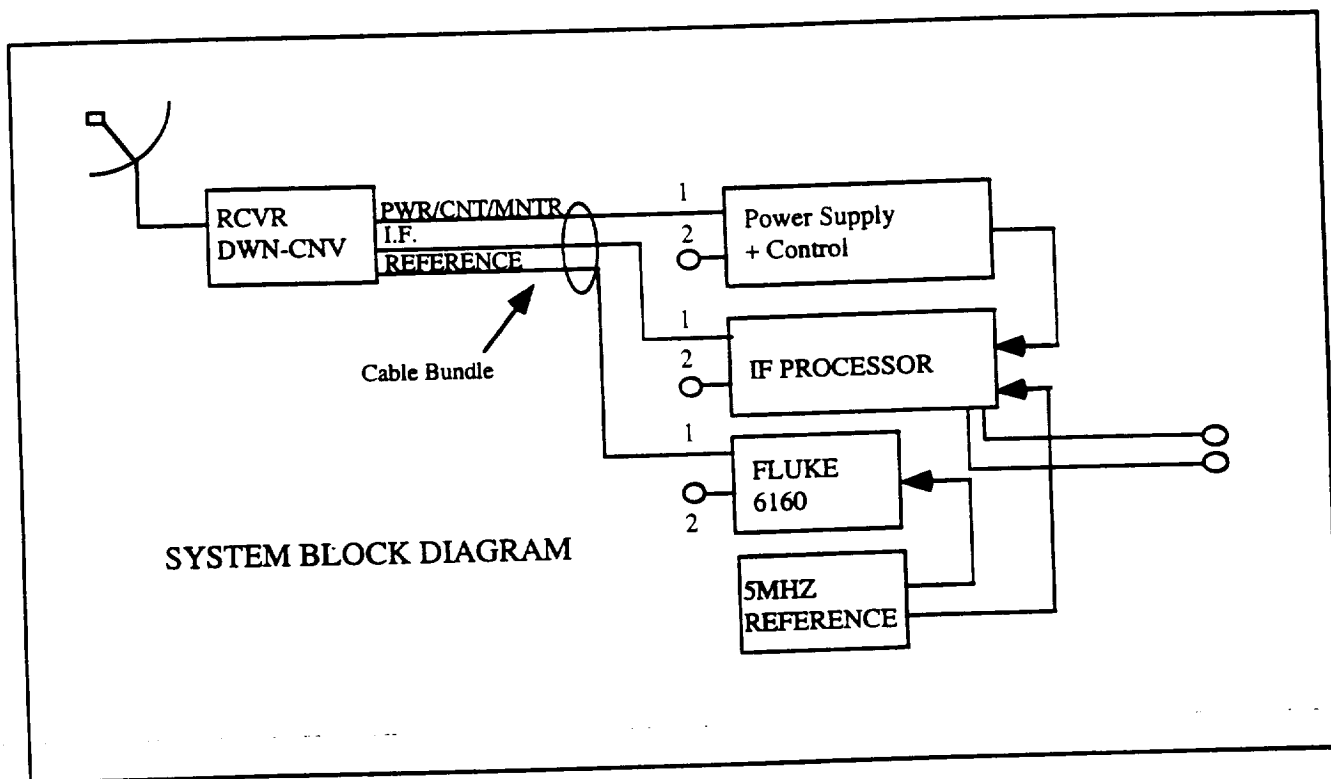
Figure 7.0   System Block Diagram

A triple conversion system is used with a first IF of 160 MHz and a bandwidth at the first IF of 23 MHz. The second conversion translates to a frequency of 21.4 MHz, with a bandwidth of 1 (2) MHz. The frequency of 21.4 MHz is a standard IF for surveillance radios, and one that a great variety of filters (both crystal and LC) is available for, so the IF bandwidth can be easily changed. The final conversion is to baseband, essentially DC-1 MHz. This final conversion is easily modifiable to allow a flexible choice of final IF before detection. This strategy permits direct digitization (FFT processing on PC based platforms) as well as experimentation with parallel filter bank approaches.

The receiver system consists of two major components:

1). Remote receiver front end containing RF circuitry to down convert the 1420 MHz band to 160 MHz, and

2). The back-end receiver, consisting of monitor circuitry for the converter, additional IF converter stages, reference oscillator for coherent locking of the receiver front ends, as well as additional test equipment.

A key feature of this system is that all of the frequency generation components used in the various conversion stages are phase locked to a common reference frequency. This reference source consists of a high quality 5 MHz temperature compensated crystal oscillator and associated buffer amplifiers. Additionally, the 5 MHz source can be derived from a Rubidium or Cesium beam clock, affording the utmost in stability and accuracy, if such a source becomes available. A commercial synthesizer drives the phase locked oscillator in the remote receivers, and in turn is locked to the 5 MHz standard. The use of a common reference frequency scheme such as this permits the remote receiver to be locked on the receive channel, regardless of external perturbations, such as weather conditions, seasonal temperature change, etc. This is particularly desirable in the event that a second receiver is added to the system for the purpose of interferometric measurements. This design will permit the phase coherent manipulation of the signals from the second receiver down converter box for interferometry based observations and experimentation. A more detailed of the circuitry and theory of operation of the front-end and back-end receivers is provided below.

Front-end Receiver

The front-end receiver consists of the LNA, image reject band-pass filter, mixer, IF pre-amplifier, IF roofing filter, level set variable attenuator, IF post-amplifier (if required), local oscillator, and required power supply regulators and control circuitry (Figure 8.0). The front-end receiver is housed in a box suitable for outdoor mounting at the terminus of the waveguide mounted on the antenna focal feed support structure (Kruth 1994).

High Electron Mobility Transistors (HEMT) FET devices are used for the first stage, followed by GaAs FET gain blocks. The device utilized for the first stage application is the Nippon Electric Company (NEC) NE32684AF Ultra Low Noise Pseudomorphic Hetero-Junction FET. This device has a measured noise figure of .3 dB (approximately 30 degrees Kelvin) at room temperature, with an associated gain of approximately 22 dB at 1400 MHz. This value represents excellent performance. Care in the amplifier design and fabrication was exercised to preserve these values. The first stage amplifier achieves .5 dB NF and 18 dB gain using this device. The design of the input matching stage for this amplifier is critical as any losses from mismatch or attenuation may directly degrade the noise figure. A simple circuit incorporating the WG-microstrip transition is utilized, with a single tuned circuit response. With this approach, it is not possible to provide much filtering, so a filter is added between the following stages.

LNA
ASSY

1420 MHZ
BPF

ATTN.
MIXER

ATTN.   160 MHZ
          BPF

160 MHZ
OUTPUT

WG
PORT

HEMT
PREAMP

AVANTEK
POSTAMP

AVANTEK
POSTAMP

LEVEL
SET
ATTN.

TO ALL
COMPONENTS

L.O. SAMPLE

POWER
SUPPLY

PLO
REFERENCE
INPUT
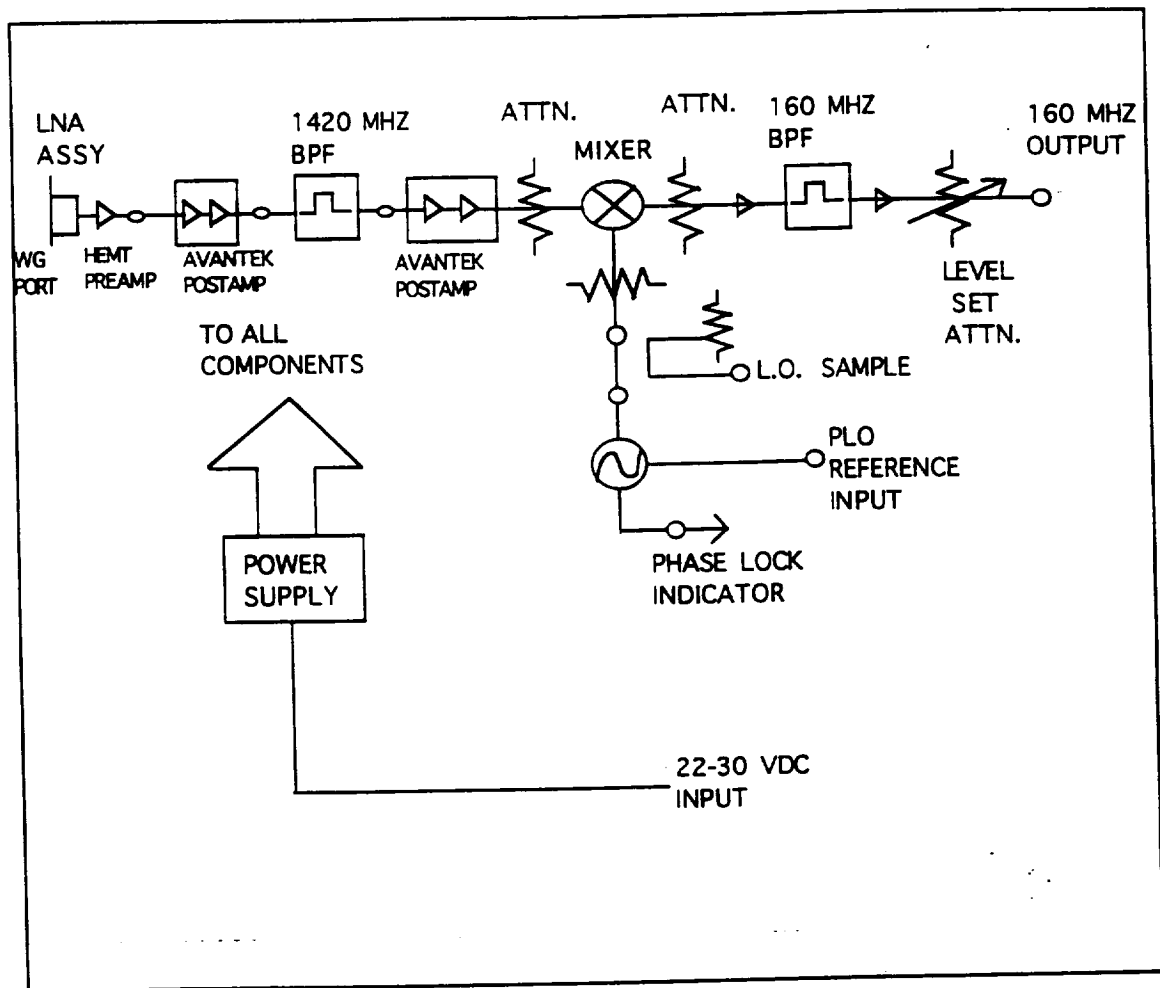
PHASE LOCK
INDICATOR

22-30 VDC
INPUT

Figure 8.0 Front-End Receiver Diagram

This stage is followed by an Avantek packaged gain block pair consisting of a UT02012 and a UT02013 amplifier cascade. This combination provides good gain (20 dB), excellent intercept point (P-sat = +21 dBm fundamental), and a modest noise figure of 2.5 dB. This controls the noise figure degradation due to second stage contribution nicely. Due to the high gain and wideband nature of the first stage amplifier, a front end pre-selection filter is necessary to block out terrestrial interference. This interference is from diverse sources such as TACAN, radar, cellular phone harmonics, INMARSAT uplinks and so on. A commercial filter was used as this became available. The bandwidth of this filter is on the order of 150 MHz, centered at 1420 MHz and the insertion loss is 2 dB. A standard double balanced mixer is used for the first converter stage. A standard drive level type is appropriate to this application and the conversion loss is 6 dB.

The 160 MHz IF amplifiers are of conventional design. A coaxial tubular bandpass filter is used to establish the bandwidth of the first converter system. Since the desired bandwidth is 2 MHz, a filter of at least 5 x this value must be used to permit future expansion of the experimental system. The bandwidth of the system is preserved down to the final stage and it is possible to use wider filters should experimental needs require this. A 20 MHz filter is used to preserve the 20 MHz system bandwidth all the way down to final detection.

The level set attenuator that is included in the design allows manual control of the gain of the receiver in order to coarsely equalize the gain of the two receivers when used together. Fine gain control is controlled in the IF processor system. The calculated end to end gain of the front-end is 68 dB. The calculated noise figure is .535 dB based on a .5 dB first stage and a 2.5 dB second stage, then an overall noise figure is attainable in the first stage, then an overall noise figure of <.4 dB (approximately 40 degrees Kelvin), is attained.

The local oscillator is a phase-locked (PLO) cavity tuned type made by California Microwave and is a "brick" style oscillator. This oscillator is a fundamental L band cavity using a low noise bi-polar transistor as the oscillator element. It incorporates a reference multiplier/harmonic mixer arrangement to permit locking. This oscillator is driven by a synthesizer at 105.0835 MHz and, as the PLO will assume the phase noise and stability character of this oscillator directly, this reference signal is high quality.

The front-end receiver package is housed in a waterproof aluminum box approximately 12" x 12" x 12", with all electrical connections made on one face. Thermal insulation and heating blankets are used to provide a relatively constant temperature environment for the outdoor receiver unit. An integral power supply is used that operates from 22-30 VDC, and uses well filtered, regulated DC-DC converters to provide the various voltages required by the system. This permits a single low voltage feed to the receiver package, for simplicity and safety.

Back-end Receiver

The back-end receiver is comprised of a synthesizer used to generate reference signals for the down-converter, an IF processor with crystal oscillator for conditioning of the IF signal, a down-converter power supply, opto-isolation system, and controlling computer and interface device. A high quality Fluke synthesizer that can generate the 105 MHz range reference signal for the receiver converters is incorporated into the back-end receiver system. This is an adaptation of the popular 6160A series that has been modified to use an external 5 MHz standard. The output of the remote receiver at 160 MHz is shipped by low loss 50 ohm coaxial cable to the indoor rack. Here the signal is buffed and split. A sample of the 160 MHz "WIDEBAND" IF is make available on the front panel of the control box. The other leg of the power splitter is applied to the 160- 21.4 MHz IF converter system. This system element used is a Watkins-Johnson IFC-162 IF converter module, a self contained, system component available from stock at K-MEC. This device uses

21.4 MHz without degrading the signal to noise ratio. The internal crystal oscillator used to convert the signal was modified so that it can be phase locked to the reference 5 MHz oscillator. Refer to Figure 9.0 for a schematic diagram of the back-end receiver (Kruth 1994).

Additional filtering is then used to establish the desired final bandwidth before detection. The final conversion brings the 21.4 MHz down the "BASEBAND" by beating against a crystal controlled oscillator. The frequency of the synthesized oscillator can be changed, along with the 21.4 MHz filtering, to allow different bandwidths at the final detection stage. Buffered sample ports are available at all pertinent points in the signal path for access to the signal. This is a useful feature for built-in tests as well as experimentation. The complete receiver system concept has been shown in block diagram form in Figure 7.0 which provides an overview of the interconnection of the various system elements. A regulated high current supply provides 26 VDC nominal for operating the outdoor receiver package.

A calibrated semiconductor noise source is incorporated into the front end LNA waveguide port of the receiver package to inject a precise amount of excess noise for calibration purposes. a precision coupler and altenvator is used to precisely set the injection level of the noise source into the first amplifier. The coupler was manufactured as part of the amplifier to minimize the impact of additional insertion loss. In fact, the scheme used did not denigrate the noise temperature, noticeably.

MRT Operator Program

The computer operator program developed for the MRT is responsible for positioning the telescope in azimuth and elevation, tracking of cosmic objects as the sky rotates, determining telescope position in altitude and azimuth via independent feedback loops, and for controlling data collection and storage in addition to controlling additional experimental parameters. The initial design of the controlling program was developed by MSU staff. The program has evolved from its initial design in order to compensate for operational characteristics of the positioning systems which have developed as these systems, themselves, have matured. This evolution has been carried out by students, along with MSU staff, after performing operational tests of the positioning system components.

The controlling program has been developed with the Labview Virtual Instrumentation software package, which provides a graphical programming environment "G", with built in accessibility to the functions of the National Instrument's LAB NB interface card. The graphically intensive language "G" is ideally suited to the production of programs used in data collection and analysis as it was initially designed to communicate with interface technologies. Virtual instruments developed with this package actually mimic hardware components such as spectrum analyzers and oscilloscopes by conditioning the signal in exactly the same way that the hardware counterpart would. This package reduces the need for expensive and space-consuming hardware.

The program determines positioning requirements based on the current Universal Time, as well as the destination coordinates (right ascension and declination) provided by the operator. After determining the local sidereal time based on this input data, and converting the coordinates of the object of interest to its current azimuth and altitude, the operator program provides the necessary control signals to the azimuth and elevation translators via digital I/O ports on the interface card. The necessary positional accuracy is achieved by monitoring the azimuth encoder and elevation clinometer. Positional accuracy of 0.10 arcdegrees is achieved via this feedback loop.

The operator program performs transit operational mode by positioning the antenna to the target location, then monitoring the analog signal from the receiver. Tracking mode additionally incorporates an algorithm to monitor the deviance of the antenna's position from the desired
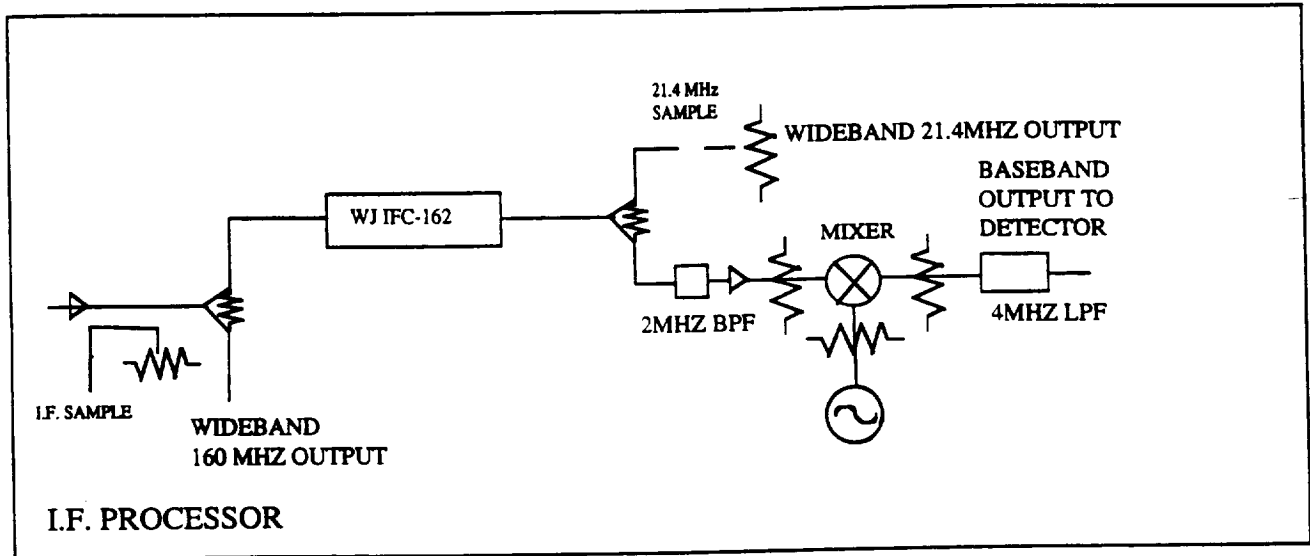
Figure 9.0   Intermediate Frequency Processor
Block Diagram

position, with the intention of achieving the aforementioned positional accuracy. It was necessary for the operator program to evolve based on experiments performed with the mechanical elements of the positioning system. The number of TTL pulses required to position the telescope in elevation and azimuth was determined empirically from numerous experiments. These values were then programmed into the program to automate positioning the telescope. Front-end (user interface) and back-end (master program diagram) are provided in figures 10.0 ~~and 11.0~~ respectively.

- 🐟

14

Theoretical Performance Characteristics of the MRT

The minimum detectable flux density, the weakest detectable radio frequency signal from space (ΔS_{min}), expressed in Janskys ($1 \text{ Jansky} = 10^{-26} \text{ w m}^{-2} \text{ Hz}^{-1}$) may be calculated (Kraus 1986):

$$\Delta S_{min} = \frac{2K \ K_s \ T_{sys}}{\varepsilon_{ap}A \ \Delta v \ \Delta t}$$

where:

ΔS_{min} = minimum detectable flux density

K_s = receiver constant ($\cong 1$)

T_{sys} = system temperature

k = Boltzman's constant (1.38×10^{-23} J*K^{-1})

ε_{ap} = aperture efficiency ($0 \leq \varepsilon_{ap} \leq 1$) dimensionless

A = aperture area (m^2)

Δv = pre-detection bandwidth in Hz

Δt = post detection integration time

Values for the MRT subsystems are obtained from laboratory measurements of the MRT front-end receiver furnished by Kruth Microwave Electronics Corporation- K-Mec; values for the antenna system are taken from Army Operational Research Group (AORG) AN-FPS 36 Radar Antenna Systems Operational Parameters) (AORG 1968). The following values are substituted:

T_{sys} = 67.77 K

Δv = 2 x 10^6 mHz

K_s = 1

ε_{ap} = 0.65

A = 50m^2

Assuming a post-detection integration time of one second produces a value of 4.066×10^{-26} J = 4.06 Janskys.

The total system temperature (T_{sys}) includes noise contributions due to the waveguide and other factors is described by (Kraus 1986):

Figure 10.0 Operator Program:
Positioning System
Front-end
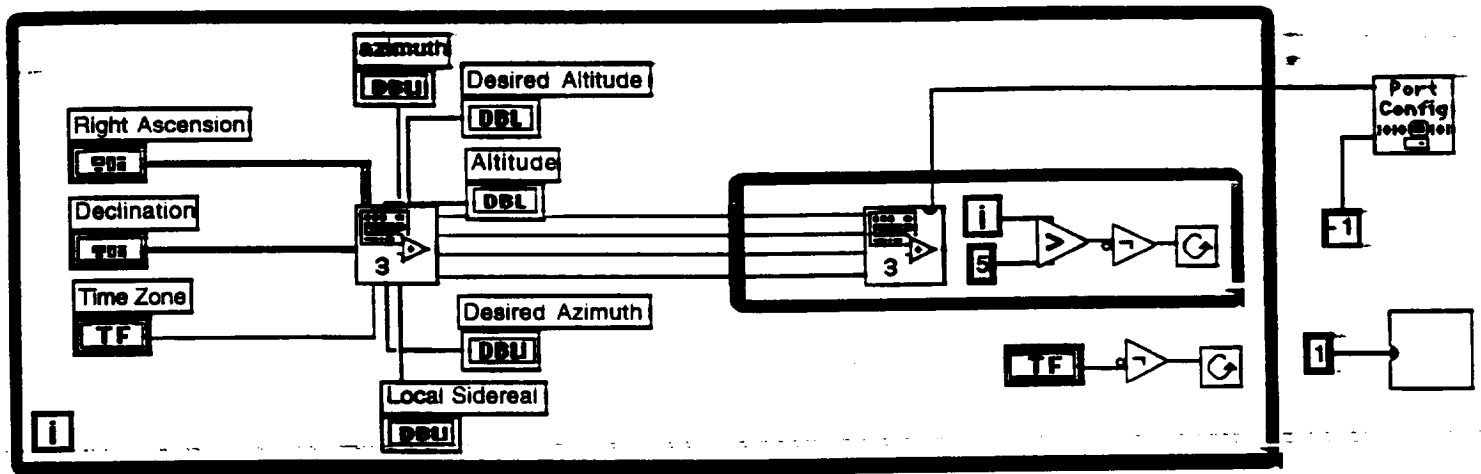
Figure 11.0 Operator Program:
Positioning System
Back-end
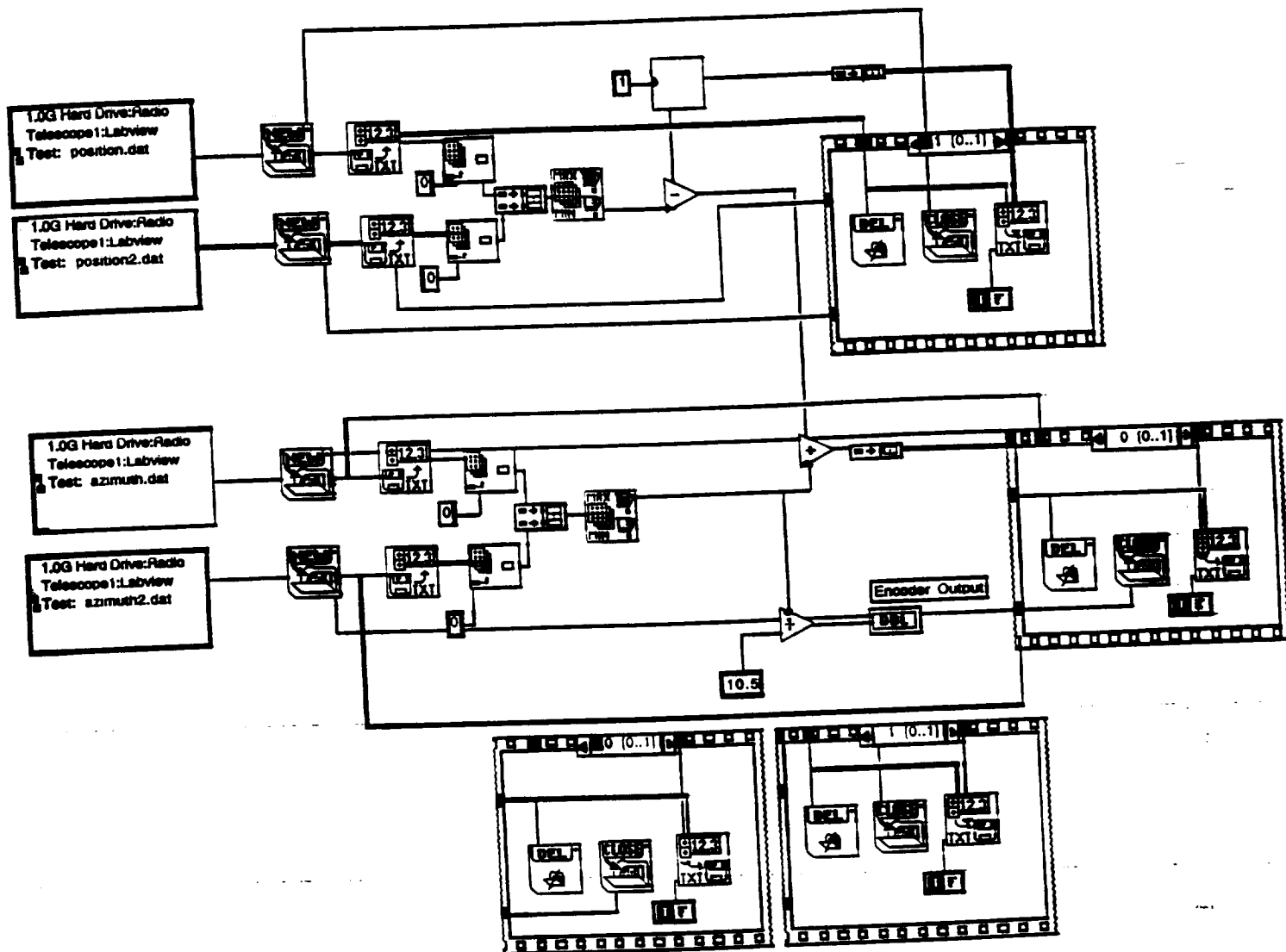
Figure 12.0 Operator Program:
Azimuth Subroutine

y=44.1036*v + 1.2485*v^2 - 6.6313*v^3 - 0.2949*v^4 + 0.8471*v^5;
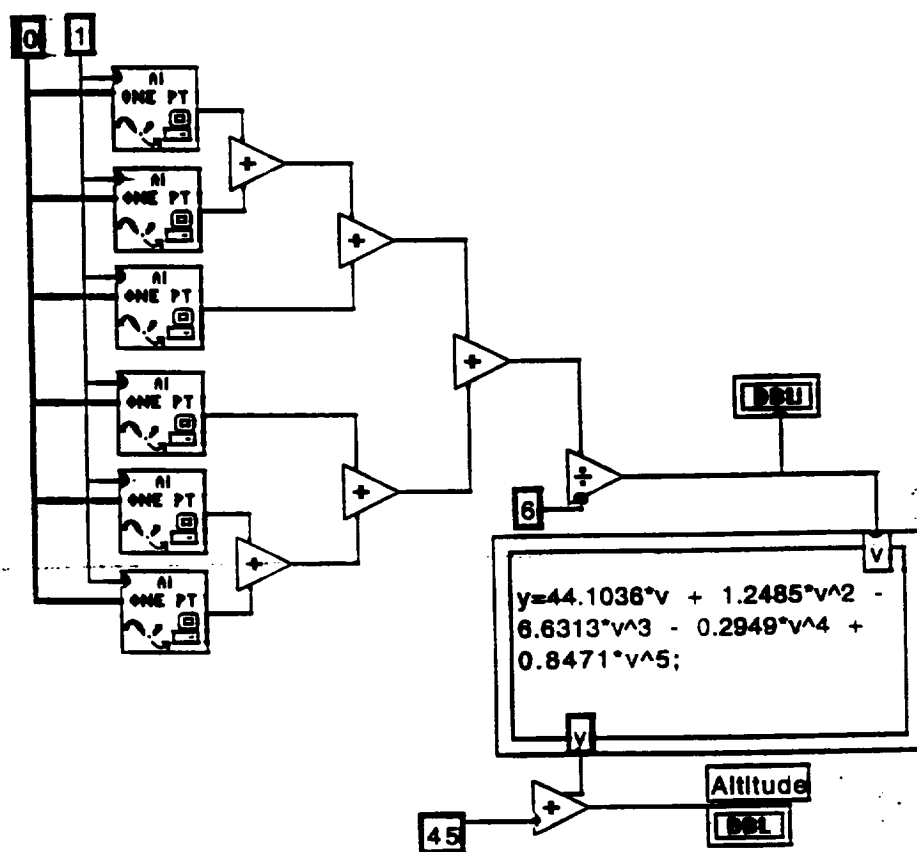
Figure 13.0 Operator Program:
Altitude Subroutine
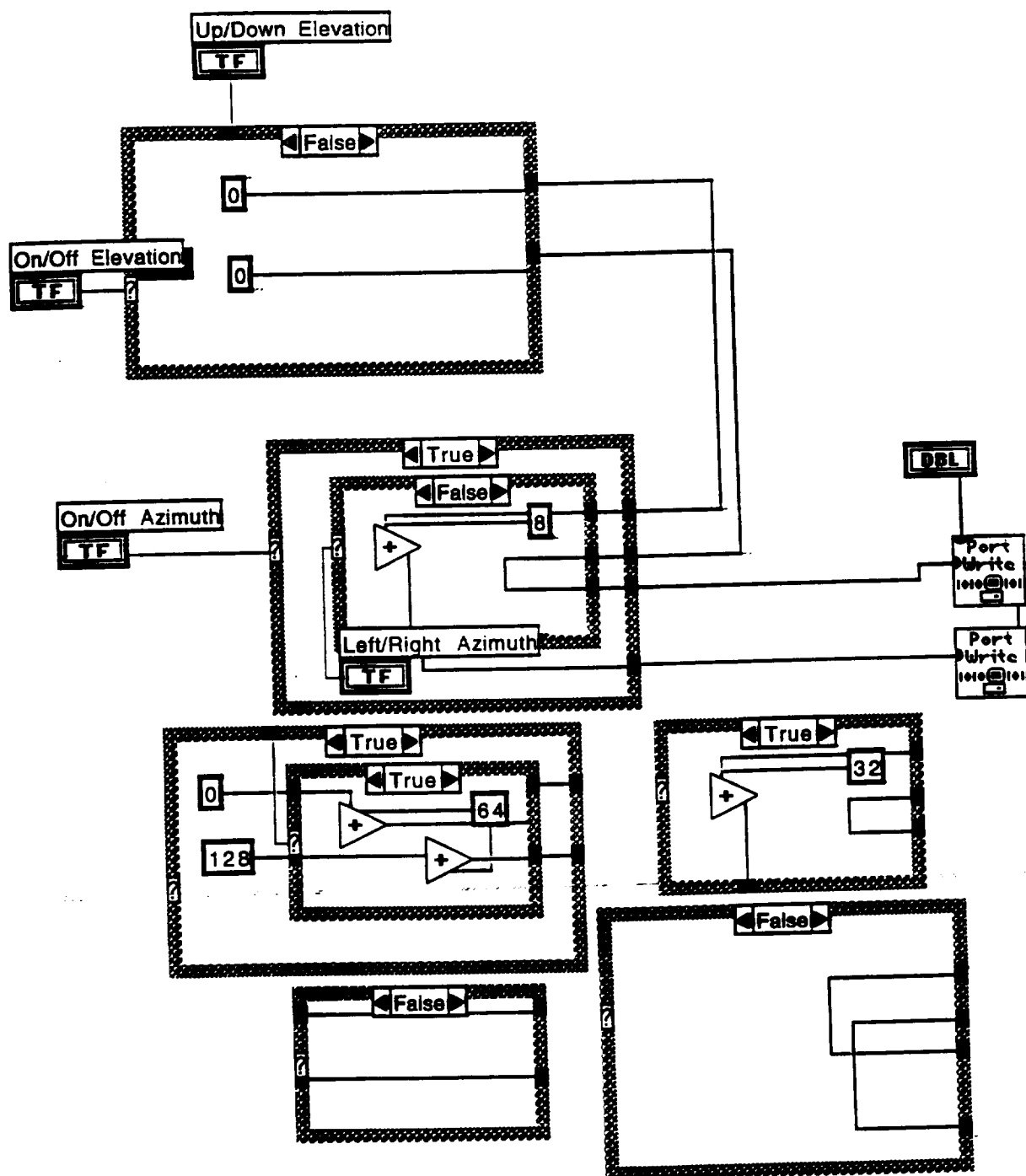
Figure 14.0 Operator Program:
Instrument Control Subroutine

$$T_{sys} = T_A + T_{Lp}[(1/\mathcal{E}) - 1] + (1/\mathcal{E}) T_R$$

where:

T_{sys} = system temperature
T_A = antenna temperature
T_{Lp} = physical temperature of waveguide

$\mathcal{E}$ = transmission efficiency

T_R = receiver temperature

Values:

T_R = 40.31° (from Kruth Microwave Electronics Corp. K-Mec)

$\mathcal{E}$ = 0.9923 (from MDL Component Book (Waveguide Manufacturer)

For WR-650, Aluminum Loss* .233 dB/100 at 1421 MHz
Assume 15' of W.G. = .03345 dB loss
Assume for dipole array efficiency = 50%
Efficiency of WG = 10(-loss/10) = 10 (-.03345/10) = 0.9923
T_{Lp} = 290°
T_A = 25° (see below)

The antenna temperature (T_A) was calculated in the following manner (5):

T_A = 3K (3K cosmic microwave background radiation)
3K (atmosphere)
2K (scattering from feed support structure)
2K (diffraction spillover to ground)
5K (Ohmic losses)
10K (scattering by inappropriate surface geometry)
Σ = 25K

Applying these values gives: T_{sys} = 25° + 2.242° + 40.31° = 67.73°

Solving for the minimum detectable cosmic temperature:

$$\Delta T_{min} = \frac{K_s \times T_{sys}}{\Delta_v \Delta_t} = 0.04787° \text{ K}$$

Recalculated system minimum sensitivity:

$$\Delta S_{min} = \frac{2K [\Delta T_{min}]}{\mathcal{E}_{ap} A}$$

$$\Delta S_{min} = \frac{2 \times 1.38 \times 10^{-23} \text{ J}}{(0.65)} \times \frac{0.04787}{50 \text{ m}^2} = 4.1357 \times 10^{-26} \cdot 4.14 \text{ Janskys}$$

The spatial resolution (expressed as half-power beamwidth- HPBW) is determined from the following relationship (Malphrus 1987):

$$HPBW = \frac{58 \lambda \text{ (m)}}{D \text{ (m)}}$$

where:

HPBW = Half-power beamwidth in degrees
λ = Operating wavelength in meters
D = Aperture diameter in meters

Calculation of the HPBW of the existing MRT system must be performed in two steps as the antenna is symmetric about a major and a minor axis.

HPBW of Major Axis:

$$HPBW = \frac{(58)(0.211 \text{ m})}{13.42 \text{ (m)}}$$

$$HPBW = 0.91192°$$

Repeating the calculation for the minor axis reveals:

$$HPBW = \frac{(58)(0.211 \text{ m})}{3.355 \text{ (m)}}$$

$$HPBW = 3.647°$$

Science Programs

The MRT will be employed in a widely varied scientific program. Research programs will range from investigating single cosmic phenomena to measuring secular variation of radio sources to mapping structures and areas of sky. The MRT will be utilized in astronomical research programs in planetary, galactic and extragalactic astronomy, and in SETI Searches. Research programs will include observing distant galaxies for variability, mapping regions of the Milky Way, spectral analyses of cosmic phenomena, and the measurement of galactic rotation utilizing measurements of the Doppler shifts of hydrogen clouds in galactic spiral arms. Astrophysically interesting phenomena such as quasars, radio galaxies, supernova remnants, giant molecular clouds, HI regions, cosmic masers, and exotic stars such as neutron stars and possible black holes will be investigated.

Research programs will include:

   *observing distant galaxies for variability

   *mapping regions of the Milky Way

   *spectral analyses of cosmic phenomena

   *galactic rotation and dynamics

Astrophysically interesting phenomena will be investigated including:

   *quasars

   *radio galaxies

   *supernova remnants

   *giant molecular clouds

   *HI regions

   *cosmic masers

   *exotic stars such as neutron stars and black hole candidates

Conclusions and Project Significance

The demilitarization initiatives that the U.S. Government has undertaken has recently produced a surplus of high-tech military equipment. Many U.S. scientists have begun to take advantage of the demilitarization efforts by acquiring and modifying surplus military equipment for use in scientific research projects. The MRT project is a classic example of the re-utilization of surplus high-tech equipment for basic science research. The success of the MRT project depends on the validity of the scientific results produced by the various research initiatives undertaken with the instrument. The validity of the scientific results is directly related to the performance characteristics of the instrument. Radio telescopes are generally rated among the largest and most sensitive scientific instruments ever produced. The scale and sensitivity of instruments is necessitated by the phenomenally weak radiation that they collect from space. In point of fact the flux density of even a moderately strong cosmic source 1420 MHz (the central operating frequency of the MRT) is on the order of a few Janskys (Jansky = 10^{-26} W/m^2/Hz). An analogy that radio astronomers use to describe the phenomenally weak signals detected by these instruments from space is to imagine converting the electromagnetic radiation into mechanical energy. If one converted all of the electromagnetic radio frequency radiation from space collected by all the radio telescopes from all over the world since the inception of the science in 1932, and converted this energy into mechanical energy it would roughly be the equivalent kinetic energy contained in a falling snowflake. If this energy were converted into electric energy it would light a 100 watt light bulb for almost one second (Malphrus 1996). Because of the inconceivably weak radiation the performance characteristics of the radio telescope must be conform to research-grade specifications to perform valid science. The instrument's performance characteristics, specifically antenna gain, minimum detectable flux density and spatial resolution are critical characteristics that effect the scientific results of a given research project.

Acknowledgments

Literature Cited

Malphrus, Benjamin K., Russell Brengelman, David Cutts, Charles Whidden. 1992. The Morehead Radio Telescope: Design and Fabrication of a Research Instrument for Undergraduate Faculty and Student Research in Radio Frequency Astrophysics. Grant Proposal Submitted to the National Science Foundation.

Malphrus, Benjamin K., Russell Brengelman, David Cutts, Charles Whidden, Phillip Hitchcock. 1996. The Morehead Radio Telescope Operator's Manual. Morehead State University. Internal Document.

Kruth, Jeff. 1994. A Receiver System for Radio Astronomy. Kruth Microwave Corporation. Internal Document.

Army Operational Research Group (AORG) AN-FPS 36 Radar Antenna Systems Operational Parameters. 1968. U.S. Army Document.

Kraus, J.D. 1986. Radio Astronomy. 2nd edition. Cygnus Quasar Publishers.

Malphrus, Benjamin K. and Richard Bradley. 1987. The National Radio Astronomy Observatory 40-Foot Radio Telescope Operators' Manual. Internal NRAO Document.

Malphrus, Benjamin K. 1996. The History of Radio Astronomy and the National Radio Astronomy Observatory: Evolution Toward Big Science. Krieger Publishers.

Kentucky Department of Education
GRANT AGREEMENT
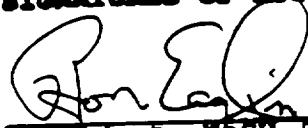
FEB 28

VENDOR: Morehead State University

PROJECT PERIOD: December 1, 1996 – August 31, 1997

PROJECT: PRISM "Bringing PRISM to the Schools"

AFC

BUDGET: $75,000.00   12 33 540 LA00 E417 0512 97 00 SF2 -4202

PAYMENT SCHEDULE: KDE will advance $50,000 effective immediately and $25,000 effective June 1, 1997 and upon completion of the following:
    1. Completion of mid-point report

PROJECT SCOPE:
1. Establish regional network to respond to local needs for improving K-12 mathematics and science education and for improving use of instructional technology.
2. Provide on-site assistance to schools; develop and implement school needs assessment and professional development.
3. Evaluate effectiveness of project.

SIGNATURES OF APPROVAL:

President, MSU, Ronald G. Eaglin   Date 12/4/96
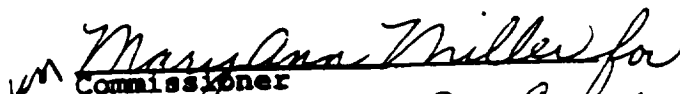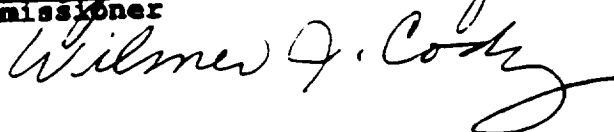
Director of PRISM   Date 4/25/96

Deputy Commissioner   Date 1/21/97

Commissioner — Mary Ann Miller for Wilmer J. Cody   Date 3/5/97

Bringing PRISM to the Schools

PROPOSAL COVER PAGE

SUBMITTED BY: ___Morehead State University_____
                        Organization

KENTUCKY DEPARTMENT OF EDUCATION REGION: # ___7_____

CONTACT PERSON: ___Benjamin K. Malphrus_____

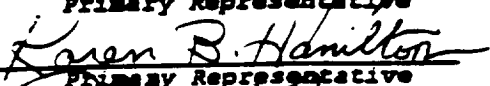ORGANIZATION: ___Morehead State University_____ PHONE: ___(606) 783-2212_____

ADDRESS: _____Morehead State University, UPO 1325___ FAX: ___(606) 783-2130_____
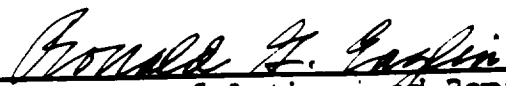
_____Morehead, KY 40351_____ EMAIL: ___b.malphr@morehead-st.edu___

TOTAL PRISM FUNDS REQUESTED: $_____79,368_____
TOTAL MATCH FUNDS: $_____17,351_____

KEY PARTNERS:
(if necessary, list additional partners on separate page)

___Morehead State University_____
        Organization   *Primary Representative*

___Region 7 Service Center_____
        Organization   *Primary Representative*

___Kentucky Educational Development Corporation___
        Organization   *Primary Representative*

___Maysville Community College_____
        Organization   *Primary Representative*

___Ronald G. Eaglin_____   ___10-4-96___
Signature of Authorized Representative(s)   Date

___Ronald G. Eaglin, President_____
Type Name and Title

___Morehead State University_____
Organization

form #1-A

EASTERN KENTUCKY
PRISM REGIONAL NETWORK

ABSTRACT

Members of the academic and business communities of Eastern Kentucky propose to establish the Eastern Kentucky PRISM Regional Network at Morehead State University (MSU) to serve Region 7. The intent of the regional network is to sustain systemic change in science and mathematics reform begun by the PRISM initiatives. The ultimate goal of these early initiatives as well as the current proposal is to strengthen the quality of science and mathematics instruction in Kentucky K-12 classrooms. The various PRISM initiatives have created a cadre of Science Resource Specialists, mathematics specialists and model school teachers throughout Eastern Kentucky. These specialists can provide the basis for a network of mathematics and science teachers in the region. The current proposal intends to extend gains made by these early initiatives by aligning the trained specialists closely with other Kentucky partners in science and mathematics in an integrated communication network.

The proposed initiative intends to support the PRISM Innovation Service initiative in its endeavor to provide schools in Kentucky with comprehensive technical assistance to improve and assess science and mathematics instruction. The proposed network center will link the resources brokered by the Innovation Service to schools via an integrated communication network of key contributors. In this way, the regional network will assist in organizing resources, increasing the awareness level of each partner's initiatives and by encouraging interaction among the various partners.

The major goal of the proposed project is to establish an integrated communication network whose purpose is to:

- Coordinate services of various initiatives in the region,
- Provide a mechanism for the delivery of PRISM and other services, and
- Sustain the State-wide Systemic Initiatives (SSI).

These goals will be accomplished via the development of a comprehensive regional communication network and the establishment of an associated center to operate and maintain the network services. The center will work with the regional partners and a Regional PRISM Advisory Committee (representatives of partner institutions) to implement the network. This project intends to link partners via an electronic network and through a series of model seminars that utilize the Kentucky Tele-Linking Network (KTLN).

The specific objectives of the proposed project are to:

1. Establish the Eastern Kentucky PRISM Regional Network
2. Develop and implement an electronic network
3. Perform a needs assessment
4. Provide a Seminar Series (KTLN) (4 tele-seminars based on needs assessment) and Internet project and participate in a statewide mini-conference
5. Develop and test an implementation plan

KENTUCKY DEPARTMENT OF EDUCATION
MEMORANDUM OF AGREEMENT

PROVIDER:

This AGREEMENT is made by and between the Kentucky Department of Education and
Morehead State University _____ (hereafter referred to as Provider)
_____
(Agency Name & Address)

on this ___16___ day of ___January___ 199_6___ .

PERIOD OF CONTRACT:

The period in which the services are to be performed under this contract is from _____
___September 1, 1995___ to ___August 31, 1996___ .

TOTAL AMOUNT OF CONTRACT:

The entire amount of this MOA shall not exceed $___42,073.00_____
(This amount must equal the Total Budget listed on the reverse side.)

FUNDS:

___ GENERAL (01)   XX FEDERAL (12)   ___ AGENCY (13)

ACCOUNT NUMBER:

Services performed are to be charged to the following Account(s):

ACCOUNT NUMBER(S)	AMOUNT OR PERCENT
~~12-33-540-LA-E41700-40-0512-96-00-4202~~	$42,073.00
12 33 540 LA00 E417 40 0512 96 00 4202	

PROJECT SCOPE:

The Provider will perform the services herein described: (Attach additional pages if necessary.)

Dr. Ben Malphrus will serve as Morehead State University's regional
coordinator for PRISM's Science Resource Specialists.

CONSIDERATION:

A. FEE

As fee for services hereinbefore set forth, the Department of Education agrees to pay the Provider
by the following method: (Unused funds must be returned to the Department of Education at the conclusion of this contract.
Carry forward is not authorized.)

Provider will bill the KY Department of Education quarterly for reimbursement
of expenses.

MAR _ 5 1996

BILLING:

Remit all invoices, bills, or requests for Payment to:
Director, Financial Services, Kentucky Department of Education
500 Mero Street · 16th Floor
Frankfort, KY 40601

CONSIDERATION:

B.   BUDGET
     SALARY $ _____
     FRINGE BENEFITS $ _____
     CLERICAL/SUPPORT STAFF COSTS $ _____
     SUPPLIES (Office/Workshops) $ _____
     SUPPLIES (Books, Pamphlets, etc.) $ _____
     OTHER RELATED COSTS (Detailed) $ _____
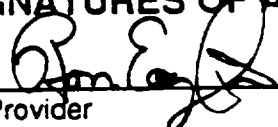
              TOTAL BUDGET $ 42,073.00
          (see attached breakdown of expenses)

CANCELLATION CLAUSE:

Either party may cancel the Memorandum of Agreement at any time for cause and may cancel without cause after thirty (30) days written notice.

SIGNATURES OF APPROVAL:

_____   2-22-96
Provider   Date
Ronald G. Eaglin, President
Morehead State University

_____   2/27/96
Associate Commissioner   Date
Department of Education
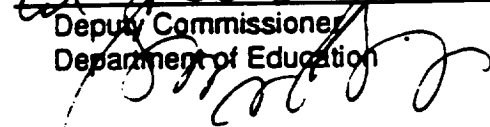
_____   2/27/96
Deputy Commissioner   Date
Department of Education

_____   3/5/96
Director Financial Services   Date
Department of Education
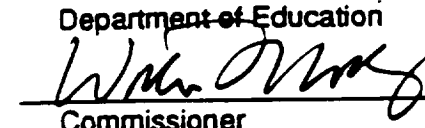
_Kevin M. Noland_____   3-5-96
Associate Commissioner, Legal Services   Date
Department of Education
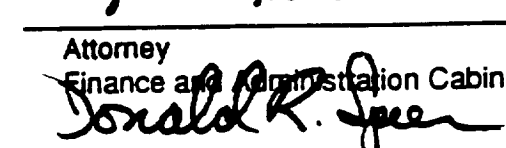
_____   3-10-96
Commissioner   Date
Department of Education

_Angela C Robinson_____   3/15/96
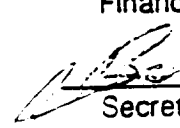Attorney   Date
Finance and Administration Cabinet

_Donald R. Speer_____   3/18/96
Commissioner   Date
Department of Administration
Finance and Administration Cabinet

_____   3-22-96
Secretary   Date
Finance and Administration Cabinet

CAMPUS OBJECTIVES GRANT PROGRAM AY 1997/98

KSGC — Kentucky Space Grant Consortium
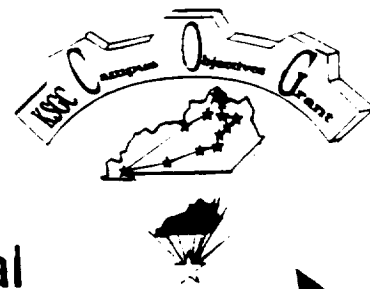
Non-Competitive Proposal

§1. Program Goals and Description: The principal goal of the KSGC is to enhance space-related research and education in Kentucky, utilizing the excitement of space sciences and missions to help increase interest and participation in science, engineering, and mathematics. The Commonwealth's primary space-science resources consist of faculty and facilities at consortium member institutions. The KSGC seeks to develop an infrastructure to increase communication, cooperation, collaboration, and support among the present and potential members of the Kentucky space-related research community, and between this population and NASA's R&D programs.

As a component of infrastructure development, each consortium member institution is eligible for a non-competitive grant of up to $1,000 to help the Campus Director facilitate KSGC objectives that are identified at the institution (award contingent upon available funding of the KSGC). The grant is to be used at the institution to support such activities as sending faculty members and students to NASA centers to explore research opportunities with NASA, copying and distributing KSGC and NASA information. and creating opportunities for interactions on the campus involving space-scientists. campus researchers, educators, students. and the public. Cost sharing is encouraged but not required; it may take the form, for example, of commitment of some of the Campus Director's time for the funded year. The Campus Director will be responsible for identifying relevant objectives at the institution, for developing opportunities for involvement of institutional personnel. for administering the grant at the institution. and for providing a brief summary report of expenses and achievements under the grant within thirty days following the end of the grant term. The funds may not be used for equipment or for the direct benefit of the Campus Director/grant administrator; however, he or she may be reimbursed for travel for the purpose of developing collaborations and infrastructure.

§2. Application for: __KSGC Campus Objectives Grant, AY 97/98__   **Proposed period:** __7/01/97–6/30/98__

KSGC Campus/Institutional Director (PI): __Benjamin Malphrus__

Consortium Institution and Address: __Morehead State University__

Phone: __(606) 783-2212__   __Morehead Astrophysical Laboratory__

FAX: __(606) 783-5002__   __Morehead, KY 40351__

E-mail: __b.malphr@morehead-st.edu__

Budget: $1,000

Request from KSGC ($1.000 max)	Cost Sharing (Optional: Campus Director time and/or other)		Total
For KSGC campus-objectives/ infrastructure-building expenses per conditions in §1: $ 1.000	B. Malphrus	$ 2,897	
	Supplies	$ 50	
		$	
		$ 2,947	
KSGC Total $ 1,000	Cost Sharing Total $ 2,947		$ 3,947

PI: _____ Signature   Benjamin Malphrus, Associate Professor   Typed Name and Title   5/23/97 Date

Fiscal Officer: __Paul R. Walters__ for   Porter Dailey, Vice President of Administration and Fiscal Services   6-4-97